

Dissertation  
zur Erlangung des Doktorgrades  
an der Mathematisch-  
Naturwissenschaftlichen Fakultät  
der Christian-Albrechts-  
Universität zu Kiel

On the role of  
microbial resilience  
in intestinal  
inflammation

Kiel, Germany, October 2017

Vorgelegt von  
Jacqueline Moltzau Anderson

---



**On the role of microbial resilience in intestinal inflammation**

Dissertation  
zur Erlangung des Doktorgrades  
an der Mathematisch-Naturwissenschaftlichen Fakultät  
der Christian-Albrechts-Universität  
zu Kiel

Vorgelegt von  
**Jacqueline Moltzau Anderson**

Kiel, Germany, October 2017



First referee (supervisor): Prof. Dr. Philip Rosenstiel  
Second referee: Prof. Dr. Hinrich Schulenburg  
Examiner: Prof. Dr. John Baines  
Chairperson: Prof. Dr. Frank Kempken

Date of the oral examination: December 12<sup>th</sup>, 2017

Approved for publication on: December 12<sup>th</sup>, 2017



Til min mor og bror.

Tusen takk.

## TABLE OF CONTENTS

<b>ACKNOWLEDGEMENTS</b>	<b>IX</b>
<b>FUNDING</b>	<b>XI</b>
<b>SUMMARY</b>	<b>XII</b>
<b>ZUSAMMENFASSUNG</b>	<b>XIV</b>
<b>DECLARATION OF AUTHOR’S CONTRIBUTION</b>	<b>XVI</b>
<b>LIST OF TABLES</b>	<b>XVIII</b>
<b>LIST OF FIGURES</b>	<b>XIX</b>
<b>LIST OF ABBREVIATIONS</b>	<b>XX</b>
<b>CHAPTER 1 – INTRODUCTION</b>	<b>1</b>
<hr/>	
<b>1.1. THE RESILIENCE PHENOMENON</b>	<b>1</b>
1.1.1. THE INSURANCE HYPOTHESIS	3
1.1.2. PERTURBATIONS	3
1.1.3. ANTIBIOTIC PERTURBATIONS	5
<b>1.2. DIVERSITY OF THE GUT MICROBIOME: BEYOND THE BACTERIAL SPACE</b>	<b>6</b>
1.2.1. POLYMICROBIAL INTERACTIONS	9
1.2.2. HOST-MICROBIOME INTERACTIONS	10
<b>1.3. INFLAMMATORY BOWEL DISEASE</b>	<b>12</b>
1.3.1. THE NOD-LIKE RECEPTOR NOD2 AS A RISK GENE FOR CROHN’S DISEASE	15
1.3.2. NOD2 REGULATES THE COMMENSAL GUT MICROBIOTA	17
<b>1.4. SECRETORY IMMUNOGLOBIN A</b>	<b>20</b>
1.4.1. SELECTIVE IGA DEFICIENCY	20
<b>1.5. FECAL TRANSFERS</b>	<b>22</b>
1.5.1. ENGRAFTMENT	24
1.5.2. WHAT IS DETERMINING THE SUCCESS OF FMT	25
<b>1.6. CHALLENGES CHARACTERIZING THE MICROBIOME</b>	<b>27</b>
1.6.2. MYCOBIOME	28
1.6.3. VIROME	28
<b>1.7. SCOPE OF THE THESIS AND AIMS</b>	<b>30</b>
<b>CHAPTER 2 – MATERIALS &amp; METHODS</b>	<b>31</b>
<hr/>	
<b>2.1. EXPERIMENTAL DESIGN</b>	<b>31</b>
<b>2.2. MICE</b>	<b>32</b>
<b>2.3. BACTERIOME</b>	<b>32</b>
<b>2.4. MYCOBIOME</b>	<b>34</b>
<b>2.5. VIROME</b>	<b>35</b>
2.5.1. NOD2	35
2.5.2. FECAL TRANSFER	38
<b>2.6. METAGENOME</b>	<b>39</b>
<b>2.7. CORRELATIONS</b>	<b>40</b>
<b>2.8. ANTIBIOTIC RESISTANCE GENES</b>	<b>40</b>
<b>2.9. SCREENING IMMUNOGLOBIN A LEVELS</b>	<b>41</b>
<b>2.10. SCREENING CALPROTECTIN LEVELS</b>	<b>42</b>

<b>CHAPTER 3 – RESULTS</b>	<b>43</b>
<b>3.1. NOD2</b>	<b>43</b>
3.1.1. BACTERIOME	43
3.1.2. ANTIBIOTIC RESISTANCE GENES	48
3.1.3. MYCOBIOME	49
3.1.4. BACTERIAL-FUNGAL CORRELATIONS	53
3.1.5. CALPROTECTIN LEVELS	55
3.1.6. VIROME	55
<b>3.2. FECAL TRANSFER</b>	<b>61</b>
<b>3.3. IMMUNOGLOBIN A</b>	<b>64</b>
3.3.1. IGA LEVELS IN WILD MICE	64
3.3.2. IGA LEVELS IN LAB MICE	66
<b>CHAPTER 4 – DISCUSSION</b>	<b>68</b>
<b>4.1. NOD2</b>	<b>68</b>
4.1.1. BACTERIOME	68
4.1.2. MYCOBIOME	71
4.1.3. CALPROTECTIN LEVELS	71
4.1.4. VIROME	72
<b>4.2. FECAL TRANSFER</b>	<b>74</b>
<b>4.3. IMMUNOGLOBIN A</b>	<b>75</b>
<b>CHAPTER 5 – CONCLUSIONS</b>	<b>77</b>
<b>5.1. CONCLUSIONS</b>	<b>77</b>
<b>5.2. FUTURE PERSPECTIVES</b>	<b>77</b>
<b>REFERENCES</b>	<b>81</b>
<b>APPENDIX</b>	<b>117</b>
APPENDIX 1 – ONLINE MATERIAL	117
APPENDIX 2 – NOD2 SUPPLEMENTAL MATERIAL	117
APPENDIX 3 – FECAL TRANSFER SUPPLEMENTAL MATERIAL	128
APPENDIX 4 – IMMUNOGLOBIN A SUPPLEMENTAL MATERIAL	130
<b>DECLARATION</b>	<b>134</b>
<b>CURRICULUM VITAE</b>	<b>135</b>

## ACKNOWLEDGEMENTS

First and foremost, I am very grateful to my supervisor Prof. Dr. Philip Rosenstiel, who supported me throughout these years, provided me with numerous opportunities, knowledge, and guidance, which allowed me to work independently and grow as a researcher. His knowledge and advice has been invaluable.

I would like to also express my gratitude to my thesis committee members Prof. Dr. Hinrich Schulenburg and Prof. Dr. John Baines, for their guidance, valuable suggestions, support, and great courses.

To Prof. Dr. Frank Kempken, Prof. Dr. Matthias Leippe, and Prof. Dr. Almut Nebel, thank you for the many wonderful conversations that have been fun, interesting, and insightful.

I am also very thankful to:

Dr. Tim Lachnit who has been and continues to be a great collaborator, friend, coffee enthusiast, and supporter.

Dr. med. Go Ito for his invaluable friendship, our many interesting discussions over lunch, and his help and support.

The IMPRS and Max-Planck-Institute for Evolutionary Biology for this wonderful opportunity. In particular to:

Dr. Kerstin Mehnert  
Prof. Dr. Bernhard Haubold  
Prof. Dr. Diethard Tautz  
Prof. Dr. Arne Traulsen  
Dr. Tobias Lenz  
Dr. Arne Nolte  
Iben Martinsen

The IKMB and the CellBio group. In particular to:

Wei-Hung Pan  
Melanie Vollstedt and the sequencing team  
Dr. Felix Sommer  
Dr. Simone Lipinski  
Dr. Robert Häsler  
Dr. Maren Falk-Paulsen  
Dr. med. Konrad Aden  
Karina Greve  
Dr. Anupam Sinha  
Philipp Best  
Florian Tran  
Maren Reffelmann  
Sabine Kock  
Melanie Nebendahl  
Angelina Offt  
Dr. Christiane Wolf-Schwerin  
Eike Zell

Iacopo Torre  
Dr. Georg Hemmrich-Stanisak  
PD Dr. Abdou Elsharawy

To Gesa Koberg and the Mathematisch-Naturwissenschaftliche Fakultät of the University of Kiel.

The VHH and in particular Sarah Vieten, who has been very helpful with the animal proposal.

The Uni Kiel Competitive Swim Team. Thank you for all the good times, for all the training, and the joy of pushing through difficult sets together (Coaches: Lena Schadte, Mario Kreft, Tobias Wyrwich, and Chris Horn).

To my friends in Kiel. In particular to:

Mario Kreft and Kirsten Dahl for their wonderful rich friendship, and generosity.

To Kristin Hagel for being a wonderful and supportive friend, the good walks together, and for translating the summary into German.

Maren Ernst for making me sweat in the pool, in yoga, and out rowing.

Charlotte and Panos for our many adventures and good times together.

Pete West-Oram for all of the good times during our evening German language classes, and the many great stories while out for good walks.

Chris Horn for all his hundreds of invitations for all sorts of different adventures and events in Kiel.

Lastly, I want to thank my mother, for her continuous and unconditional love and encouragement, and to my brother for his constant support and great wit.

## FUNDING

This work was supported by the IMPRS of the Max-Planck-Institute for Evolutionary Biology and CAU, the Origin and Function of Metaorganisms SFB1182 (C2), and Systems Medicine of Chronic Inflammatory Bowel Disease SysmedIBD. The work leading to these results has received funding from the European Union Seventh Framework Programme (FP7/2012-2017) under grant agreement n°305564, the DFG CRC1182 C2, CRC877 B9 and the BMBF as part of the e:Med framework (“sysINFLAME”, grant 01ZX1306), the Cluster of Excellence “Inflammation at Interfaces” (ExC 306) and SYSCID in the European Union’s Horizon 2020 research and innovation programme under grant agreement No 733100.

## SUMMARY

Loss-of-function variants in the nucleotide-binding oligomerization domain-2 (NOD2) gene, impairing the recognition of the bacterial cell wall component muramyl-dipeptide, are associated with an increased risk for developing Crohn's disease (CD). A disturbed control of gut microbial communities is hypothesized as a causative mechanism contributing to increased susceptibility for chronic intestinal inflammation through this genetic variation. Here, the influence of NOD2 on the longitudinal dynamics of the intestinal microbiota was demonstrated using wild-type (WT) C57BL/6J and knock-out (KO) NOD2 mice treated with broad-spectrum antibiotics. The microbial community composition was determined by 16S, ITS1, and viral sequencing. The presence of virus-like particles was also identified by transmission electron microscopy, and the occurrence of antibiotic resistance genes was assessed using qPCR. Additionally, since intestinal secretory immunoglobulin A (SIgA) is important in the regulation of the bacterial community, IgA levels were determined across different genotypes of both wild and lab mice to assess whether a pattern could be detected.

Antibiotics caused a significant increase in resistance genes and altered the microbial gut community in both genotypes. However, while bacterial diversity decreased, fungal diversity increased, serving as an indicator of gut dysbiosis and impaired host health. Strikingly, the viral community explained 99.2% of the bacterial community variation, and was found to be highly diverse, composed predominantly of bacteriophages, and a low abundance of eukaryotic viruses. Interestingly, a significant difference between the genotypes was observed, where the NOD2 genotype impaired bacterial resilience leading to delayed recovery. A delayed resilience was also detected in the virome of both genotypes, whereas, the fungal community remained perturbed. A pattern of IgA levels was not detected in the wild mice; however, a significant difference across time was observed in the ATG16L1 lab

mice, where IgA levels increased as mice aged. Moreover, a significant difference was also observed when comparing male wild mice with male lab mice where higher IgA levels were found in the wild mice.

These results demonstrate a complex relationship between gut bacteria, fungi, and viruses, where antibiotic perturbation creates niche availability and the expansion of potentially opportunistic genera. Importantly, NOD2 seems to license resilience of gut microbial communities, as evidenced by the delayed recovery. This may promote colonization with pathobionts and may contribute to the development of chronic intestinal inflammation.

## ZUSAMMENFASSUNG

Varianten von Funktionsverlustmutationen im Nukleotid-bindenden Oligomerisationsdomäne-2 (NOD2) Gen, welches die Erkennung der bakteriellen Zellwandkomponente Muramyl-Dipeptid beeinträchtigt, hängen mit einem erhöhten Risiko für die Entwicklung von Morbus Crohn zusammen (CD). Eine gestörte Kontrolle mikrobieller Darmgemeinschaften, basierend auf dieser genetischen Variation, wird als ein ursächlicher Mechanismus angenommen, der zu einer erhöhten Anfälligkeit für chronische Darmentzündungen beiträgt. In diesem Zusammenhang wurde der Einfluss von NOD2 auf die longitudinale Dynamik intestinaler Mikrobiota durch den Wildtyp (WT) C57BL/6J und Knockout-Mäusen (KO) NOD2, die mit Breitbandantibiotika behandelt wurden, gezeigt. Die Zusammensetzung der mikrobiellen Gemeinschaft wurde durch 16S, ITS1 und viraler Sequenzierung bestimmt. Das Vorhandensein von virusartigen Partikeln wurde auch durch Transmissionselektronenmikroskopie nachgewiesen. Zudem wurde das Auftreten von Antibiotikaresistenzen anhand von qPCR bemessen. Da das intestinale sekretorische Immunglobulin A (SIgA) darüber hinaus eine wichtige Rolle in der Regulation bakterieller Gemeinschaften spielt, wurde der IgA Gehalt verschiedener Genotypen von Wild- und Labormäusen zur Überprüfung eines möglichen Musters bestimmt.

Die Antibiotika verursachten einen signifikanten Anstieg der Resistenzgene und veränderten die mikrobielle Darmgemeinschaft beider Genotypen. Während die bakterielle Diversität abnahm, stieg die Pilz-Diversität jedoch an, was als ein Indikator für Darmdysbiose und eine beeinträchtigte Gesundheit des Wirtsorganismus gesehen wird. Auffallend ist, dass die virale Gemeinschaft 99.2% der Variation in der bakteriellen Gemeinschaft erklärt und als besonders divers, hauptsächlich aus Bakteriophagen zusammengesetzt und mit einer geringen Häufigkeit von eukaryotischen Viren beschrieben werden kann. Interessant ist auch der beobachtete signifikante Unterschied zwischen den

Genotypen, wobei der NOD2-Genotyp die bakterielle Resilienz beeinträchtigte, was zu einer verzögerten Wiederherstellung führte. Eine verzögerte Resilienz wurde auch in dem Virom beider Genotypen gefunden, wobei die Pilz-Gemeinschaft gestört bleibt. Ein Muster des IgA Gehalts wurde im Wildtyp nicht gefunden; hingegen jedoch ein signifikanter Unterschied über die Zeit in der ATG16L1 Labor-Maus, wo der IgA Gehalt mit dem Alter der Maus anstieg. Darüber hinaus wurde ein signifikanter Unterschied bei dem Vergleich zwischen männlichen Wild- und Labor-Mäusen gefunden, wobei Wild-Mäuse einen höheren IgA Gehalt aufwiesen.

Diese Ergebnisse zeigen eine komplexe Beziehung zwischen Darmbakterien, Pilzbefall und Viren, in der durch Antibiotikaeinwirkung Nischenverfügbarkeit und die Ausbreitung potenziell opportunistischer Gattungen entstehen. Es ist wichtig zu erwähnen, dass NOD2 anscheinend die Resilienz von Darm-Mikrobengemeinschaften zulässt, wie durch die verzögerte Wiederherstellung bewiesen. Dies kann die Kolonisierung mit Pathobionten fördern und zur Entwicklung einer chronischen Darmentzündung beitragen.

## DECLARATION OF AUTHOR'S CONTRIBUTION

Here, I present my doctoral research titled, "On the role of microbial resilience in intestinal inflammation", which took place from December 2014 to December 2017. The experimental design of all projects was done with the guidance of my supervisor Prof. Dr. med. Philip Rosenstiel. All written work included herein is my own. The work included herein was primarily conducted by myself, with the following exceptions:

The combined work of the bacteriome, mycobiome and detection of antibiotic resistance genes via qPCR was submitted to *Microbiome* on July 5<sup>th</sup>, 2017, with author contributions as follows. Fecal samples were collected by Dr. Maren Falk-Paulsen and Dr. Simone Lipinski. Wei-Hung Pan, Richa Bharti, and myself performed data analysis. Dr. Ateequr Rehman and myself performed the wet lab for the bacteriome and mycobiome. I performed experimental design, wet lab, and analysis for the detection of antibiotic resistance, with guidance from Dr. Robert Häsler. The final, as well as all previous versions of the manuscript were written by myself. All authors read and approved the final manuscript.

The viral work which resulted in the publication in *Gastroenterology* is my own. Additionally, the publication's materials and methods section for the virome was written by myself. All versions of the manuscript were edited by myself. All other work which comprises the publication was performed by the other authors.

The work comprised of the NOD2 virome and metagenome was conducted in collaboration with Dr. Tim Lachnit. Dr. Lachnit performed the extractions of VLPs, and the analysis of the raw data post sequencing. Experimental design, wet lab, library preparation and sequencing were performed by myself. Metagenomic wet lab, library preparation, sequencing, and initial data analysis was performed by myself.

The work comprised of the IgA levels in wild mice was conducted in collaboration with Dr. Marie Vallier and Prof. Dr. John Baines. Dr. Vallier provided the wild mice samples from France, their genetic background, and histological intestinal scores. Dr. Go Ito provided the lab ATG16L1 mice samples. All other samples were obtained myself. Determining IgA levels in all samples and subsequent analysis was performed by myself.

The work which contributed to the publication in *Nature Reviews Microbiology* was conducted in collaboration with the other authors. The section on fecal microbial transfer was written by myself. All versions of the manuscript were edited and revised by myself.

The thesis has contributed to the following publications:

**Moltzau-Anderson J**, Pan WH, Rehman A, Falk-Paulsen M, Lipinski S, Häsler R, Bharti R, Rosenstiel P. NOD2 influences intestinal microbial resilience after antibiotic perturbation. (*Microbiome*, submitted July 5<sup>th</sup>, 2017; under revision)

Sommer F., **Moltzau Anderson J**, Bharti R, Raes J., Rosenstiel P. (2017). The resilience of the intestinal microbiota influences health and disease. *Nature Reviews Microbiology*. doi:[10.1038/nrmicro.2017.58](https://doi.org/10.1038/nrmicro.2017.58)

Ott J.S., Waetzig H.G., Rehman A., **Moltzau Anderson J.**, Bharti R., Cassidy L., Thley A., Fickenscher H., Seegert D., Rosenstiel P., Schreiber S. (2016). Intestinal microenvironment transfer: a case series for therapy of *Clostridium difficile* infection. Gastroenterology <http://dx.doi.org/10.1053/j.gastro.2016.11.010>.

In preparation:

**Moltzau Anderson J.**, Lachnit T, Falk-Paulsen M, Lipinski S, Rosenstiel P. Antibiotics cause delayed resilience in the diverse murine virome. (Manuscript in preparation).

---

Jacqueline Moltzau Anderson

**LIST OF TABLES**

TABLE 1 - PERMANOVA on Bray-Curtis distance of the bacterial community	45
TABLE 2 - PERMANOVA on Bray-Curtis distance of the fungal community	50

**LIST OF SUPPLEMENTARY TABLES**

APPENDIX 2 TABLE S1 - Summary of antibiotic resistance genes and assay	122
APPENDIX 2 TABLE S2 - Exchangeable correlation matrix of phylum level bacteria	122
APPENDIX 2 TABLE S3 - Exchangeable correlation matrix of genus level bacteria	123
APPENDIX 2 TABLE S4 - ANOSIM global test of the viral community	123
APPENDIX 2 TABLE S5 - Pairwise test for time groups 0 and 14 of the viral community	124
APPENDIX 2 TABLE S6 - Pairwise test for time groups 0 and 21 of the viral community	125
APPENDIX 2 TABLE S7 - Pairwise test for time groups 0 and 71 of the viral community	125
APPENDIX 2 TABLE S8 - Pairwise test for time groups 0 and 86 of the viral community	127
APPENDIX 3 TABLE S1 - Characteristics and treatment outcome of patients	128
APPENDIX 4 TABLE S1 - Characteristics of wild mice	130
APPENDIX 4 TABLE S2 - Intestinal scores of wild mice	131
APPENDIX 4 TABLE S3 - Characteristics of wild mice with high fecal IgA levels	132
APPENDIX 4 TABLE S4 - Summary of wild mice intestinal scores with high IgA levels	133

## LIST OF FIGURES

Cover picture was taken under microscopy (TEM) of phages isolated from a NOD2 KO sample.

FIGURE 1 - Alternative stable states	2
FIGURE 2 - Community dynamics in response to perturbations	4
FIGURE 3 - Distribution of the human virome	8
FIGURE 4 - Structure of NOD1 and NOD2	15
FIGURE 5 - NOD2 response in the healthy gut and Crohn's disease	18
FIGURE 6 - Fecal microbial transfer as a perturbation	23
FIGURE 7 - NOD2 experimental design	43
FIGURE 8 - PCoA based on Bray-Curtis of bacterial community	45
FIGURE 9 - Relative abundance of genus level bacterial community composition	46
FIGURE 10 - Bacterial taxa indicating resilience	48
FIGURE 11 - PCoA based on Bray-Curtis of fungal community	50
FIGURE 12 - Relative abundance of genus level fungal taxa	51
FIGURE 13 - Relative abundance of class level fungal community composition	52
FIGURE 14 - Shannon index of class level fungal diversity	53
FIGURE 15 - Significant correlations between bacteria and fungi	54
FIGURE 16 - Fecal calprotectin levels in WT and NOD2 KO mice	55
FIGURE 17 - Transmission electron micrographs of virus-like particles	56
FIGURE 18 - MDS plot of the viral species composition based on Bray-Curtis	58
FIGURE 19 - Viral community composition in WT and NOD2 KO mice	59
FIGURE 20 - Distance-based redundancy plot of bacteria fitted to the viral community	60
FIGURE 21 - Genome of phage with mapping similarity to <i>Phage ctd1</i>	61
FIGURE 22 - PCoA and Shannon index of the bacterial community across time	62
FIGURE 23 - Virome composition of the donor and patient 4 across time	63
FIGURE 24 - Fecal IgA levels in wild mice	65
FIGURE 25 - Fecal IgA levels in lab mice	66
FIGURE 26 - Fecal IgA levels in male wild and lab mice & serum IgA levels	67
FIGURE 27 - Experimental design of two pulse disturbance events	78

## LIST OF SUPPLEMENTARY FIGURES

APPENDIX 2 FIGURE S1 - Mean organ weight from WT and NOD2 KO mice	117
APPENDIX 2 FIGURE S2 - PCoA based on Jaccard of bacterial community	118
APPENDIX 2 FIGURE S3 - Relative abundance of phylum level bacterial composition	118
APPENDIX 2 FIGURE S4 - PCoA based on Jaccard & Chao1 index of fungal community	119
APPENDIX 2 FIGURE S5 - Relative abundance of fungal community composition	120
APPENDIX 2 FIGURE S6 - Relative abundance of phylum level fungi in individuals	121
APPENDIX 3 FIGURE S1 - Relative abundance of the bacterial community of patient 4	129

**LIST OF ABBREVIATIONS**

ABR - Antibiotic resistant genes  
 AMPs - Anti microbial peptides  
 ATG16L1 - Autophagy-related 16 Like 1  
 CD - Crohn's disease  
 cDNA - Complimentary deoxyribonucleic acid  
 Cp - Ciprofloxacin  
 dsDNA - Double stranded DNA  
 FFT - Fecal filtrate transfer  
 fl/fl – Flanked by LoxP  
 FMT - Fecal microbiota transplantation  
 GEE - Generalized estimating equations  
 H1 - Haplotype  
 hBD1-3 - Human beta-defensins 1 to 3  
 HD5 - alpha-defensins 5  
 HD6- alpha-defensins 6  
 HMP - Human Microbiome Project  
 IBD- Inflammatory bowel disease  
 IEC - Intestinal epithelial cells  
 IMEnT - Intestinal microenvironment transfer  
 ITS (1/2) - Internal transcribed spacer region (1/2)  
 KO - Knock out  
 LLRs - Leucine rich repeats  
 MDP - Muramyl dipeptide  
 MetaHit - Metagenomics of the Human Intestinal Tract  
 MID - Multiplex identifier barcodes  
 MLCK - Myosin light chain kinase  
 NBD - Nucleotide binding domain  
 NF-KB - Nuclear factor kappa-light-chain-enhancer of activated B cells  
 NLR - Nuclear-binding oligomerization (NOD) domain-like receptors  
 NOD(1/2) - Nucleotide-binding oligomerization domain (1/2)  
 OTU - Operational taxonomic unit  
 PCoA – Principle coordinates analysis  
 PR - Prevalence ratio  
 RCDI - Recurrent *Clostridium difficile* infection s  
 rDNA - Ribosomal deoxyribonucleic acid  
 RIP2 - Receptor-interacting serine/theonine-protein kinase 2  
 rRNA - Ribosomal ribonucleic acid  
 RT - Room temperature  
 SIgA - Secretory immunoglobulin A  
 SIgAD - Secretory immunoglobulin A deficiency  
 ssDNA - Single stranded DNA  
 qPCR – Real-Time quantitative polymerase chain reaction  
 TEM - Transmission electron micrographs  
 TMRCA - Time to most recent common ancestor  
 UC - Ulcerative colitis  
 VLPs - Virus-like particles  
 VWF - von Willebrandd factor  
 WT - Wild type



# Chapter 1 – Introduction

Microbial communities are the drivers of key ecosystem processes in diverse habitats including the human body. Yet, microbial community behavior in perturbed environments remains a challenge to predict. Understanding how the community responds to a perturbation is important for determining how this same community maintains stability, through resistance and resilience. In the mammalian gut, a long evolutionary history exists between bacteria specialized for the gut habitat and the host. While the host provides both a habitat and energy resources by nutrient intake, associated microbes assist in digestion, pathogen resistance, and the regulation of both the immune system and metabolism<sup>1</sup>.

Numerous studies have shown the disruptive effect antibiotics can have on these processes<sup>2,3</sup>. Concerns related to the use of antibiotics include pathogen resistance to antibiotics, the alteration of the microbial composition, and related acute and chronic health problems. The increasing rates of inflammatory bowel disease in the developed world have been hypothesized to be related to the disruption of the interaction within and between the human microbiota and the host<sup>1</sup>.

Though essential to the health of the human host, there is a clear gap in knowledge regarding the responses of the bacterial, fungal, and viral communities to perturbations. The work presented in this thesis aimed to determine the composition of the bacterial, fungal, and viral gut communities and to better understand how they respond to a single pulse antibiotic perturbation.

## 1.1. The Resilience Phenomenon

Community stability is defined by both the resilience and resistance to environmental change. Pimm (1984)<sup>4</sup> defined resilience as the community's ability to recover back to a quasi-

stable state following a perturbation. Resilience, then, is a measure of the strength, or how often the perturbation occurs to alter the community function. In ecology, a perturbation is defined as a causal event that can change the immediate environment or directly change the community<sup>5</sup>.

A well-known perspective of stability, known as ecological resilience, states that there exist many stable states for which a community may reside<sup>5-7</sup>. A community can then shift to a new stable state when conditions are unfavorable resulting from a perturbation. This has been further developed by the concept of a stability landscape<sup>5,8</sup> (Fig. 1), where a ball represents the community existing in state of equilibrium (basin). When a perturbation occurs, a force is

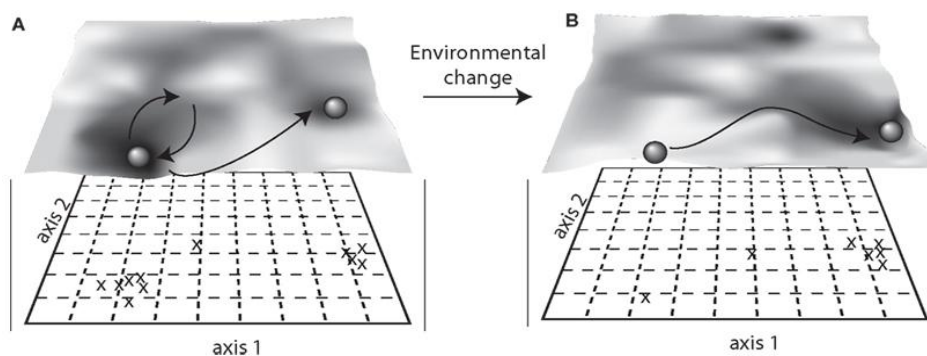


**Figure 1.** Illustration of alternative stable states from Shade *et al.*, 2012<sup>5</sup>.

applied to the ball within its basin. If the force is minimal, the community may resist the perturbation and the ball remains unmoved in the basin. In some cases, the ball may shift from its basin, but then return to its original basin, demonstrating resilience (Fig. 1A). However, if the perturbation is great enough, a strong force will be applied to the ball, which may shift it into a new basin representing an alternative stable state. This may also result if the resistance or resilience of the community is low. Once in this new basin, or alternative stable state, the ball's return to its original basin (with the community's previous composition and function) may be

difficult. Additionally, a ‘catastrophic regime shift’ may permanently shift the ball to a new basin (i.e. through extinction of species).

### **1.1.1. The Insurance Hypothesis**

There is a strong relationship between species diversity and ecosystem stability. Specifically, the insurance hypothesis states that species diversity stabilizes ecosystem functional properties, and as such, larger numbers of species enhances the probability that a system will provide a consistent level of performance over time despite fluctuating environmental perturbations<sup>9,10</sup>. In short, the insurance hypothesis refers to the buffering capacities of the community to return to a stable state in response to a perturbation either through a single stabilizer, otherwise known as a driver species (keystone species), or through multiple means. Resilient communities are usually characterized by a high species diversity, suggesting that they may be more stable based on their response to an environmental perturbation. Studies have shown that when the resilience of a community is low, transitory changes to the structure occur, which may increase the community’s susceptibility to invasion (by non-indigenous transient species), and thus cause functional changes. In the case of the gut microbiota, this change in function may be harmful for the health of the host, and in turn may additionally lead to the colonization of (opportunistic) pathogens<sup>5</sup>.

### **1.1.2. Perturbations**

Within the human gut, bacterial communities are constantly exposed to perturbations. Perturbations can include antibiotics, fecal transfers, a change in diet, or a pathogen, to name a few<sup>11</sup>. Depending on the duration, perturbations are further classified as pulses (Fig. 2A,B), short-term events, or presses (Fig. 2C), long-term or continuous events. However, a perturbation depends on many factors, including its spacial and temporal scales, frequency, intensity, extent,

and periodicity<sup>5</sup>. Additionally, since community stability is defined by both resistance and resilience, it is imperative to distinguish between these two in order to understand the implications of a communities' response to perturbations. Resistance then, is the degree to which a community withstands change in the face of a perturbation (Fig 2A), whereas the resilience is

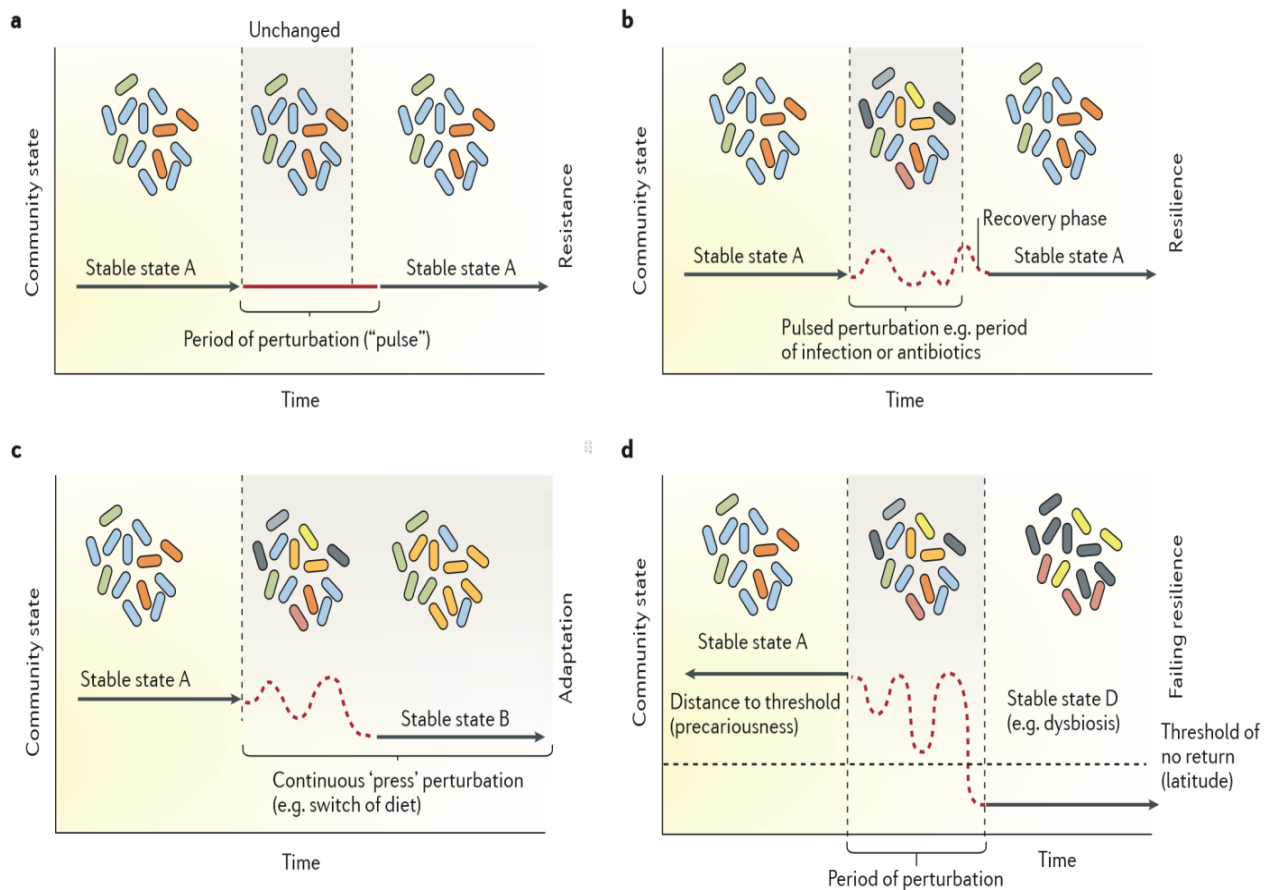


**Figure 2.** Illustration of community dynamics in response to perturbations, from Sommer *et al.*, 2017<sup>11</sup>

the community's ability to return to its original state after a perturbation (Fig. 2B). Moreover, long-term perturbations, such as a press, can lead to a community's shift to an alternative stable state (Fig. 2C).

A perturbation may also demonstrate a community's lack of resistance or resilience by shifting to a permanent alternative stable state (Fig. 2D). In the human gut, this may lead to a state of dysbiosis, whereby the microbial communities play a causative role in the manifestation of a disease and is ultimately detrimental to the health of the host<sup>11</sup>. Finally, compounded perturbations may also occur, which occur simultaneously, or within the recovery time of a previous perturbation.

### 1.1.3. Antibiotic Perturbations

The human use of antibiotics for treatment is a very recent adoption<sup>12</sup>. With the emergence of resistant and multi-resistant strains, most studies have focused on addressing these adverse effects. Few studies have reported on the effect of antibiotic perturbation on the human gut microbiota and the resilience phenomenon<sup>1,2,13</sup>. In one study, the distal gut microbiota of three individuals were examined over a 10 month period, within which two rounds of the antibiotic ciprofloxacin (Cp) was administered for 5 days each. Each course of antibiotic was separated by a period of 6 months, and stool samples were collected for bacterial 16S rRNA sequencing. Interestingly, taxa that were closely related to those that had been wiped out during antibiotic administration replaced them in abundance, but were later replaced by the original taxa after termination of Cp<sup>1</sup>. Additionally, although the composition of the gut microbiota had stabilized in all subjects at the conclusion of the study, they were all altered from their original state.

Similarly, a long-term study on the effects of antibiotic treatment on the microbiota found that post-antibiotic equilibrium states are themselves resilient, where the use of clindamycin disrupted *Bacteroides* for up to two year<sup>2</sup>. Another similar study further demonstrated that a cocktail of antibiotics, composed of metronidazole, clarithromycin, and omeprazole, and

administered for one week in three individuals with dyspepsia, resulted in a shift in the throat and gut microbiota for up to four years<sup>13</sup>. All studies also demonstrated some persistence of antibiotic resistance genes. In the case of the study administering ciprofloxacin, recovery from the second round of antibiotic administration was much faster than the initial round<sup>1</sup>. Yet, this same study also demonstrated that in a different case, the first round of antibiotics had a nearly complete recovery, whereas in the second round, recovery occurred to a different stable equilibrium. Thus, these studies demonstrate that the microbial resilience to future antibiotic treatments can have considerable individual variation. Furthermore, antibiotics can cause a shift in the microbial composition to an alternative stability state, for which the consequences remain unclear.

## **1.2. Diversity of the Gut Microbiome: beyond the bacterial space**

Previously, bacterial cells were believed to far outnumber human cells, constituting as much as 90% of the total number of cells associated with the human body<sup>14,15</sup>. However, a recently revised estimate determined that the number of bacteria within the human body is within the same order of human cells<sup>16</sup>. Commensal bacteria colonize all mucosal surfaces, with the intestinal tract harboring the largest bacterial load, currently estimated at  $3.9 \times 10^{13}$  bacteria<sup>16</sup>. The host microbiota performs numerous essential roles, such as the production of short-chain fatty acids, the development of the intestinal epithelium and a mature immune system, protection against pathogens, and the production of inflammatory and anti-inflammatory products<sup>17,18</sup>. Thus, microbial dysbiosis is considered central to the origin of numerous diseases.

Although little attention has been directed towards antibiotic perturbations on the community composition and function of the gut microbiota<sup>1,2,13</sup>, fewer still have done so looking

at the long-term effects of such impacts on a polymicrobial community<sup>19,20</sup>. Notably, most research has focused on bacteria (bacteriome) and their impact on gut health. The interactions of polymicrobial populations, made up of bacteria, fungi, and viruses have largely been ignored despite the potential for each to contribute to infection and inflammation<sup>21</sup>. Furthermore, fungi (mycobiome) and viruses (virome) also play an important role and contribute to gut community stability.

Humans have a fungal microbiome that is orders of magnitude smaller than that of the bacteriome<sup>22</sup>. The gut mycobiome has been estimated to be less than 0.1% in human feces<sup>21,23</sup>. However, this ‘rare biosphere’ has been shown to be more diverse, with the genus *Candida* including approximately 160 species, of which most are adapted to a mammalian host<sup>23</sup>. Similarly to many commensal bacteria, acquisition of *Candida* species occurs at birth, or through later human contact, and different body sites harbor specific fungal population<sup>23,24</sup>.

Few studies have reported on the mutualistic relationship between the host and the gut mycobiome, as most have focused on the role of fungi as pathogens. However, recent studies have demonstrated the importance of a stable mycobiome in regulating mucosal health, where a perturbation of the mycobiome resulted in enhanced immune responses<sup>25,26</sup>. These findings have led to the suggestion that fungi are keystone species within the gut, for which more studies are needed to elucidate the dynamics of the mycobiome during health and disease.

Finally, viruses have been shown to be extremely diverse, varying in their genetic material, genome sizes, life cycles, transmission routes, or persistence<sup>27-30</sup>. Humans are colonized by large populations of viruses consisting of viruses that infect eukaryotic cells (eukaryotic viruses) and those that infect bacteria (bacteriophages) (Fig. 3)<sup>28,31</sup>. Human feces are estimated to contain at least  $10^9$  virus-like particles per gram<sup>32</sup>, and although many of these

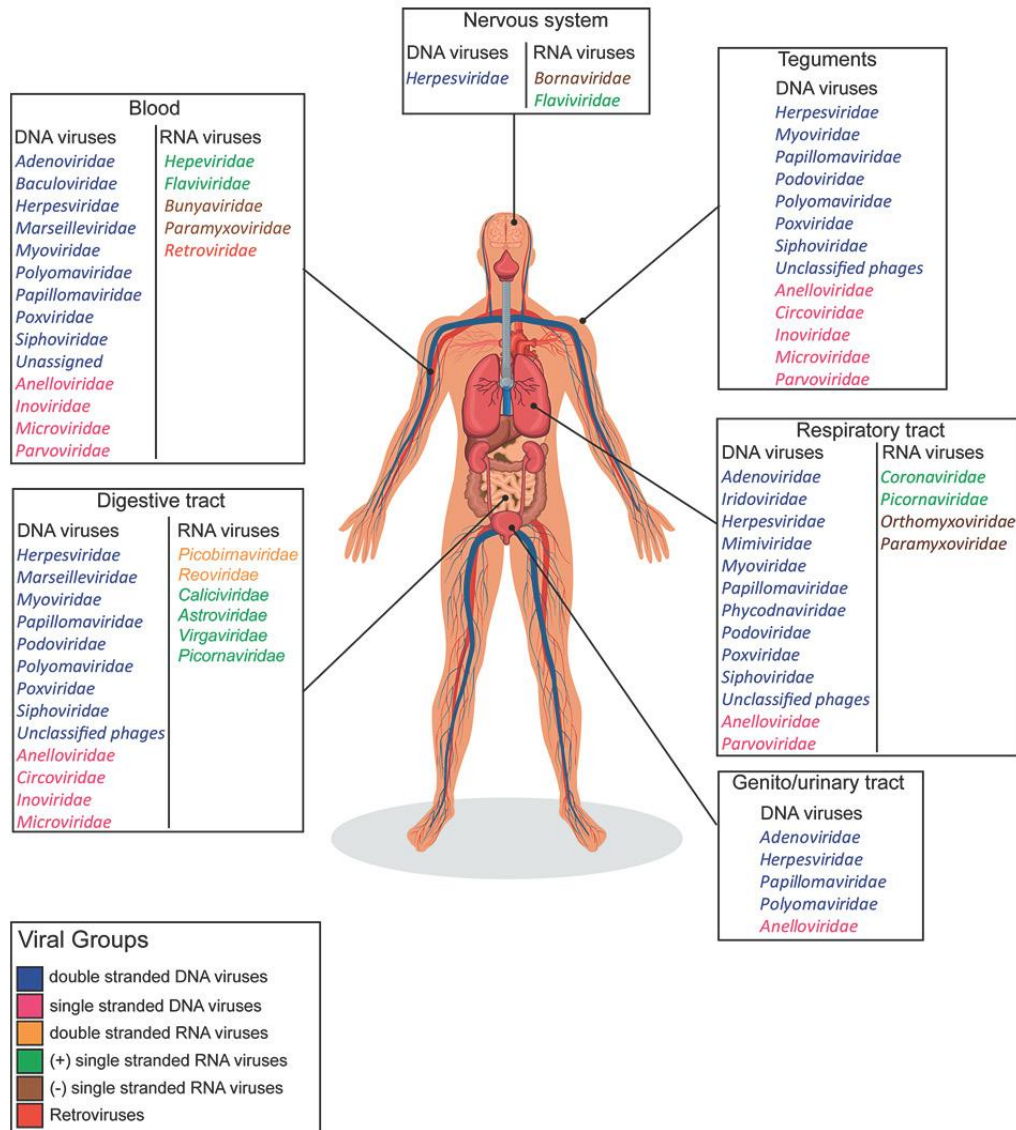


**Figure 3.** Illustration of the distribution of the human virome, from Popgeorgiev *et al.*, 2013<sup>28</sup>

viruses have been identified as bacteriophages, the majority remains unidentified<sup>33–35</sup>. Furthermore, host-genomes are also frequently composed of virus-derived genetic elements (retroviral elements and prophages)<sup>28,31,36</sup>.

Metagenomic analysis of human gut viruses has also revealed extreme interpersonal diversity. This is in part likely due to the already considerable individual variation in the bacterial strains present in the gut, for which differences in phage predators are influenced<sup>35,37</sup>. It

is well established that phages can be highly selective for different bacteria, and as such, phage sensitivity (phage typing) has been used for decades as an effective means of differentiating between different bacterial strains<sup>38,39</sup>. Rapid within-host viral evolution may also influence the large variability among individuals. In a long-term study investigating the viral community of an adult individual, Microviridae, a family of bacteriophages, was demonstrated to have high substitution rates, causing the sequence divergence values to be sufficient to distinguish new viral species by the conclusion of the study<sup>32</sup>. Moreover, individual virome compositions has been suggested to be relatively stable, with an estimated 80% of viral forms to be persistent throughout a 2.5 year long study<sup>32</sup>, with similar findings also observed in studies of shorter duration<sup>33,35</sup>.

### **1.2.1. Polymicrobial Interactions**

Despite the low abundance of the gut mycobiome, studies on the gastrointestinal and oral ecosystems have indicated that fungi influence bacterial behavior through different interactions, such as positive and negative influences between, as well as among, microbiome members<sup>21,40</sup>. This may be represented as co-occurrence or co-exclusion phenomenon, in addition to metabolic needs, quorum sensing exchanges, and the production of antimicrobial agents. Bacteria and fungi are also able to produce biofilms, which serve to protect bacteria and/or fungi from desiccation, antibiotic diffusion, or immune cell attacks, and results in the development of multiresistant strains to antimicrobial agents<sup>21,40</sup>.

Additionally, co-infections by pathogens forming mixed communities have higher virulence and resistance, in addition to different resilience properties compared to those of single species communities<sup>41</sup>. Viruses have also been found to have various effects on the bacterial community, by impacting bacterial diversity in a community, stimulating evolutionary change in

bacterial hosts, and providing selective advantages to bacterial hosts<sup>19</sup>. Viruses are an integral part of the gut microbial community and are mostly comprised of bacteriophages. Yet, little is known about how they respond to disturbances within a human host. Although antibiotics do not target bacteriophages directly, they do target their bacterial hosts, and thus the virome is thought to reflect changes in the bacterial community. Several studies have shown that the gut virome serves as a reservoir of antibiotic resistance genes<sup>19,42-44</sup>. In a murine model, certain antibiotics were shown to increase the reservoir of antibiotic resistance genes in the fecal virome<sup>42</sup>. Antibiotics have also been shown to induce prophages in the swine gut, which transmitted antibiotic resistance genes to other acceptor strains<sup>43</sup>. Importantly, recent evidence from studies of mice with mutations in ATG16L1 has demonstrated that eukaryotic viruses can alter intestinal disease by interacting with IBD risk genes and the bacteriophage community<sup>45,46</sup>. Moreover, an enteric eukaryotic virus was shown to replace the beneficial function of the commensal bacteria in germ-free and antibiotic treated mice<sup>45</sup>. Thus, viruses also play an important role in the resilience of microbial communities in response to antibiotic perturbations.

### **1.2.2. Host-Microbiome Interactions**

Within the gut, the majority of the intestinal bacterial microbiota reside in the large intestine, of which 99% is composed of Bacteroidetes, Firmicutes, Proteobacteria, and Actinobacteria<sup>47</sup>. The intestinal mucosa is continuously exposed to these large numbers of bacteria and their products, and it is this interaction that elicits basal level immune responses, which both regulate and protect the host from pathogenic and commensal bacteria. With an ever changing microbiota over the duration of a hosts' lifetime<sup>48</sup>, signaling pathways and their outcome resulting from an immune response will also change. These effects are of particular importance when considering the impact of antibiotic treatment, which has been shown to cause

numerous, and even permanent changes to the microbiome, particularly when exposed in infancy<sup>49</sup>. Moreover, changes disrupting the homeostasis of these interactions may play a role in the susceptibility and progression of chronic inflammatory diseases, such as Crohn's disease<sup>50</sup>.

Within the past 10 years, research has shown that the microbiota is essential in order to prime the innate and adaptive immune system in a process that begins shortly after birth<sup>51,52</sup>. Epithelial cells serve as the first line of defense in the initial recognition of microbial presence, in addition to other resident and migrating cell types<sup>53</sup>. This is established by tight junctions and the mucus layer of the intestinal epithelial cells, where highly specialized intestinal epithelial cells (IEC), such as Paneth and goblet cells, provide innate immune functions<sup>53</sup>. In addition, intestinal epithelial cells also sense microbial communities and respond through coordinated immune responses. The association of microbial dysbiosis, intestinal inflammation, and bacterial translocation, suggest that barrier dysfunction may play a central role in the pathogenesis of gastrointestinal inflammation<sup>53,54</sup>. Moreover, numerous studies have shown a strong association between barrier dysfunction and intestinal inflammation with a dysregulation of epithelial cell death<sup>53,55,56</sup>. The clearance of infected host cells, through apoptosis or other forms of cells death, is important during infection as a means of inhibiting microbial replication and survival. These strategies allow infected cells to be expelled from the epithelium quickly, thus preventing persistent infection<sup>57</sup>.

Another important component of the intestinal barrier includes AMPs as a means of preventing the microbiota from crossing the epithelium. However, AMPs are also responsible for shaping the microbiota, while the microbiota in turn can also shape AMPs<sup>58</sup>. A major factor in maintaining the balance between the host and the microbiota are AMPs in conjunction with the enteric mucus layer<sup>59</sup>. One important group of AMPs are defensins, which are classified by the

patterns of their disulfide bonds into the main classes of alpha- and beta-defensins. These are produced at almost all body sites and exhibit a diverse antimicrobial spectrum<sup>59,60</sup>. The human beta-defensins 1 to 3 (hBD1-3) are mainly expressed by epithelial cells, where hBD-2 and hBD-3 exhibit broad antimicrobial and anti-viral spectra, and hBD-1 exhibits broad activity against several commensal and fungi<sup>61,62</sup>. On the other hand, alpha-defensins-5 and -6 (HD5 and HD6) are the main antimicrobial peptides produced specifically by Paneth cells<sup>63</sup>. HD5 is a potent antimicrobial against bacteria, fungi, and viruses, whereas HD6 has been shown to self-assemble to form fibrils and nanonets to surround and trap bacteria<sup>63</sup>. Paneth cells are a crucial factor for pathogen defense and regulation of the commensal microbiota in small intestinal immunology<sup>63</sup>. In ileal Paneth cells, NOD2 is highly expressed, and provides a critical mechanism for regulating ileal microbiota via the secretion of anti-bacterial compounds<sup>17</sup>. Thus, NOD2 is a regulator of the ileal microbiota and Crohn's disease. Interestingly, impairment of the induction of the defensin molecules in humans are associated with colonic Crohn's disease<sup>62,64</sup>. Moreover, it was demonstrated in a mouse model that an orally applied AMP was able to reduce inflammation and infectious symptoms<sup>65</sup>. Together, these studies demonstrate the importance of AMPs to host health and its role in Crohn's disease when disrupted.

### **1.3. Inflammatory Bowel Disease**

Inflammatory bowel disease (IBD) is a complex chronic and relapsing inflammatory disease with genetic and environmental risk factors, in addition to commensal microbial factors. The precise cause of IBD remains unknown, although evidence suggests that an aberrant immune response toward the commensal gut microbiota, in a genetically susceptible host, is likely triggered by environmental factors. There are two primary subtypes of IBD composed of Crohn's

disease (CD), commonly localized the ileum and proximal colon, though it can involve any part of the gastrointestinal tract, and ulcerative colitis (UC), which is restricted to the colon.

Microbial communities are important for physiological homeostasis in the mammalian gut, and changing environmental factors affect the gut microbiota and likely contribute to the development and pathogenesis of IBD. At the time of diagnosis, patients already have an altered mucosal-associated bacterial community favoring aerotolerant species<sup>66</sup>. During the early stages of disease onset and prior to treatment, consistent trends across studies include an enrichment of Proteobacteria and Enterobacteriaceae, and a decrease in community diversity in conjunction with a decrease in protective taxa (i.e. *Lachnospiraceae*)<sup>67-72</sup>. The gut microbiota during active IBD is unstable and perturbed, and can directly alter both bacterial composition and gene expression, and in mice, *Escherichia coli* genes, which are highly induced by inflammation, have been shown to affect the severity of colitis<sup>73</sup>.

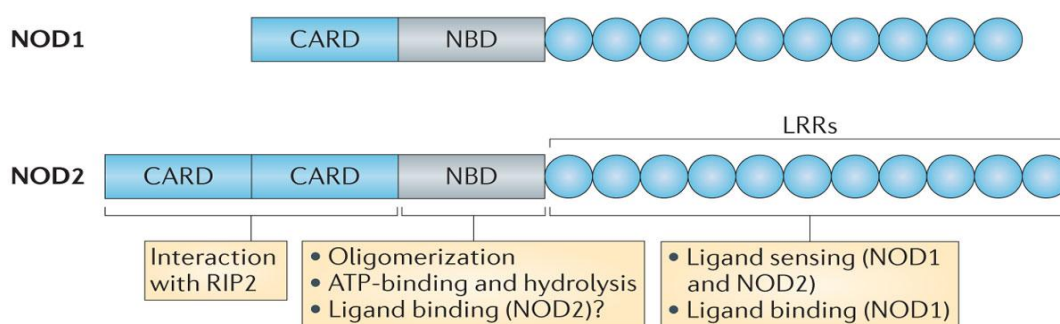
In IBD, a wealth of genetic risk variants have also been identified, which points to the involvement of innate immune genes (e.g. NOD2, RIP2, TLRs) in the etiology of the disease. Currently, over 200 distinct loci conferring either risk or protection from the development of CD and UC have been identified through genome-wide association studies, with a majority common to both diseases<sup>74-76</sup>. Of these, many alter production or secretion of proteins, antimicrobial peptides, mucus, bile acids, antibodies, and proteases, ultimately affecting barrier function and/or autophagic clearance of intracellular bacteria<sup>75</sup>. Thus, variants in genes regulating the innate immune response and associated with IBD, affect the interactions between the immune cells and bacterial communities. Nucleotide-binding, oligomerisation domain 2 (NOD2) was the first identified susceptibility gene for IBD<sup>77,78</sup>. An intracellular recognition protein, NOD2 senses the essential bacterial cell wall product muramyl dipeptide (MDP), derived from peptidoglycan, and

is highly expressed in specialized intestinal epithelial cells, such as Paneth cells<sup>79–82</sup>. Remarkably, approximately one third of all CD patients have a deleterious mutation on at least one NOD2 allele<sup>77</sup>, making NOD2 alone a very strong predictor of CD incidence. In humans, Crohn's disease risk alleles on the NOD2 locus disrupt and destabilize the NOD2 protein<sup>83</sup>, and it is assumed that this genetic variation is interacting with the intestinal microbiota as an environmental factor to precipitate disease manifestation. Additionally, impaired NOD2 function has been shown to have a distinct subtype of microbial dysbiosis, where patients with NOD2 mutations have an increase in adherent microbes to the intestinal mucosa<sup>84</sup> and significant shifts in the relative abundances of *Escherichia* species<sup>85</sup>.

In mice, NOD2 is an established risk gene for CD and mice with the NOD2 (KO) are useful to study inflammatory bowel diseases, innate immunity, and bacterial susceptibility. These mice have a dysbiotic microbiota and exhibit abnormal immune system morphology and a susceptibility to induced colitis<sup>86</sup>. Additionally, NOD2 deficient mice have an increased commensal microbial load (rDNA), yet the active bacterial component (rRNA) has a lower diversity<sup>86</sup>. NOD2 deficiency was also previously shown to increase disease risk in WT mice, post colonization with the fecal microbiota from NOD2-deficient (KO) mice<sup>87</sup>. Conversely, transfer of the fecal microbiota from WT to NOD2 deficient mice reduced disease risk and caused long-term changes in the gut microbial communities. Thus, NOD2 plays a key role in shaping the gut microbiota, further demonstrating the dysbiotic microbiota as an important factor of disease risk, and the role of NOD2 in the protection against intestinal inflammation. Interestingly, a global increase of IBD has been reported<sup>88,89</sup>. Yet, genetic factors cannot solely be driving the increasing global incidence of both CD and UC<sup>90</sup>, further suggesting that environmental factors are also contributing to its development<sup>1</sup>.

### 1.3.1. The NOD-Like Receptor NOD2 as a risk gene for Crohn's disease

NLR proteins are members of innate immunity effector molecules characterized by a central oligomerization domain (NBD/NOD) and a protein interaction domain, leucine rich repeats (LLRs) at the C-terminus<sup>91</sup>. NLR proteins play an important role in shaping the immune system by recognizing pathogens and damage-associated molecular patterns (i.e. PAMPs and DAMPs), and eliciting innate immune responses<sup>17</sup>. Although abundance of NLR protein members may vary dependent on cell types, humans have 22 NLR members and mice have 34 members, indicating that NLRs have evolved to develop specificity to numerous pathogens<sup>17,91</sup>. Most NLRs have a distinct protein-protein association domain and these variations of the amino-acid terminal are used to categorize NLRs into major subfamilies, including NLRCs (containing CARD) and NRPs (containing Pyrin), among others<sup>17</sup>. NOD2 is a cytosolic protein (110 kDa) characterized as part of the NLRC subfamily, having two CARD domains, whereas NOD1 contains a single CARD<sup>92</sup> (Fig. 4). The NOD2 gene is located on the human chromosome 16p21, and two NF- $\kappa$ B-binding sites are present upstream from the transcription start site. It is well established that numerous risk alleles for complex diseases are present throughout human



Nature Reviews | Immunology

**Figure 4.** Illustration of the structure of NOD1 and NOD2, from Philpott *et al.*, 2013<sup>91</sup>.

populations. In the NOD2 gene, there are three main polymorphisms that have been found to be strongly associated to Crohn's disease: (i) a frameshift mutation at 1007 (1007fs); (ii) a glycine to arginine conversion at amino acid residue 908 (G908R); and (iii) an arginine to tryptophan conversion at amino acid residue 702 (R702W)<sup>77,78,93</sup>. Interestingly, all three mutations are located close to, or even within the LRR domain, which recognizes MDP. Furthermore, Crohn's disease risk alleles on the NOD2 locus have been shown to be maintained by natural selection, where the deleterious haplotype of NOD2 is advantageous in diploid individuals<sup>83</sup>. Moreover, NOD2 mutations are mainly Caucasian alleles, having spread through hitchhiking with a high-frequency haplotype (H1) specific to Europeans<sup>83,94</sup>. Interestingly, estimates of time to most recent common ancestor (TMRCA) have shown the presence of the H1 haplogroup before human migration Out-of-Africa. Additionally, TMRCA for Europeans further revealed H1 to be older than the H2 or H3 haplotypes, which were also present in Africa<sup>83</sup>. With a strong distribution dissimilarity between single populations and major geographical regions, the regional diversity of NOD2 mutations and the exclusive H1 haplotype within Europe suggests that there is a regional selective pressure that is advantageous to this group<sup>83,94</sup>. Furthermore, three variants within the leucine rich repeat (LRR) domain of NOD2 are highly disease specific and are associated with CD. They also share a common ancestral allele, known as the H5 haplotype, which is characterized by the upstream coding variant SNP5. Interestingly, the main CD associated NOD2 mutations have occurred on the SNP5 allele primarily within the geographical region of Europe<sup>94</sup>. Thus, it has been suggested that natural selection acting on the NOD2 locus is due to balancing selection, and the existence of the H1 haplotype prior to Out-of-Africa migration further supports that its constant frequency may be advantageous within European populations<sup>83</sup>.

### 1.3.2. NOD2 Regulates the Commensal Gut Microbiota

In the healthy human intestine, the intestinal epithelium, in conjunction with epithelial tight junction and mucus layer, are an effective barrier against the gut microbiota. However, a dysfunctional mucosal barrier can lead to a direct interaction between bacterial products and immune cells (i.e. macrophages and dendritic cells), which respond by producing cytokines (i.e. IL-23) and chemokines. Lymphocytes are then further recruited when high levels of chemokines are produced, creating inflammation in CD through a positive feedback cycle<sup>17</sup>. However, the dysregulation of the NOD2 pathway alone has been found to be insufficient to induce intestinal inflammation, as NOD2 deficient mice do not develop spontaneous colitis<sup>47</sup>. Thus, although the exact mechanism for which NOD2 mutations contribute to Crohn's disease remains unknown, it has been suggested that NOD2 dysfunction leads to an alteration of the host-microbial interactions resulting in a loss of homeostasis<sup>50</sup>.

One possible mechanism resulting in these alterations includes altered antimicrobial activity of Paneth cells. NOD2 is highly expressed in Paneth cells, which secrete antibacterial compounds<sup>78,80</sup>. Furthermore, bactericidal activity from terminal ileum crypts have been shown to be induced by bacterial components, such as LPS<sup>95,96</sup>. Interestingly, the 1007fs mutation in NOD2, one of three major mutations associated to Crohn's disease (R702W, G908R, and 1007fs), causes a decrease in the expression of alpha-defensin<sup>64,97</sup>. Although NOD2 deficient crypts in mice were found to not have morphological defects, MDP could not induce effective bacteria-killing activity of both Gram-positive and Gram-negative bacteria<sup>47</sup>, and a reduced expression of a subgroup of alpha-defensins was also found<sup>82</sup>. Additionally, RIP2 deficient crypts were also found to be reduced in their ability to kill bacteria. Thus, loss of function mutations in NOD2 does not interfere with normal Paneth cell development; however, it may

facilitate bacterial entry into epithelial cells, resulting from an impaired bactericidal capacity through defective regulation of defensin expression<sup>82</sup> (Fig. 5).

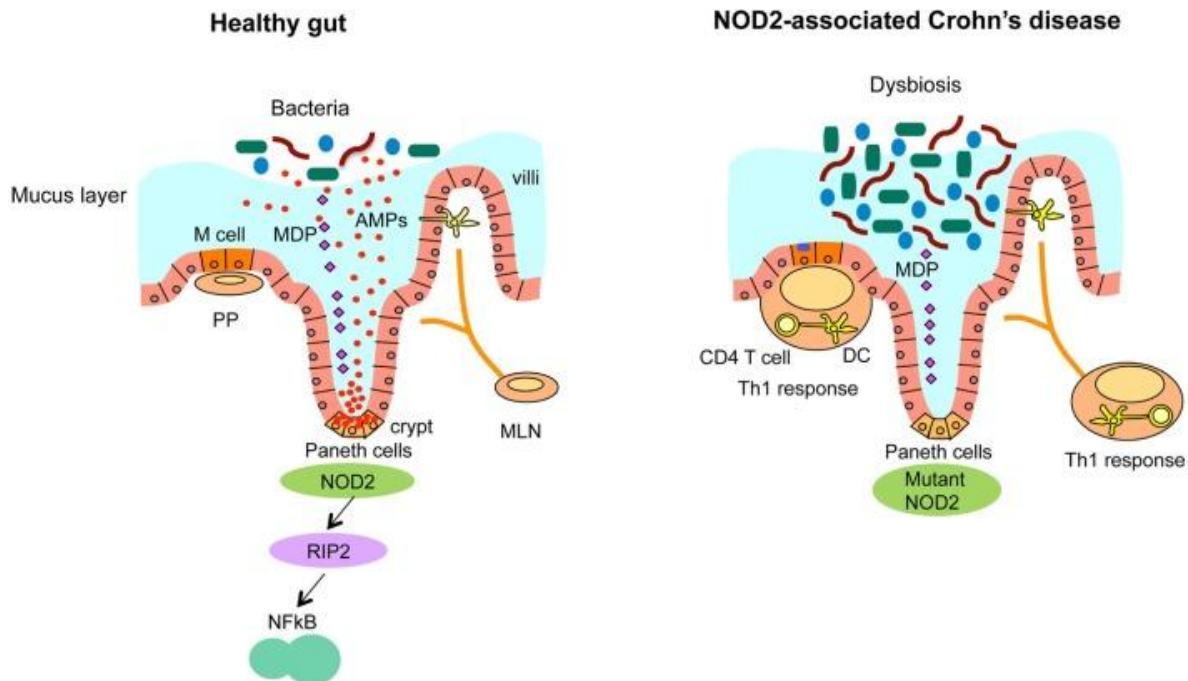


**Figure 5.** Illustration of NOD2 response in the healthy gut and Crohn's disease, from Sidiq *et al.*, 2016<sup>17</sup>.

NOD2 is essential for controlling the commensal microbiome in the terminal ileum, without which an increased bacterial load for *Bacteroides* and Firmicutes was found in NOD2 deficient mice<sup>47</sup>. Interestingly, in a study to determine whether NOD2 prevents de novo colonization of pathogenic bacteria, NOD2 showed a significantly delayed clearance of *H. hepaticus* compared to wild-type mice<sup>47</sup>. Both human and mouse studies have given support to the importance of a dysbiotic gut microbiome in the etiology of Crohn's<sup>50</sup>. Thus, in a negative feedback loop, the NOD2-RIP2 pathway plays an important role in regulating the commensal bacteria, while simultaneously the commensal bacteria are important for inducing this signaling pathway. RIP2 kinase is required for downstream signaling of NOD2 by activating downstream signaling cascades, including NF- $\kappa$ B and MAPK, together resulting in the activation of immune

response genes<sup>47</sup>. Through NF- $\kappa$ B, toll-like receptor (TLR) agonists enhance the NOD2 signal cascade, and thus the immune response. Importantly, NOD2 is also expressed in myeloid cells, and in non-Paneth epithelial cells, though at a lower level, inhibiting bacterial growth directly via beta-defensin secretion, or indirectly via the development of mature intestinal lymphoid tissues<sup>17,50,98,80</sup>. It is possible that the varied locations of NOD2 expression may be necessary for responding to different commensals and pathogens.

Mutations in autophagy-related 16 Like 1 (ATG16L1) gene are also a risk factor for CD<sup>99</sup>. NOD2 is capable of recruiting ATG16L1, which is an essential component for autophagy. However, studies have shown that NOD2 mutants failed to recruit ATG16L1<sup>100</sup>. Thus, NOD2 and ATG16L1 have important roles for regulating the gut microbiota. Autophagy is a pivotal component of the innate immune response to intracellular bacteria. Several studies have demonstrated that NOD2 activates autophagy to augment intracellular bacterial killing<sup>100,101</sup>. Moreover, a functional association between NOD2 and ATG16L1 has been demonstrated via a link between autophagy and bacterial sensing by NOD proteins<sup>100</sup>. Furthermore, in a process that involves NOD2, ATG16L1, and RIP2, MDP-activated autophagy increased bacterial killing and MHC class II-dependent antigen presentation in primary human dendritic cells<sup>101</sup>. Thus, genetic risk variants, defective lysozyme degradation and intestinal autophagic responses, are likely altering the gut microbiota and enhancing CD susceptibility<sup>101,102</sup>. However, in turn, two different mechanisms are also separately regulated by commensal bacteria, selective lysozyme trafficking and final secretion<sup>95</sup>. Interestingly, NOD2-mediated lysozyme trafficking in Paneth cells was found to be directed by the commensal bacteria<sup>103</sup>, and plays an important role to promote host defense against infections. Thus, NOD2 expression is in turn regulated by signals from the microbiota. Taken together, these results demonstrate that NOD2 restricts the

commensal bacterial from over-expansion and further protects the host from pathogen colonization in the intestine.

## **1.4. Secretory Immunoglobulin A**

Intestinal secretory immunoglobulin A (SIgA), an antibody class produced by plasma cells within the lamina propria, is important in the regulation of the commensal bacterial and viral populations<sup>104</sup>. Unique to the mucosa, SIgA binds to surface molecules of pathogens, and thus functions by blocking these microorganisms from contact with the host's cells<sup>105,106</sup>. In the absence of intestinal IgA, the commensal microbial community may expand and escape the gastrointestinal tract, thus activating the immune system both locally and systemically<sup>104</sup>.

### **1.4.1. Selective IgA Deficiency**

Selective IgA deficiency (SIgAD) is the lack, or low amounts of secretory immunoglobulin A and is the most common form of primary immunodeficiency affecting approximately 1/600 individuals in the western world<sup>107,108</sup>. Yet, variability in the prevalence of different ethnic groups suggests a genetic basis for the disorder. Additionally, familial inheritance pattern is observed depending on the gender of the parents, where affected mothers are more likely to pass the defect. Interestingly, as many as 85-90% of IgA-deficient individuals are asymptomatic, sufferers only experiencing an increase in gastrointestinal infections and cases of diarrhea compared to IgA normal individuals<sup>104</sup>. However, SIgAD has also been associated with an increase in gastrointestinal diseases, such as malabsorption, celiac disease, ulcerative colitis, and malignant proliferation<sup>104</sup>. In a study examining autoimmune disorders in patients with IgA deficiency compared to the general population in Sweden, individuals with IgA deficiency were found to have a 35-fold higher prevalence ratio (PR) for celiac disease<sup>108</sup>. In addition, the study

also found a 5-fold higher PR for IBD, a 5.7-fold higher PR for Crohn's disease, and a 3.9-fold higher PR for ulcerative colitis, indicating that individuals with IgA deficiency had a higher prevalence for autoimmune disorders<sup>108</sup>.

In IBD, the intestinal microbiota plays a role in driving an inflammatory response<sup>109</sup>. To identify specific members of the microbial gut community that may affect IBD, a study predicted that relative levels of bacterial coating with IgA could be used. Using a combination of flow-cytometry based bacterial cell sorting and 16S rRNA gene sequencing, the microbial community was sorted into bacteria that had high IgA coating (IgA+) and bacteria that had low IgA coating (IgA-). High IgA coating was found to represent a distinct subcommunity within the gut microbiota and was associated to known pathogens driving intestinal inflammation<sup>109</sup>. In another study investigating the role of SIgA, baseline intestinal levels of IgA in WT C57BL/6J mice had been determined and differentiated into high and low IgA levels<sup>110</sup>. Interestingly, co-housed WT C57BL/6J mice with IgA-high and IgA-low levels resulted in all mice to be IgA-low<sup>110</sup>. To determine whether a specific microbial pool could cause the IgA-low phenotype, IgA-low mice were pre-treated with a broad spectrum antibiotic cocktail before performing a fecal transplant either from IgA-high or IgA-low mice. The study found that ampicillin reversed the IgA-low phenotype, indicating that microbes sensitive to ampicillin were responsible for the IgA-low phenotype. Thus, the IgA-low phenotype was found to be dominant, bacterially driven, and transmissible, making fecal IgA a marker of microbial variability<sup>110</sup>. However, IgA levels, and determinants thereof, still remain undetermined in many other murine lines and wild mice.

## 1.5. Fecal microbiota transplantation

Fecal microbiota transplantation (FMT) is the transfer of stool, or portions of stool, from a healthy donor into the gastrointestinal tract of a recipient. First described in 1958 as a treatment for pseudomembranous colitis, FMTs have garnered attention as an effective form of treatment for recurrent *Clostridium difficile* infections (RCDI) with a success rate of over 90%<sup>111–113</sup>. In addition to being used as a treatment for RCDI, FMTs are also an effective tool for functional studies in animal models<sup>114</sup>. Despite FMT's success in treating RCDI and its potential to treat other gastrointestinal disorders, such as IBD, the mechanisms behind the restoration of gut functions remain unknown. Moreover, changes observed in the recipients' gut bacterial community are generally attributed to the bacteria from the donor's feces. Other components of the FMT are largely ignored, and few studies report on the long-term effects. Additionally, the criterion of a healthy donor varies across studies and screening focuses largely on infectious pathogens. There is an urgent need for investigations to characterize and better understand the effects of FMTs in the recipient. Moreover, FMTs can be better understood as a perturbation to the recipients' microbiome, and as such, stresses the importance of future studies on community stability and resilience.

FMTs are widely acknowledged for its efficacy in modifying the gut microbiota<sup>115,116</sup>. As such, FMTs fall under the classification of a pulse (short-term) perturbation, followed by a recovery, or resilience period (Fig. 6). In such a scenario, several hypothetical outcomes are possible, where the ideal outcome is the long-term transfer of the functional properties of the donor to the recipient leading to stable state similar to the donor community (Fig. 6A, B; stable state C). However, it is also possible that the perturbation is too weak with the recipient's community returning to its initial dysbiotic state (dysbiotic stable state A). Finally, it is also

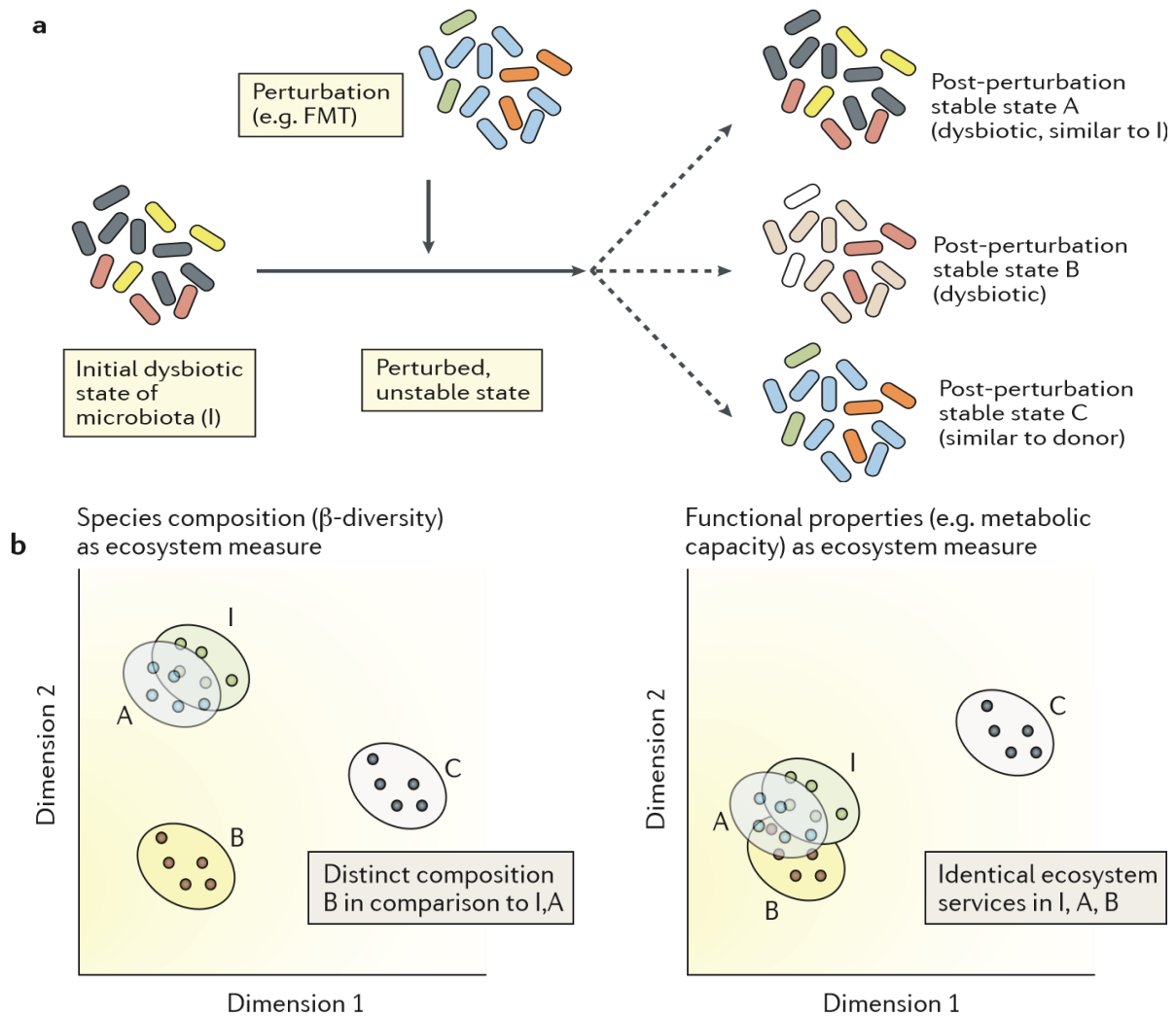


**Figure 6.** Illustration of a fecal microbial transfer as a perturbation, from Sommer *et al.*, 2017<sup>11</sup>.

possible for the perturbation to cause the recipient's community to shift to an alternative stable state, which is still dysbiotic, but distinct from initial state (dysbiotic stable state B).

However, most FMTs are usually preceded by antibiotic treatment, or a bowel lavage, and are usually only administered to patients for whom other treatments have been ineffective, as seen in RCDIs. Thus, FMTs should be evaluated in light of multiple perturbations that can occur either simultaneously, or within the recovery time, or resilience, of a preceding perturbation (compounded perturbation). Interestingly, multiple perturbations appear to have a greater likelihood of leading to a shift in the microbial community<sup>112,113,117,118</sup>. In CDI patients pre-

FMT, a greater relative abundance of the phyla Proteobacteria and Firmicutes is observed<sup>112,113,119</sup>. In some cases, CDI patients have been shown to have more than 99% of the reads classified as Proteobacteria or Firmicutes<sup>113</sup>. It is well established that patients with CDI have a perturbed gut microbiota compared to healthy donors who have a greater relative abundance of Bacteroidetes and Firmicutes, with Proteobacteria, Verrucomicrobia, and Actinobacteria present only at a low relative abundance<sup>113,120,121</sup>. However, despite the similarity in taxa among donors, individual variation is observed in the relative abundance of the taxa<sup>112,113,119</sup>. Furthermore, although patient samples post-FMT are generally found to have similar taxa to the donor, the relative abundance varies between recipient and time point. Despite this variation, samples post-FMT generally shows an increase in Bacteroidetes and Firmicutes compared to the matched pre-FMT samples<sup>113,119</sup>. A greater community diversity is also observed in both the healthy donors and the recipients post-FMT compared to pre-FMT samples. Additionally, compared to pre-FMT samples, a lower abundance of Proteobacteria and Actinobacteria is usually observed<sup>113,119</sup>.

### **1.5.1. Engraftment**

Surprisingly, engraftment, or the success of the transfer to colonize, occurs quickly with recipient microbial communities resembling donor composition and leading to a resolution of gastrointestinal symptoms and CDI within two or three days post-FMT<sup>111,113,122</sup>. Additionally, engraftments appear to be enduring, with most engraftments from donors shown to remain for nearly 4 months. In a study investigating strain engraftment, donor-specific species were identified 70 days post-FMT in the recipient<sup>119</sup>. Donor and recipient strains have even been shown to coexist; however, the colonization success was greater for conspecific strains compared to new species<sup>111</sup>. Interestingly, new species were found to follow a similar level of fluctuation

over a similar time frame, as seen in the healthy donors. However, the origin of newly observed species remains to be determined. It is uncertain whether they originate from the donor, other environmental sources, or in the gut of the recipient. Yet, these studies demonstrate the importance of species level diversity in population dynamics and as a consequence, the potential role some species have on resilience. Additionally, it is important to consider that most FMT studies are preceded by antibiotic treatment. Interestingly, in contrast to findings in FMT patients with RCDIs, recipients that did not use antibiotics for at least 3 months prior, or during FMT treatment, but received a bowel lavage prior to the FMT, gradually lost the similarity to the donor composition<sup>111</sup>. Antibiotics may therefore serve as a means to increase the success of FMT engraftment in the recipient by clearing out a majority of the recipients' gut bacterial community, and potentially also pathogens<sup>112,117</sup>. Though most authors acknowledge some effect from antibiotics used by patients with RCDI, it remains to be determined whether antibiotics serve as a tool for the facilitation and success of engraftment. However, 1/3 patients with RCDI successfully treated with a FMT are re-infected with CDI after a subsequent treatment of antibiotics for an unrelated infection<sup>113,123</sup>, further stressing the need to evaluate multiple perturbation events in future FMT studies.

### **1.5.2. What is determining the success of FMTs**

Currently, a standardized method for FMTs does not exist, and is a major problem for identifying the factors responsible for the successful outcome of the FMT. Moreover, FMTs are now also being considered as a means of treating other gastrointestinal disorders, such as multi-resistant pathogens. Several studies have observed that compared to pre-FMT samples, a significant reduction in the number of antibiotic resistant genes (ABR) in the recipients' samples occurred one or two months post-FMT<sup>115,124</sup>. However, a possible transfer of resistance through a

FMT was observed by the authors, where the *vanB* resistance gene was identified in all patients post-FMT and in all donors used, but not in the pre-FMT samples<sup>115</sup>. Thus, despite the reduction of ABR genes, FMTs may also introduce new resistant genes into the recipient. Fecal donors and healthy donors harbor a large repertoire of resistant genes, making the transfer of ABR genes a likely scenario in FMTs. In light of these results, stringent donor screening should be implemented. Yet, antibiotic resistant genes are not the sole cause for concern when considering what is transferred during a FMT. Notably, FMT studies have focused solely on the bacteria community and their impact on gut health, excluding the potential for the mycobiome or virome to contribute to either health or disease. Viruses in particular, including bacteriophages, may play an important role in human immunity and the mucosal health<sup>112,118</sup>.

Importantly, the structure of the gut microbiota is also influenced by host genetics. In a study investigating over 400 twin pairs, specific bacterial taxa were found to be more heritable than others<sup>125</sup>. The interaction between the gut microbiota and the host genotype may also affect the outcome of the transplant, where the resolution of CDI was higher in FMT from related donors compared to unrelated donors<sup>114</sup>. In numerous body sites a significant association between the microbiome composition and host genetic variation was found to be driven by immunity-related pathways, especially in host genes which were associated with diseases, such as IBD<sup>126</sup>. Additionally, high levels of genetic differentiation among human populations were identified in host genomic regions associated with the microbiome<sup>126</sup>. Moreover, multiple mouse models have shown that a disease promoting microbiota can be dominant after a FMT in previously stable wild-type (WT) mice, again highlighting the transfer of disease susceptibility<sup>87,110,127</sup>.

Finally, other body sites also play a role in the establishment of the microbial communities. For instance, the oral cavity plays a role in the development of diverse microbes in the lower respiratory tract<sup>20</sup>. The oral microbiota composition can also influence pregnancy outcome by entering the uterine environment through the bloodstream<sup>128</sup> and has been found to resemble the placental microbiome more than the vaginal, fecal, nasal, or skin microbiomes in normal term pregnancies<sup>129</sup>. Bacterial products from the gut can also affect distal organs. In a study manipulating the gut microbiota of germ-free maternal mice, permeability of the blood-brain barrier in their offspring was influenced in utero and persisted into adulthood<sup>130</sup>. Ultimately, community structures remain distinct, demonstrating that each body site hosts a unique community. Although these studies indicate that the gut selects for a separate community, the influence of other body sites cannot be ignored.

Although FMT perturbations have been shown to be highly effective to treat RCDI, and have the potential to treat other gastrointestinal disorders, factors responsible for the stability of gut polymicrobial communities need to be investigated, particularly in light of different perturbation events (pre-FMT). Though essential to the health of the human host, only a limited understanding of the mechanisms responsible for these responses is currently available. Moreover, thorough screening of donors and the compatibility of the donor and recipient is of particular importance when considering future FMTs.

## **1.6. Challenges Characterizing the Microbiome**

In the last two decades, DNA sequencing technology has revolutionized the characterization of microbial communities, prior to which culturing, morphological, and physiological characteristics were relied upon<sup>131-133</sup>. In particular, the Human Microbiome

Project (HMP) and the Metagenomics of the Human Intestinal Tract (MetaHit) have helped to define the commensal bacteriome of various human body site<sup>24</sup>. However, the characterization of the fungal and viral diversity is still lacking, largely due to issues regarding methodology, and the lack of a database as rich as that for bacteria.

### **1.6.1. Mycobiome**

The primary choice for molecular identification of fungi is the nuclear ribosomal internal transcribed spacer (ITS) region<sup>134,135</sup>. Its two spacers (ITS1 and ITS2) are highly variable and species specific, whereas the 5.8S gene is highly conserved<sup>131</sup>. However, identifying and extracting the ITS1 and ITS2 region from data sets is difficult and often leads to a high proportion of false-positives, as many ITS sequences are incorrectly defined in public sequence databases. Additionally, surrounding the ITS region are the highly conserved SSU and LSU genes, which creates false matches using a BLAST search, since the conserved parts of sequence will match regardless of whether or not the variable part does. To work around this, the software tool ITSx<sup>131</sup> was implemented, which extracts full length ITS sequences of either the ITS1 or ITS2 region, in addition to the 5.8S, from both high-throughput and Sanger sequencing. Additionally, the ITSx software can also remove non-ITS sequences from the data set, which altogether greatly improves sequence similarity searches and reduces sequences that would otherwise exaggerate diversity estimates.

### **1.6.2. Virome**

The general steps for characterizing the virome consist of four steps: (i) purification and enrichment of VLPs present in the sample, (ii) extraction of nuclear acids (including cDNA synthesis and amplification), (iii) library preparation and sequencing, and (iv) bioinformatic analysis of the sequence data<sup>136</sup>. However, studying the virome has numerous challenges. Firstly,

the majority of the genetic material in a sample is of non-viral origin (i.e. bacteria), causing difficulties with extraction and isolation, contamination and amplification, as well as data analysis post sequencing. Secondly, viruses lack universally conserved genetic regions, in addition to also being both genetically and morphologically diverse<sup>137</sup>. Taken all together, these limitations often lead to viral sample loss during processing, and usually focus only on viral DNA, overlooking viral RNA in the microbiome. Moreover, a major limitation is the lack of validated methods for understanding the role of the human or mouse gut virome in health and disease. Thus, to characterize the virome in the gut, key-steps include the enrichment of viral-like-particles (VLPs) from a sample, and random amplification, should the starting material need to be increased prior to NGS library preparation<sup>137</sup>. However, there is no singular method that will yield flawless results. For instance, filtration is a widely used method for VLP enrichment by removing bacterial and host cells, as well as larger debris, such as plant material. The most popular filters contain 0.45- $\mu\text{m}$  or 0.22- $\mu\text{m}$  pore sizes<sup>136-138</sup>. Although filters efficiently remove bacteria, they also remove large viruses (i.e. Herpes virus) and giant viruses (i.e. Pandora virus and *Megavirales*), which have similar physical dimensions to small bacteria<sup>29,30,137,139</sup>. Thus, careful consideration should be taken in order to obtain the most optimal results.

## 1.7. Scope & Aims

NOD2 plays a key role in shaping the gut microbiome, and loss-of-function variants in the NOD2 gene are associated with an increased risk for developing Crohn's disease. Understanding how the microbial community responds to a perturbation is important for determining how this same community maintains stability, through resistance and resilience.

The work presented in this thesis aimed:

- to investigate the influence of NOD2 on the longitudinal dynamics of the bacterial, fungal, and viral gut community's response to a single pulse antibiotic perturbation,
- and to establish a pattern of IgA levels in wild mice, and in lab mice.

## Chapter 2 – Materials and Methods

### 2.1. Experimental Design

**Single Pulse Disturbance Event.** A mouse model deficient in the Crohn's Disease risk gene, NOD2, was used to investigate the role of this innate immune receptor for microbial resilience after a catastrophic perturbation. We treat C57BL/6J (WT) and NOD2 (KO) mice for two weeks with broad-spectrum antibiotics composed of ampicillin (1 g/L), vancomycin (500 mg/L), neomycin (1 g/L), and metronidazole (1 g/L) (Sigma Aldrich)<sup>127</sup> and followed fecal microbiota composition for 10 weeks (Figure 7A). Using 16S rRNA phylogenomic analysis (V3-V4 region) and ITS1 and viral sequencing, we determined the community composition of the gut bacterial, fungal, and viral communities, respectively. Additionally we assessed the occurrence of selected known antibiotic resistance genes using qPCR.

**Intestinal Microenvironment Transfer (IMEnT): Sterile Fecal Transfer.** Five patients, each with symptomatic chronic-relapsing *Clostridium difficile* infection (CDI) were administered a single intestinal microenvironment transfer (IMEnT) with sterile stool filtrate, as opposed to a fecal microbiota transfer (FMT). Composition of the bacterial and viral communities were determined from the donors, the sterile filtrates, and the patients. Patient fecal samples were collected prior to the transfer, 1 week after, and 6 weeks after. Additionally, proteome analysis was also performed. Patient characteristics are summarized in Appendix 3 Table S1.

**Intestinal Secretory Immunoglobulin A (SIgA) Levels.** Additionally, the study aimed to establish a pattern of IgA levels in different murine lines, and if differences are observed, to also compare IgA levels to wild mice to study further variations. Fecal IgA levels from a population of wild *M. m. domesticus* was collected from the area of Espelette, France. Interestingly, IgA levels, and determinants thereof, still remain undetermined in most murine lines and wild mice.

## 2.2. Mice

All animal experiments were approved by ethical committees of respective institutes, and conducted according to local guidelines and regulations. A single Nod2-deficient male mouse was crossed to a C57Bl/6J female to obtain heterozygous offspring. Heterozygous mice (F1) were then used to generate WT and NOD2 KO breeder pairs (F2). Male offspring of the next two generations were used and maintained in single cages under specific-pathogen free (SPF) conditions for the experiment. At the onset of the study (Fig. 1A; day 0), mice were approximately 52 weeks old. We treated C57BL/6J WT and NOD2 KO mice for two weeks with broad-spectrum antibiotics composed of ampicillin (1 g/L), vancomycin (500 mg/L), neomycin (1 g/L), and metronidazole (1 g/L) (Sigma Aldrich)<sup>127</sup>. Fecal pellets were collected immediately from mice throughout the 86 days and stored at -80 °C until needed. Mice were monitored and weighed regularly, and sacrificed at the conclusion of the study. Organ and tissue samples were collected and stored at -80°C for future use.

## 2.3. Bacteriome

**16S DNA profiling.** Fecal pellets were used to investigate the bacterial community. DNA was isolated using the PowerSoil DNA Isolation Kit (MoBio) according to the manufacturer's directions. Individual amplicons were tagged with specific multiplex identifier (MID) barcodes and pooled for library construction before sequencing. The 16S rRNA gene variable region V3-V4 was amplified and sequenced on an Illumina MiSeq 2x150 bp platform at the Institute for Clinical Molecular Biology of Christian-Albrechts University of Kiel, Germany.

**16S Statistical Analysis.** Sequencing reads were initially processed for quality control and downstream analysis using Mothur<sup>140</sup>. The V3-V4 contigs with size  $\leq 450$ , homopolymer count

=6, and zero ambiguities with mean quality score  $\geq 25$ , were considered for further alignment with SILVA reference database. The sequences not aligning to the target region of 16S rRNA gene were discarded from analysis. Chimeric sequences were detected using the Chimera.Uchime algorithms and were removed from the analysis. Sequence classification was done using the RDP taxonomic database (released May 2015; 10,244 bacterial and 435 archaeal 16S rRNA gene) using the k-Nearest neighbor algorithm (cutoff=60). Reads showing matches with eukaryotic, chloroplast or mitochondrial sequences were excluded from analysis. A standard cut-off of minimum of 1190 reads per sample was used to eliminate sampling bias and uneven depth of coverage. Following this, the sub-sampled dataset was used to compute a distance matrix for assigning sequences into operational taxonomic units (OTU) by a 97% similarity cut-off.

Beta diversity ( $\beta$ -diversity) estimation for distance based methods Bray Curtis and Jaccard metrics and statistical analysis of dissimilarity was studied with Adonis/PERMANOVA using Vegan package in R V.3.2.5<sup>141</sup>. Alpha diversity ( $\alpha$ -diversity) estimation for diversity and richness based methods Shannon and Chao1 index was performed using in-house scripts in R V.3.2.5<sup>141</sup>. Paired Wilcoxon test was performed for time wise analysis and non-parametric Mann-Whitney test was performed for genotype comparison using Graphpad 5.0. To determine the proportional abundance of the top 16 OTUs present, which covered an average of 90% of the microbial population, we employed the generalized estimating equation (GEE) model<sup>142</sup>. The significant level of abundance changes in selected OTUs at different time points (days) compared to the baseline (day 0), was calculated. The correlation structure was settled as exchangeable.

## 2.4. Mycobiome

**Fungal ITS1 rRNA profiling.** Isolated DNA, as described above, was used to investigate the mycobiome. PCR amplification was carried out in two steps. The ITS1-F(F) (5' *CTTGGTCATTTAGAGGAAGTAA* 3')<sup>143</sup> and ITS2(R) (5' *GCTGCGTTCATTCGATGC* 3')<sup>144</sup> primers were used to amplify the ITS1 region of the fungal rRNA region. The 25 µL PCR mixture contained 12.5 µL Master Mix (Phusion HotStart Flex 2X Master Mix, NewEngland Biolabs), 1 µL of each primer (1.25 µM), 7.75 µL PCR-clean water, 0.75 µL DMSO, and 2 µL of DNA template. Reactions were held at 94°C for 2 min, with amplification proceeding for 40 cycles, with 1 cycle consisting of 94°C for 15 s, 55°C for 30 s, and 72°C for 45 s; a final extension was performed for 10 min at 72°C. The second amplification was performed for each sample to contain a linker sequence, a sample specific index, and an Illumina adapter. The 25 µL PCR mixture contained 12.5 µL Master Mix (Phusion HotStart, Flex 2X Master Mix, NewEngland Biolabs), 0.5 µL of each primer (2.25 µM), 8.75 µL PCR-clean water, 0.75 µL DMSO, and 2 µL of first-round product. Reactions were held at 94°C for 2 min, with amplification proceeding for 20 cycles, with 1 cycle consisting of 94°C for 15 s, 55°C for 30 s, and 72°C for 45 s; a final extension was performed for 10 min at 72°C. Prior to pooling samples, aliquots of each amplified product were electrophoretically separated in a 1.5% LE agarose (Biozym) stained with SYBR Safe Gel Stain (ThermoFisher) and visualized under UV illumination. Molecular weight ladders were included in each run (100 bp DNA Ladder, Invitrogen). Paired-end sequencing (2x300 bp) was performed on an Illumina MiSeq sequencer at the Institute for Clinical Molecular Biology of Christian-Albrechts University of Kiel, Germany.

**ITS1 Statistical Analysis.** Paired-end sequencing (2x300 bp) on an Illumina MiSeq sequencer resulted in 7990874 pairs of reads. Demultiplexing of the raw sequencing data was processed using the package `sabre` V.1.00 (<https://github.com/najoshi/sabre>) using the paired-end setting. The PIPITS pipeline was used to process paired-end reads for fungal community analysis<sup>145</sup>. Read-pairs were joined on the overlapping regions of sequences with PEAR<sup>146</sup>. Assembled reads were then quality filtered with `FASTQ_QUALITY_FILTER` (FASTX-Toolkit) (Hannon, <http://hannonlab.cshl.edu>). Files were then converted into FASTA format with `FASTQ_TO_FASTA` (FASTX-Toolkit). The highly variable ITS1 subregion was extracted from sequences using the software `ITSx` V.1.0.11<sup>131</sup>. Of the 7849824 input sequences, 7334632 contained an ITS1 subregion. ITS1 sequences were clustered into operational taxonomic units (OTUs) with `VSEARCH` (Rognes, <https://github.com/torognes/vsearch/>) at 97% sequence similarity, and chimera detection and removal was performed using the UNITE UCHIME reference data set (<http://unite.ut.ee/repository.php>). Representative sequences were assigned taxonomic classification with the RDP Classifier against the UNITE fungal ITS reference dataset<sup>147</sup> from which an OTU abundance table was generated with a confidence threshold of 97% sequence identity. 7244071 reads were used to generate the OTU table. Three samples in the WT at day 14 were discarded due to poor quality and low number of reads.

## 2.5. Virome

### 2.5.1. NOD2 Virome

**Sample Processing.** Two fecal pellets per sample were resuspended in 15 mL PBS buffer containing 0.01 M sodium sulfide and 10 mM EDTA for 30 min on ice. Samples were centrifuged twice at low speed (ThermoScientific Heraeus Multifuge 3SR) at 4°C for 30 min to

remove bacteria and contaminating plant material. The resulting supernatants were sterile filtered and ultracentrifuged at 22,000 x rmp (Beckman SW41 rotor) at 4°C for 2 hrs. Viral pellets were then resuspended in 200 µL Tris buffer (50 mM Tris, 5 mM CaCl<sub>2</sub>, 1.5 mM MgCl<sub>2</sub>, pH 8.0), from which 5 µL sub-samples of isolated viruses were collected for morphological characterization by negative staining in 2% (w/v) aqueous uranyl acetate and visualized by transmission electron microscopy (TEM) (Technai Bio TWIN) at 80 kV with a magnification of 40,000-100,000. To the samples, 2 µL benzonase was added and incubated at 37°C for 2 hrs to remove remaining nucleic acid contamination.

To extract viral DNA and RNA, 22 µL of a 0.1 volume of 2M Tris-HCl (pH 8.5)/0.2 M EDTA, 10 µL of 0.5 M EDTA, and 268 µL of formamide were added to the sample and incubated at RT for 30 min. Subsequently, 1 µL of glycogen, and 1024 µL of ethanol were added, and samples were mixed gently and incubated overnight at RT. The next morning, samples were centrifuged at 12,000 x g at 4°C for 20 min, washed with 70% ethanol, and resuspended in 100 µL of TE buffer and 1 µL of mercaptoethanol, after which 10 µL of 10% SDS and 3 µL of Proteinase K were added and incubated for 20 min at 37°C and 15 min at 56°C. Then, 400 µL of DNA extraction buffer CTAB (100 mM Tris pH 8.0, 1.4 M NaCl, 20 mM EDTA, 2% CTAB) and 1 µL mercaptoethanol were added and samples were incubated at 56°C for 15 min. To the resulting supernatant, an equal volume of chloroform:isoamylalcohol (24:1) was added, and samples were centrifuged at 13,000 x g for 5 min. The supernatant was collected, to which 1 µL of glycogen, 10 µL mercaptoethanol, and a 0.7 volume of isopropanol were added and incubated overnight at -20°C. The next morning, samples were centrifuges at 13,000 x g at 4°C for 20 min, after which the supernatants were collected, washed with 500 µL of 70% ethanol, and stored at -80°C.

Following extraction of VLPs, ethanol was removed from samples and pellets were air-dried and resuspended in 20  $\mu$ L of RNase free filtered water. Amplification was performed using a modified Complete Whole Transcriptome Amplification Kit (WTA2) (Sigma-Aldrich) as described previously<sup>137</sup>. PCR products were then purified using the GenElute PCR Clean-Up Kit (Sigma-Aldrich). Samples were stored overnight at -20°C prior to library construction.

**Library Construction.** Libraries were generated as described previously<sup>137</sup> using the NexteraXT kit (Illumina). After quantification, normalized pools of all samples were sequenced on an Illumina MiSeq using the 2 x 150bp sequencing kit (Illumina).

**Viral community composition.** Nextera XT adapters and sequence reads were trimmed from Illumina paired-end reads (2x150 bp) using Trimmomatic V.0.36<sup>148</sup>. Trimmed and quality controlled reads of all samples were cross assembled using SPAdes V.3.1.10<sup>149</sup> to generate a reference viral metagenome. Contigs with a minimum length of 1000 bp and a minimum total read coverage of 10 were selected and used as OTUs representing the mice viral community. Reads from each sample were then mapped separately against representative viral OTUs using Bowtie2<sup>150</sup> and SAM tools<sup>151</sup>. The normalized coverage of each OTU was used as a proxy for the relative abundance of each virus per sample<sup>152</sup>. Using blastn against the NCBI nucleotide database and tblastx against the NCBI refseq viral database<sup>153</sup>, OTUs of the reference viral metagenome were classified with an e-value cut off at  $10^{-5}$ . Verification of results from tblastx prediction was performed using PHASTER<sup>154</sup> by analyzing the protein composition of the nucleotide sequence<sup>155</sup>. Viral community composition was analyzed using PRIMER V.7<sup>156,157</sup>, and abundance data was standardized and log+1 transformed. Estimation of similarity between all samples was calculated by Bray-Curtis similarity and multidimensional scaling analysis

(MDS), and pairwise comparison of viral community composition between different treatment groups and time points was analyzed using a similarity test (ANOSIM global test)<sup>157</sup>.

### **2.5.2. Efficacy of Sterile Fecal Transfer**

**Sample Processing.** Virus-like particle purification and DNA extraction were performed as described previously<sup>33</sup>, with some modifications. Fecal samples were resuspended in 0.5 mL SM buffer and centrifuged four times at 2,500 x *g* for 10 min, with the resulting supernatant passed sequentially through a 0.45- $\mu$ m and a 0.22- $\mu$ m pore diameter filter (Whatman/GE Healthcare; Munich, Germany). Each sample was treated twice with 0.2 volumes of chloroform and centrifuged at 5,000 x *g* for 10 min at 4°C, and the aqueous phase was treated with 1 U of DNase I and 70  $\mu$ L of 10 X DNase buffer (Sigma-Aldrich; Taufkirchen, Germany), followed by incubation at 65°C for 10 min.

To extract viral DNA, 0.1 volumes of 2 M Tris-HCl/0.2 M EDTA, 1 volume of formamide, 1  $\mu$ L of glycogen, and 100  $\mu$ L of a 0.5 M EDTA solution were added per 1 mL of sample. The sample was subsequently washed with 2 volumes of ethanol and centrifuged for 20 min at 13,800 x *g* at room temperature. The resulting pellet was then washed twice with 70% ethanol and resuspended in TE buffer followed by 10% SDS and 20 mg/mL solution of Proteinase K (Sigma-Aldrich) for 1 h at 37°C, after which 5 M NaCl and 10% cetyltrimethylammonium bromide/0.7 M NaCl were added. Samples were then mixed with an equal volume of chloroform and centrifuged at 13,800 x *g* for 10 min at room temperature. To the resulting supernatant, an equal volume of phenol:chloroform:isoamyl alcohol (25:24:1) was added, and the mixture was centrifuged at 13,800 x *g* for 10 min. The aqueous phase was recovered, an equal volume of chloroform was added and the resulting mixture was centrifuged again at 13,800 x *g* for 10 min, prior to adding 1  $\mu$ L of glycogen with 0.7 volumes of isopropanol

and incubating overnight at 4°C. The next morning, samples were centrifuged at 13,800 x g for 30 min at 4°C, washed with 1 mL of 70% ethanol, air-dried, and resuspended in 50 µL of deionized water.

**Library Construction.** Libraries were generated using the TruSeq Nano DNA kit (Illumina) according to the manufacturer's instructions. After quantification, normalized pools of all samples were sequenced on an Illumina MiSeq using the 2x150 bp sequencing kit (Illumina).

**Quality control, metagenomic assembly, and taxonomic assignment.** Truseq adaptors and low quality reads (length <55) were filtered from the Illumina paired-end reads (2x150 bp) using Trimmomatic V.0.33<sup>148</sup>. These pre-processed paired-end reads were assembled using SPAdes V.3.7.0 assembler, by implementing “meta” function with wide k-mer range (21 to 77)<sup>158</sup>. The assembled contigs were classified at various taxonomical levels using the kmer based approach as described previously<sup>159</sup>. In brief, reads were subdivided into complete sets of 31 bp length-overlapping sequences (k-mers). Subsequently, these k-mers were compared against a large database (40,000 whole microbial genomes in the One Codex reference database) that contains information on known k-mers unique to specific taxonomic groups such as different bacterial clades or viruses. After comparison, each contig was assigned to a closely matched specific clade. Each sample was then summarized as a group of signature sequences depicting the presence of specific groups of organisms<sup>159</sup>.

## 2.6. Metagenome

**Profiling.** A total of 40 samples were selected, representative of 5 KO and 5 WT individual mice from days 0, 14, 21, and 71. DNA was isolated using the PowerSoil DNA Isolation Kit (MoBio) and 15 µL of each sample was loaded into the appropriate well of a 96 well plate. Samples were

sent for library construction and pooled using the NexteraXT kit (Illumina) and sequenced on an Illumina HiSeq 2500 platform with a coverage of 2x150 bp.

## 2.7. Correlational Analysis

**Relationship between fungal and bacterial community.** Correlations were calculated between fungi and bacteria at the genus level using Pearson's correlation with a cutoff mean >0.5% relative abundance (20 x 16 correlations respectively). Differences in genotype over time were then compared for each combination from fungi and bacteria (ttest,  $P < 0.05$ ), of which 36 were found to be significant. Heatmaps were generated by R package (*pheatmap*).

**Relationships between viral and bacterial community.** To investigate whether changes in the bacterial community composition were associated to the viral community, RELATE was used in PRIMER V.7<sup>160</sup>, and the analysis was based on the relative abundance of viral and bacterial OTUs. Predictor variables were then fitted to the relative abundances of bacterial OTUs using distance-based linear modeling (DistLM) to investigate the variability in the viral community that could be explained by changes in the bacterial community, or vice versa. Bacterial community datasets were  $\log(x+1)$  transformed and analyzed against the viral community composition with  $R^2$  selection criteria using the forward selection procedure, and distance-based redundancy analysis was used to visualize results<sup>161,162</sup>.

## 2.8. Antibiotic Resistance Genes

**Detection of antibiotic resistance genes using real time qPCR.** To identify antibiotic resistance genes present in the bacterial community, 11 antibiotic resistance predesigned TaqMan® real-time PCR gene expression assays were selected to target genes conferring

vancomycin resistance in *Enterococcus*, and AmpC, extended-spectrum beta-lactamases (ESBL) and carbapenem resistance in Enterobacteriaceae (as listed in Appendix 2 Table S1A). Microfluidic real time PCR was employed according to the manufacturer's guidelines (Thermo Fisher Scientific, USA) using the Fast Universal PCR Master Mix (Applied Biosystems) and carried out on a ViiA 7 system (Thermo Fisher Scientific, USA).

Isolated fecal DNA samples from WT and KO mice were taken from days 0, 14, 21, and 71 for a total of 84 samples per TaqMan® PCR assay (10 KO and 11 WT per time point). A 10 µL reaction was prepared with 4.5 µL of TaqMan® Fast Universal PCR Master Mix (Applied Biosystems), 0.5 µL TaqMan® assay, 1 µL of template (stool sample), and 4 µL PCR water, respectively. Assays were run on a ViiA 7 real-time PCR system (Applied Biosystems) using the following cycling conditions: 95°C for 20 s, followed by 45 cycles of 95°C for 1 s and 60°C for 20 s. All assays were performed in duplicate with a positive control of bacterial DNA and a negative control of water. Real-time PCR data was analyzed with ViiA™ 7 RUO software, employing the ddCT-method as previously published<sup>163</sup>. A Fisher's exact test was performed to determine nonrandom significant associations between the genotypes, days, and antibiotics.

## 2.9. Screening Immunoglobulin A Levels

**Profiling.** Fecal pellets were collected from wild mice (from the area of Espelette, France) and lab mice (NOD2 (KO), C57BL/6J, Atg161condVilCre (KO and fl/fl)). All samples were stored at -80°C. Fecal pellets were weighed and reconstituted in an equal volume of PBS containing 0.1% Tween 20 (Thermo Scientific) and vortexed for 20 min, or until homogenized. Samples were then centrifuged for 10 min at 12,000 rpm at 4°C. The clear supernatants were collected and stored at -20°C until further analysis. Serum from NOD2 (KO) and C57BL/6J from the Single

Pulse Disturbance Event study was also collected from day 86, diluted 20,000 fold, and stored at -20°C. IgA levels were estimated from the supernatants and diluted serum using the Mouse IgA ELISA Kit (Thermo Scientific) according to the manufacturer's directions. All samples were performed in duplicate.

**Wild Mice (Espelette, France).** A total of 46 wild mice were selected for detection of IgA levels from feces (Appendix 4 Table S1). Samples were composed of three different genotypes, which included C57BL/6J, RIISJ, and heterozygotes. Samples were further grouped by geography (farm), haplotype (mitochondrial D-loop), haplogroup (grouping of the haplotypes)<sup>164</sup>, population (analysis of 18 neutral microsatellite markers with STRUCTURE), and gender. Histology was performed for all mice of the ileum, cecum, proximal colon, and distal colon (Appendix 4 Table S2).

**Lab Mice.** Fecal pellets were collected from 27 Atg161condVilCre (KO and fl/fl) mice housed at the ZTH. Samples were grouped according to gender and age in weeks.

## 2.10. Screening Calprotectin Levels

**Profiling.** Fecal pellets were collected from C57BL/6J (WT) and NOD2 (KO) mice from the Single Pulse Disturbance Event study. All samples were stored at -80°C. Fecal pellets were weighed and reconstituted in an equal volume of PBS containing 0.1% Tween 20 (Thermo Scientific) and vortexed for 20 min, or until homogenized. Samples were then centrifuged for 10 min at 12,000 rpm at 4 °C. The clear supernatants were collected and stored at -20°C until further analysis. Murine S100A8/S100A9 (calprotectin) was determined by ELISA (Immundiagnostik AG; Bensheim, Germany) according to the manufacturer's directions. All samples were prepared in duplicate.

## Chapter 3 – Results

### 3.1. NOD2

#### 3.1.1. Bacteriome

##### WT mice recover earlier from antibiotic induced weight loss.

Mice were administered a combination of broad-spectrum antibiotics for two weeks, and then allowed to recover for 72 days (Fig. 7A). Antibiotics were shown to have the desired effect of causing a perturbation, where both C57BL/6J WT and NOD2 KO mice lost substantial weight (between 20-25%), indicative of gut dysbiosis (Fig. 7B). Rapid weight loss occurred from the

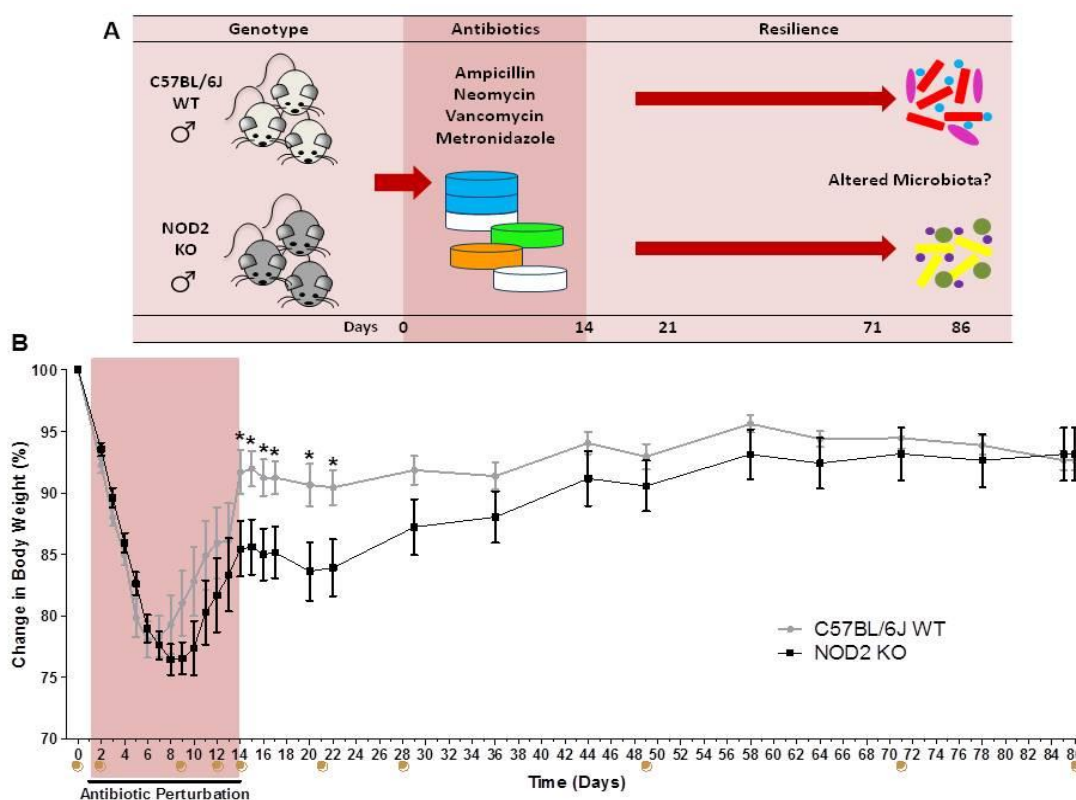


**Figure 7.** (A) Schematic of experimental design showing administration of broad-spectrum antibiotics to C57BL/6J (WT) and NOD2 KO for two weeks. Mice were subsequently monitored for a total of 86 days to investigate genotype effect on the gut microbial resilience. (B) Percent change in body weight of C57BL/6J (WT) (gray circles) and NOD2 KO (black squares) mice. Percent body weight was calculated based on initial body weight at the time of the experiment. Each point represents the means  $\pm$  SEM values (WT = 11, and KO = 10). Brown circles indicate days where fecal pellets were collected. The asterisks (\*) indicates significance difference ( $P < 0.05$ ) between the two genotypes and was evaluated using the Student's *t*-test.

onset of antibiotic administration to day 6 in the WT and day 8 in the KO, after which an increase in weight was observed despite antibiotic administration occurring until day 14. Interestingly, the greatest difference in weight between the genotypes was observed from days 14-22 ( $P < 0.05$ ). Additionally, weight recovery occurred earlier and faster in WT mice compared to KO; however, both showed the same weight recovery by day 86. A significant difference ( $P = 0.02$ ) in liver weight was observed between genotypes at the conclusion of the study (day 86), with a greater liver weight observed in KO mice compared to WT (Appendix 2 Fig. S1A). Yet, no significant difference was observed in spleen and caecum weight, or colon length, though some individual variation was observed (Appendix 2 Fig. S1B, C, D).

**Loss of NOD2 causes delayed recovery in bacterial gut community composition post antibiotic perturbation.**

Beta diversity analysis of principle coordinate analysis (PCoA) distinguished clustering based on genotype and day, where a phenotypic variation between the two genotypes could be observed (Fig. 8; Appendix 2 Fig. S2A-D). In the WT, a clear clustering based on the day was observed (Fig. 8A), where day 14 and day 21 clustered in distinguished groups. Interestingly, days 71 and 86 clustered more closely with day 0 (pre-treatment), demonstrating community resilience.

On the other hand, although day 14 clustered as a separate distinguished group in the KO, the community at day 86 is distributed across days 71, 21, and 0, demonstrating a delayed recovery (Fig. 8B). Comparing both genotypes together, no difference was observed at day 0 (pre-treatment) (Fig. 8C). However, resilience was only observed in the WT, where day 86 clustered together with day 0, whereas in the KO a wide distribution occurred. Interestingly, outliers were present in both genotypes, and some were found to have an antibiotic resistance gene, indicating

that antibiotic resistance genes present in the bacterial community can significantly alter the composition (Fig. 8A and B, Appendix 2 Fig. S2, and Table S1B).

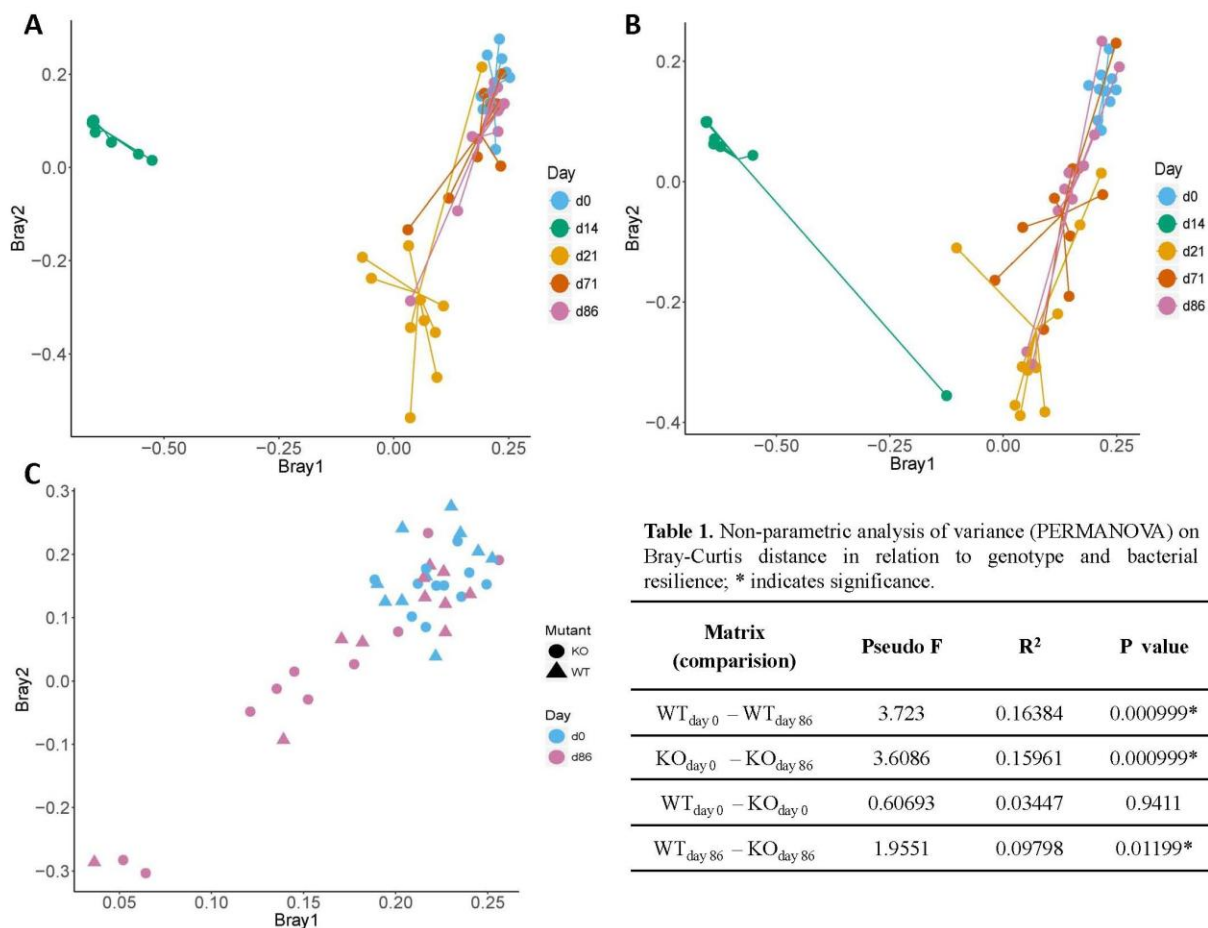


**Figure 8.** Principle coordinate analysis (PCoA) of bacteria where Bray1 explains 19.4% and Bray2 explains 7.1% in (A) WT across time (days 0, 14, 21, 71, 86) and (B) KO across time (days 0, 14, 21, 71, 86), and (C) KO (circles) and WT (triangles) at day 0 (blue) and day 86 (pink).

### Perturbation leads to genotype variation of gut bacterial community composition.

The most abundant phyla in both genotypes were Bacteroidetes and Firmicutes (Appendix 2 Fig. S3A, B). An increase in the relative abundance of Proteobacteria was observed during the antibiotic period. Verrucomicrobia was found to have a greater relative abundance after the antibiotic period in both WT and KO (Day 21), despite a general recovery of community diversity from day 14. In the KO, Verrucomicrobia and Tenericutes also had a greater abundance

at day 28. Importantly, resilience was observed in both WT and KO, where community composition at day 86 more closely resembled community composition at day 0 (pre-treatment), though differences in relative abundance are still observable, particularly in the KO.

The most abundant genera in both genotypes were *Barnesiella* and unclassified *Lachnospiraceae* (Fig. 9A, B). During the antibiotic period (days 1-14) *Escherichia/Shigella* were the most abundant. A variety of temporal patterns was evident in both genotypes, such as taxa that became more abundant after antibiotic treatment and throughout the remainder of the study (e.g. *Parabacteroides*), and those that became less abundant (e.g. *Bacteroides*; Figure 9D).

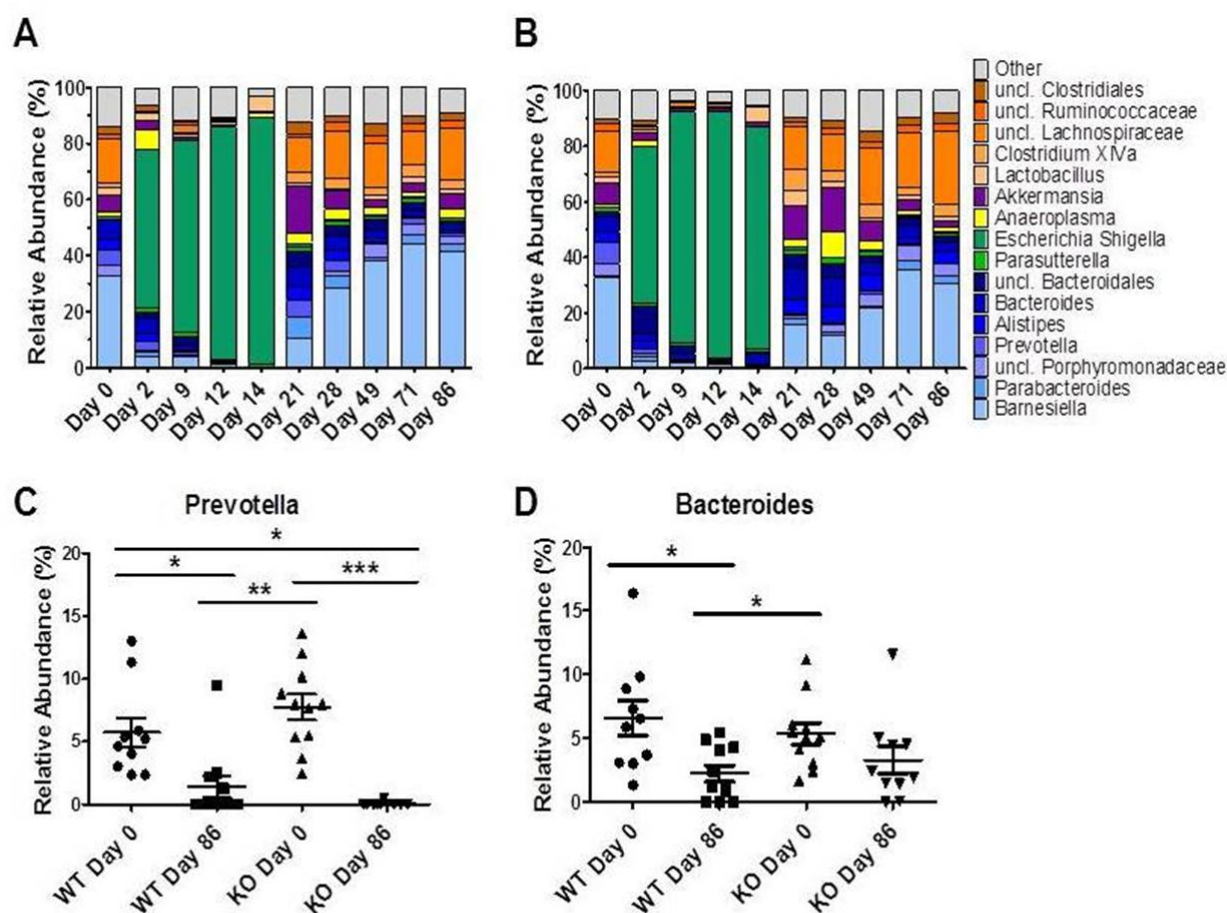


**Figure 9.** Relative abundance (%) of 16S bacterial community composition across all time points in (A) WT and (B) KO at phylum level. (C) Relative abundance (%) of *Prevotella* in WT and KO at day 0 (pretreatment) and day 86, and (D) Relative abundance (%) of *Bacteroides* in WT and KO at day 0 (pretreatment) and day 86. Each point represents an individual. \*P < 0.05, \*\*P < 0.005, \*\*\*P < 0.0005.

Differences between the genotypes were also observed, where immediately post antibiotic treatment (days 21 and 28) there was an increase in the relative abundance in *Akkermansia*, *Anaeroplasma*, and *Lactobacillus* in the KO, whereas in the WT an increase in abundance was observed in *Prevotella* and *Parabacteroides*.

As observed in the PCoA plots, the antibiotic period had a marked effect on the bacterial gut community. At the phylum level, day 14 was significantly different in both the WT and KO when compared to day 0 and day 86 (Appendix 2 Fig. S3A, B), where Bacteroidetes, Proteobacteria, and Firmicutes had the greatest observable differences. Interestingly, the phylum Verrucomicrobia showed a significant difference in the KO from day 0 to day 86, where a decrease in the relative abundance occurred (Appendix 2 Fig. S3B). On the other hand, no difference was observed in the WT from day 0 to day 86, demonstrating recovery. Thus, Verrucomicrobia demonstrated resilience in the WT, whereas the KO does not exhibit recovery as seen in the WT. At the genus level, the dominant genera in both genotypes were *Barnesiella* and *uncl. Lachnospiraceae*. Interestingly, *Escherichia/Shigella* were dominant during the antibiotic period. Significant differences were also observed in both genotypes in *Prevotella* and *Bacteroides*, which all decreased in relative abundance from day 0 to day 86 (Fig. 9C, D).

We then identified 11 bacterial taxa indicating resilience and generated a heatmap based on the relative abundance for longitudinal comparisons among individual samples (Fig. 10). The resulting bacterial taxa were further grouped into three categories where groups I and II demonstrated significant resilience only in the WT, whereas group III showed significant resilience independent of genotype.

To further investigate the longitudinal (day) effect in the bacterial community composition overall (irrespective of genotype) compared to the WT at day 0 (pre-treatment), we

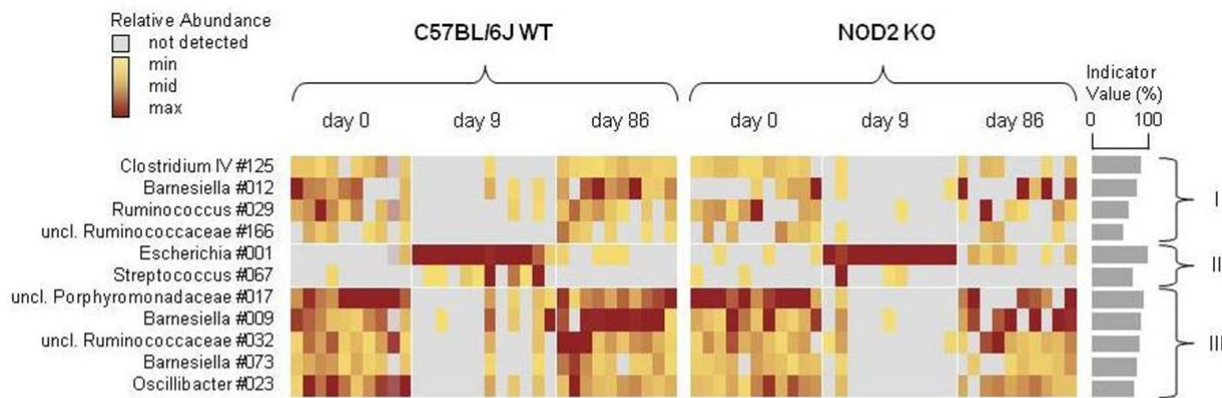


**Figure 10.** Bacterial taxa indicating resilience. Bacterial taxa were selected by their ability to display resilience (indicator species for day 0 vs. day 9 and day 9 vs. day 86, while not being an indicator for day 0 vs. day 86). The resulting 11 bacterial indicator taxa were grouped into three categories: I) bacterial taxa showing significant resilience only in C57BL/6J (WT) animals while being depleted after antibiotic treatment and regained at day 86; II) bacterial taxa showing significant resilience only in C57BL/6J (WT) animals while being enriched after antibiotic treatment and regained at day 86 and III) bacterial taxa showing significant resilience independent of genotype while being depleted after antibiotic treatment and regained at day 86. Relative abundances are color coded, each column represents an individual animal, and indicator values shown are obtained from C57BL/6J (WT) animals during the resilience period (day 9 to day 86). Data for days 2, 12, 14, 21, 28, 49 and 71 were omitted from the figure for visualization purposes.

generated a correlation matrix known as the generalized estimating equations (GEE) (Appendix 2 Table S2 and S3). At the phylum level, significance was observed in most taxa from day 2 to day 14 compared to WT day 0. However, only Verrucomicrobia was significantly different at day 86. At the genus level, *Prevotella* and *Clostridium XIVa* were significantly different at all time points compared to WT day 0. These results demonstrate a strong day effect, particularly in *Barnesiella* and *Escherichia/Shigella*, with numerous additional significant differences observed across all taxa, compared to day 0.

### 3.1.2. Antibiotic Resistance Genes

#### Presence of antibiotic resistance genes in bacterial community significantly increased after antibiotics.

Resistance genes commonly associated to the bacterial phylum Proteobacteria (AmpC resistance) and Firmicutes (vancomycin resistance) were detected in both WT and KO individual mice (Appendix 2 Table S1A, B). As expected, vanC2-C3-2 and vanA2 genes were present; however,

ACT/MIR and BIL/LAT/CMY genes were also identified, although they were not associated to the antibiotics used in this study. Furthermore, a significant difference was observed where most resistance genes were present at the conclusion of the antibiotic administration (day 14) and subsequent days (days 21 and 71) compared to prior (day 0) ( $P = 0,048$ ; Appendix 2 Table S1B). However, a difference associated with genotype was not observed with the current set of genes (Appendix 2 Table S1A, B).

### **3.1.3. Mycobiome**

#### **Long-term changes detected in fungal gut community.**

To further elucidate the role of NOD2 on the gut microbiome, we performed ITS1 sequencing to assess the composition of the fungal gut community. Beta diversity analysis of PCoA based on genus-level abundances revealed clustering according to genotype and day (Fig. 11A, B). In both genotypes, day 0 (pre-treatment) clustered together, though the distribution was large. In the KO, day 14 also clustered together (Fig. 11B). On the other hand, a more distinct clustering occurred in the WT according to the day, compared to the KO (Fig. 11A), with day 71 also clustering largely together. Comparing both genotypes together, clustering of samples occurred according to day rather than genotype, although some heterogeneity was observed (Fig. 11C).

Importantly, contrary to the WT bacterial community, PCoA plots demonstrated a lack of resilience in fungal community of both genotypes. These observations were further supported using PCoA based on Jaccard (Appendix 2 Fig. S4A-C).

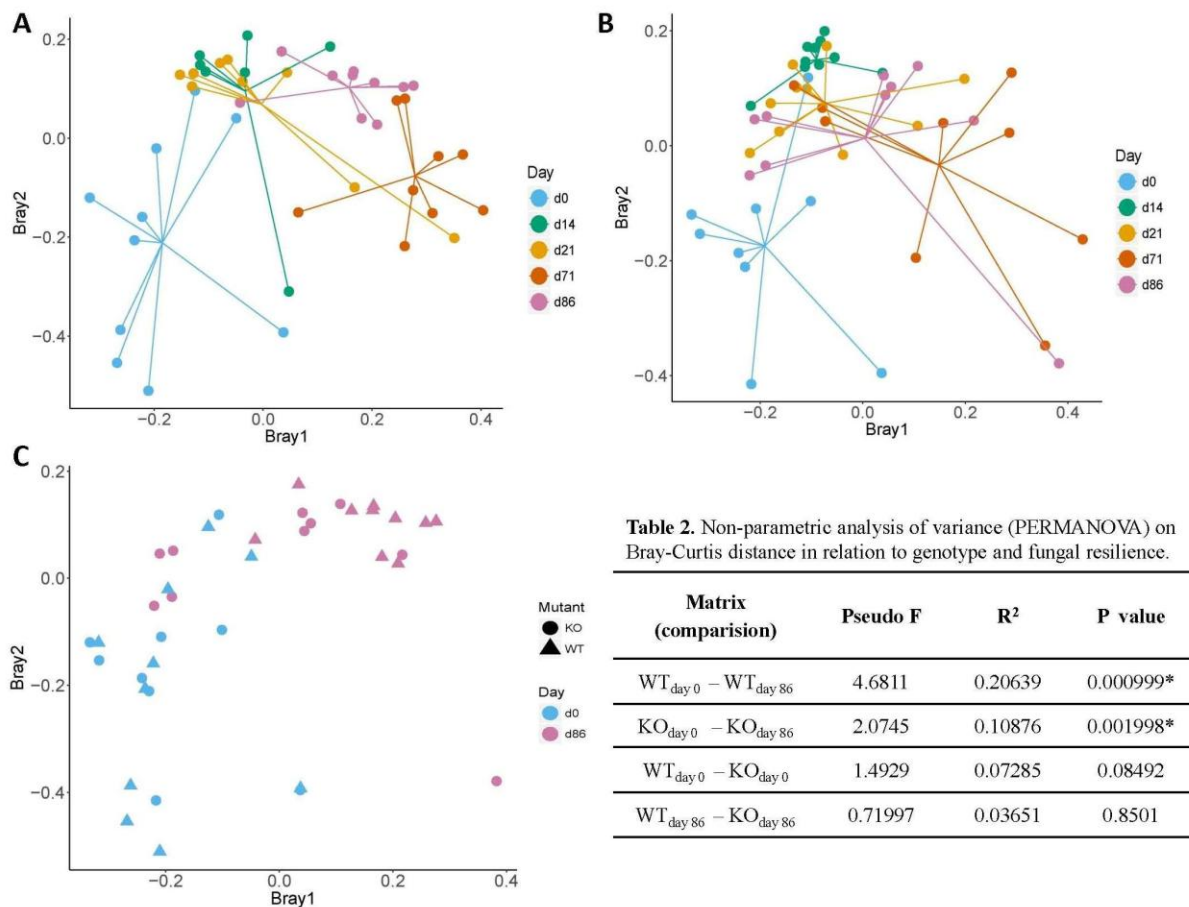


**Figure 11.** Principle coordinate analysis (PCoA) of fungi where Bray1 explains 10.47% and Bray2 explains 8.39% in (A) WT across time, (B) KO across time, and (C) WT (triangles) and KO (circles) at day 0 (pre-treatment) (pink) and day 86 (blue).

### Antibiotic perturbation significantly increased fungal gut diversity.

The dominant phylum in both genotypes was Ascomycota and Basidiomycota (Appendix 2 Figure S5A). Compared to day 0, a greater relative abundance of unidentified fungi was seen from day 14 to day 86, with the greatest abundance occurring in the WT at day 86. Furthermore, as supported by PCoA analysis, resilience at day 86 was not observed in either genotype, although the KO appeared to be more resilient compared to the WT. Comparable to the phylum level bacterial community composition, both genotypes were similar to one another; however, a greater variation in community composition was observed at the class level, highlighting the importance of investigating lower taxonomic levels (Figure S5B). Furthermore, as seen in the

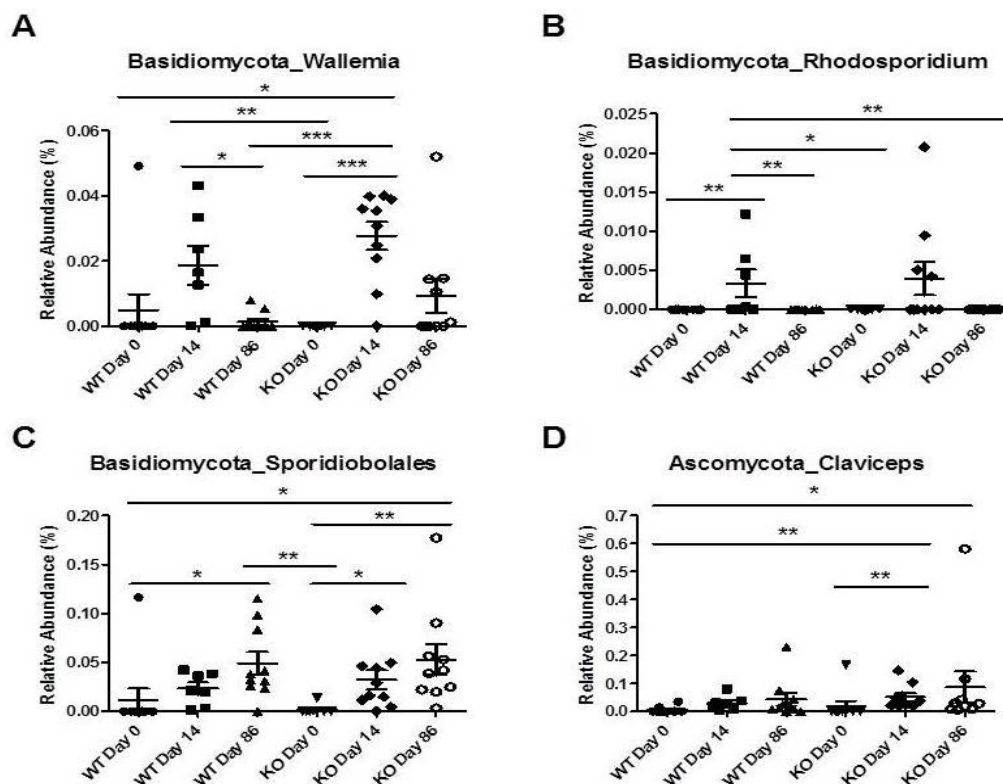


**Figure 12.** Fungal relative abundance (%) at genus level in WT and KO across time (days 0, 14, 86) in (A) *Wallemia*, (B) *Rhodosporidium*, (C) *Sporidiobolales*, and (D) *Claviceps*. \* $P < 0.05$ , \*\* $P < 0.005$ , \*\*\* $P < 0.0005$ .

bacterial community, numerous significant shifts occurred in the mycobiome at the class level after antibiotic administration (Fig. 12 and 13).

A high level of individual variation was observed in the mycobiome samples of both genotypes at both the phylum and class level (Fig. 13 and Appendix 2 Fig. S6). Remarkably, the community shifted towards a uniform distribution of greater diversity across all individuals in both genotypes at day 14 (Fig. 13 and Appendix 2 Fig. S6). Community shifts continued to occur for the duration of the study, with individuals remaining largely varied from day 0 (pre-treatment) (Fig. 6A and Appendix 2 Fig. S6).

To characterize fungal Alpha diversity across time, the Shannon diversity index was used. Strikingly, fungal diversity significantly increased in both genotypes at all time points, compared

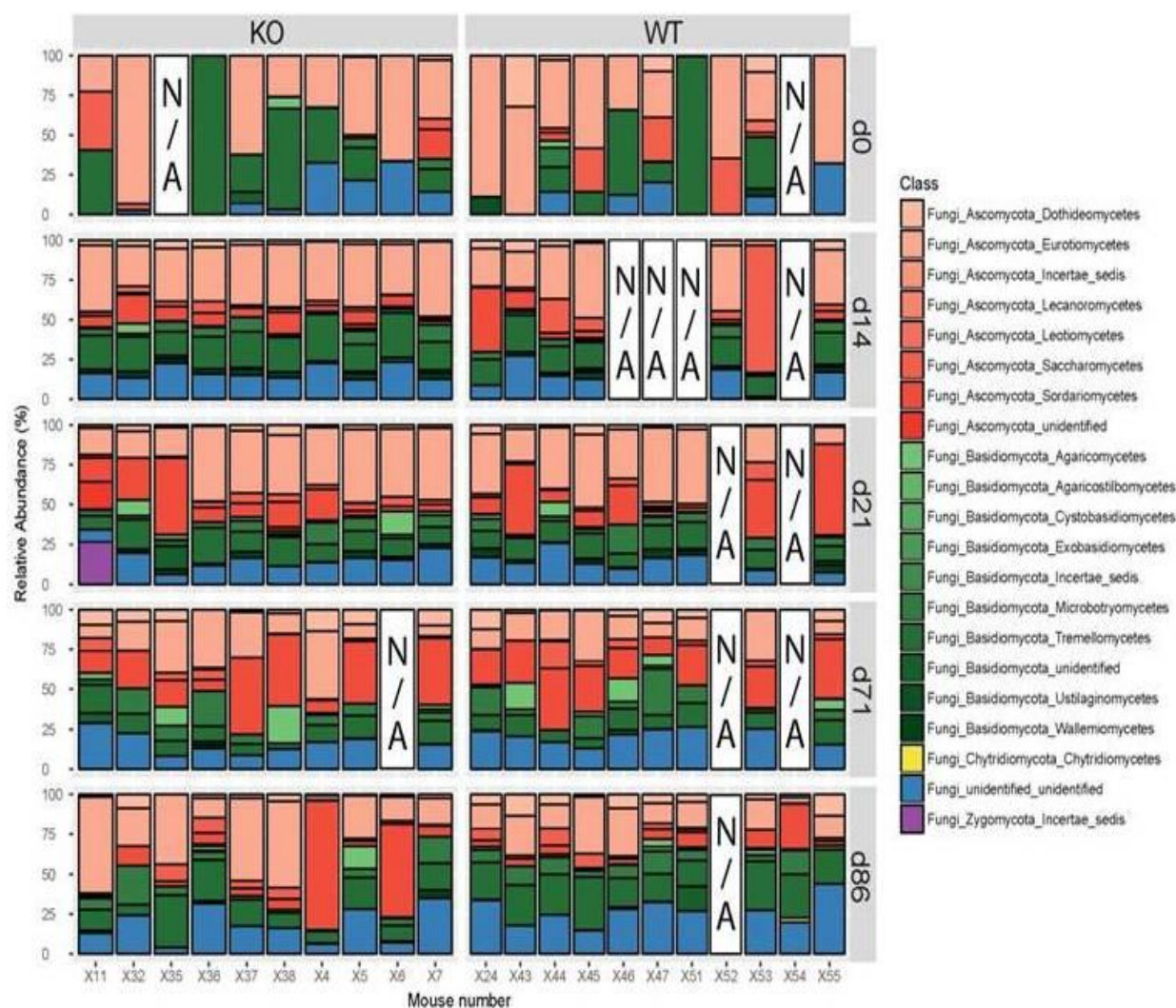


**Figure 13.** ITS1 fungal relative abundance (%) of class level community composition in all KO and WT individuals across time (days). N/A indicates sample unavailable.

to day 0 (Fig. 14). Furthermore, at the conclusion of the study, the KO was found to significantly decrease in fungal diversity compared to the WT (Fig. 14;  $P = 0.028$ ). We then examined the richness of the fungal community using the Chao1 index (Fig. S4D). Similar to the Shannon diversity observations, all time points were significantly different compared to day 0, with species richness significantly increased in both genotypes after antibiotics. However, while Shannon diversity remained high after day 21, Chao1 richness decreased, particularly in the KO.

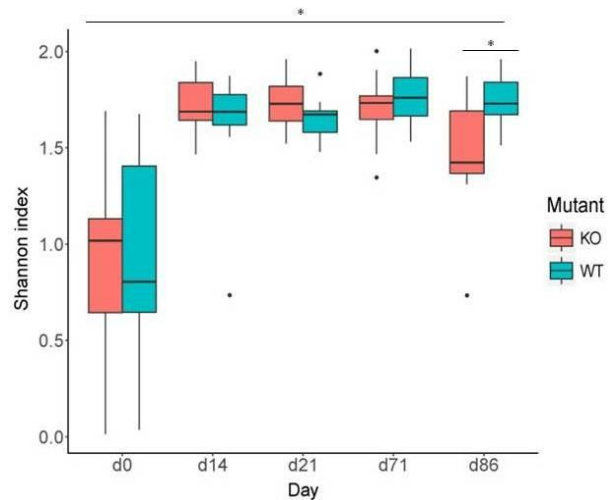


**Figure 14.** Shannon index demonstrating fungal diversity at class level in WT and KO across time (days). All time points in both genotypes are significant when compared to day 0 (pre-treatment) (Student's t-test,  $P < 0.05$ ). At day 86, comparing KO and WT is significant (Student's t-test,  $P = 0.028$ ).

### 3.1.4. Bacterial-Fungal Correlations

We then investigated whether specific bacterial taxa were associated to members of the mycobiome across all time points according to genotype (Fig. 15A, B). We hypothesized that the differences in the genotypes would indicate possible key interactions between bacteria and fungi, which would have been altered from the antibiotic perturbation and may have played a role in the delayed recovery in the KO. A higher number of significant correlations were observed in the KO compared to the WT (Fig. 15A, B). Interestingly, a pattern across bacterial taxa was observed only in the KO, where the bacterial genera *Barnesiella*, *Prevotella*, *Escherichia/Shigella*, and *uncl. Ruminococcaceae* had at least three significant correlations to specific fungi. In particular, 9 significant correlations were observed between *Prevotella* and different fungal taxa, indicating that *Prevotella* may play a role in the delayed recovery of the NOD2 KO. However, a pattern was observed in both genotypes when fungi with at least three significant correlations to specific bacteria were considered. In the WT these were Hypocreales, Sporidiobolales, and Wallemiaceae, while in the KO these were Clavicipitaceae, Xylariales and Wallemiaceae.

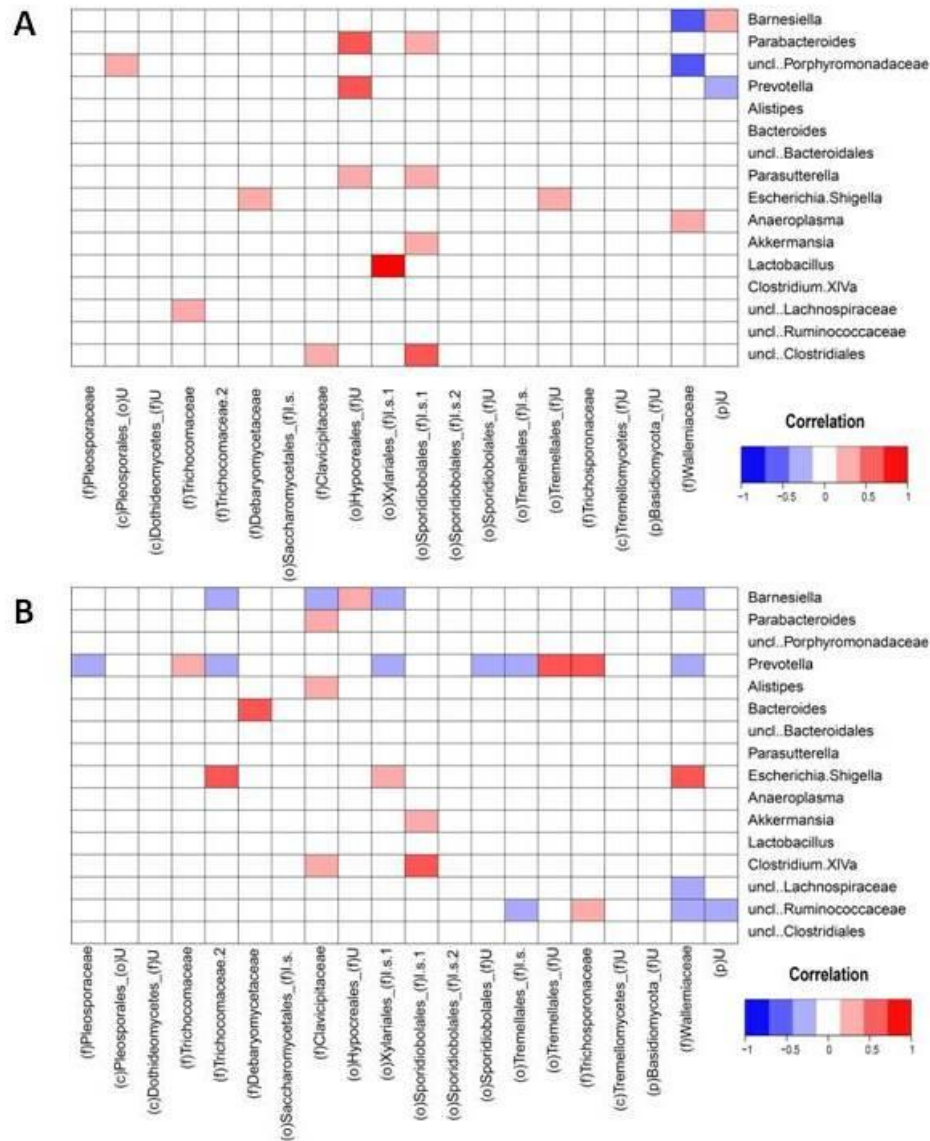


**Figure 15.** Significant correlation (Student's t-test,  $P < 0.05$ ) between fungi and bacteria in (A) WT and (B) KO. Blue to red gradient indicates negative and positive correlations. White spaces indicate no correlations observed.

Interestingly, Wallemiaceae was shared in both genotypes, yet was only significantly positively correlated to *E. Shigella* in the KO. When comparing the relative abundance of both genotypes, it is apparent that *Wallemia* increases at day 14 compared to day 0; however, from day 14 to day 86, a significant decrease was observed in the WT, but not in the KO where large individual variation was present (Fig. 12A).

### 3.1.5. Calprotectin Levels

Calprotectin levels were measured to determine the presence of inflammation in the gut. Interestingly, despite the greater relative abundance of the bacterial pathogen *Escherichia/Shigella* from day 0 to day 14 (Fig. 9A, B), calprotectin was not induced in the NOD2 KO at day 14 (Fig. 16). Moreover, compared to day 0 and prior to the antibiotic perturbation, a decrease in

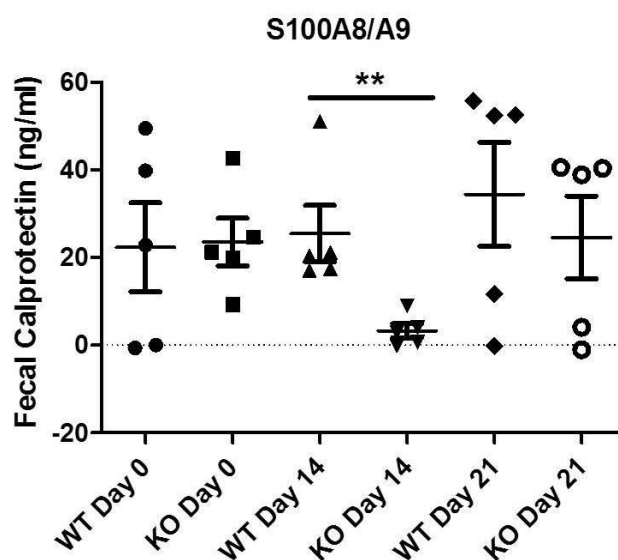


**Figure 16.** Fecal calprotectin levels in WT and NOD2 KO mice (n = 5) across time (days) compared to day 0 (pre-treatment) (Student's t-test, \*\*P < 0.005).

calprotectin was observed at this time in the NOD2 KO, whereas the WT at day 14 remained stable. After cessation of antibiotics (day 22), elevated levels of calprotectin was observed in both genotypes. However, large variations exist between individuals.

### 3.1.6. Virome

#### Presence of virus-like particles.

The presence of virus-like particles from fecal samples were observed by transmission electron microscopy, which revealed morphologically distinct isolates (Fig. 17)<sup>165</sup>. RNA virus-like particles with morphological similarity to the Peste des Petits Ruminants (PPR) virus or the

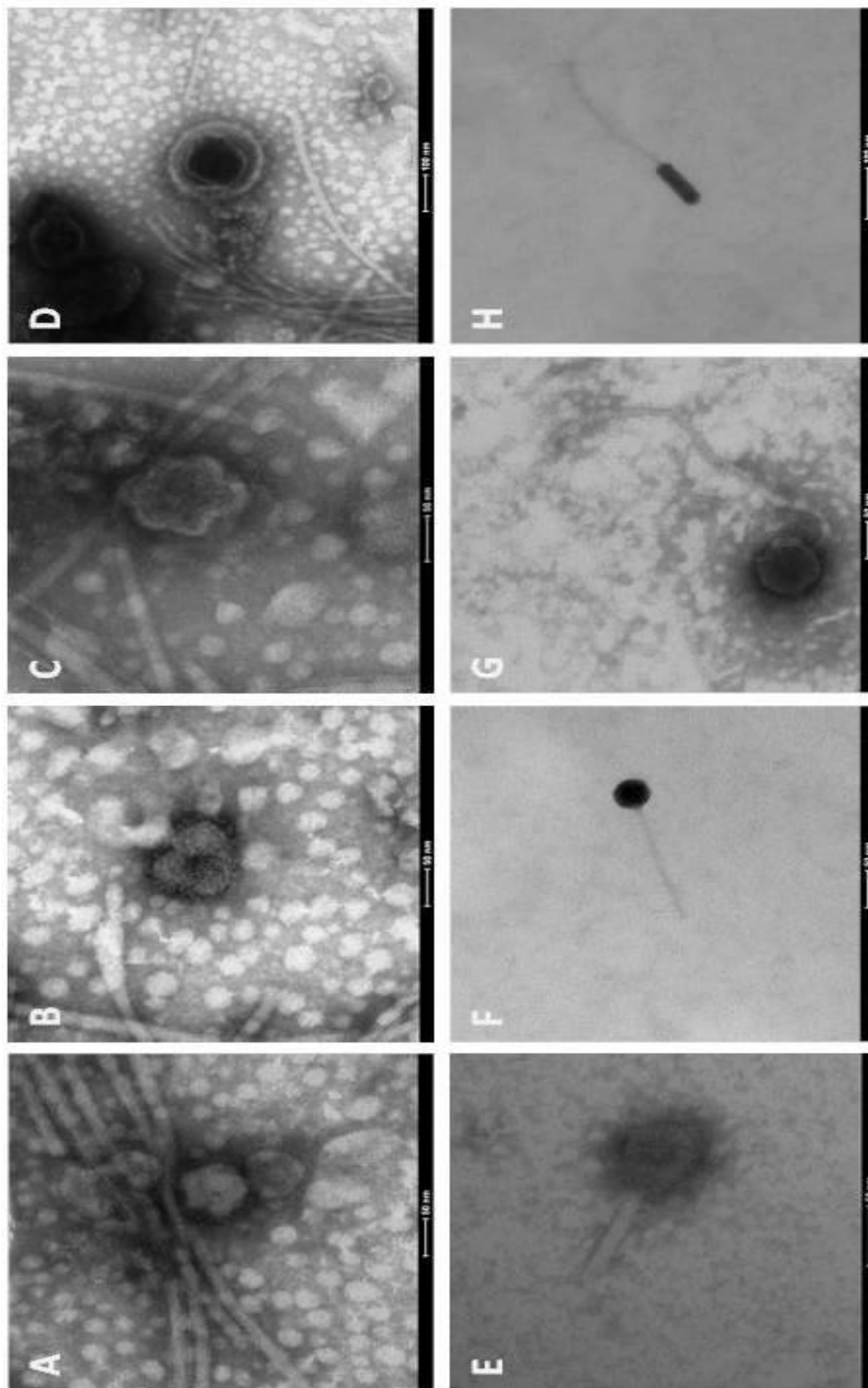


**Figure 17.** Transmission electron micrographs of purified virus-like-particles (VLPs) from WT and NOD2 KO mouse fecal samples stained with 2% aqueous uranyl acetate. (A-C) RNA virus-like particles with morphological similarity to PPR virus or MMTV virus, (D) encapsulated virus, and (E-F) bacteriophages Myoviridae (G-H) bacteriophage Siphoviridae.

Murine Mammary Tumor virus (MMTV) were observed (Fig. 17A-C), in addition to viruses with morphological similarity to filamentous bacteriophages, as defined by a filament-like shape. However, these filamentous bacteriophages are likely the tails of other phages which have cleaved off during sample processing (Fig. 17A-D). Numerous diverse bacteriophages were present (Fig. 17E-H), and were distinguished by the structure of a head, or capsid, and in some cases a tail, although other phage morphologies exist beyond this structure (i.e. without a tail). The Myoviridae family morphology was present, with an icosahedral (20 sides) head and a rigid tail (Fig. 17E-F). The structure of a phage lambda ( $\lambda$ ) displaying the Siphoviridae family morphology, which commonly infects *E. coli*, was also identified (Fig. 17G-H). The protein head of capsid is icosahedral (Fig. 17G) and elongated (Fig. 17H), containing the nucleic acid. The head is joined to a tail possessing a long thin tail fiber at its end (for host recognition). The tails are composed of a hollow tube, through which the nucleic acid passes into the host during infection.

#### **Delayed resilience in viral gut community composition post antibiotic perturbation.**

Multidimensional scaling analysis of the viral community based on viral OTU level demonstrated a clear clustering based on day (Fig. 18). Samples at day 0, prior to treatment, clustered together and underwent large changes shifting after 14 days of antibiotic treatment. Post antibiotic treatment, the viral community shifted from day 14, and appeared to recover by clustering more closely with day 0, with the average dissimilarity declining from a maximum dissimilarity at day 14 from day 0 (SIMPER analysis = 62,37) to day 86 from day 0 (SIMPER analysis = 53.2) (Fig. 18 and Appendix 2 Tables S5-8). However, the community at day 86 did not fully recover and remained significantly different from day 0 (Fig. 18 and Appendix 2 Tables S4 and S8). Additionally, no significant difference between the genotypes was detected.

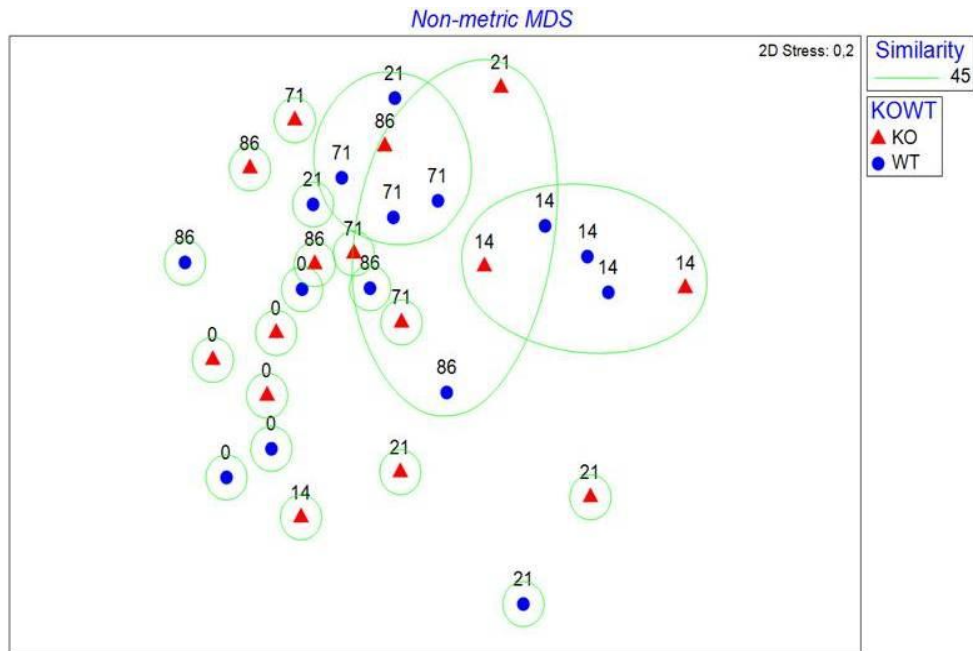


**Figure 18.** Non-metric multidimensional scaling analysis (MDS) of the viral species level community composition based on Bray-Curtis.

### High inter-individual variation of viral community composition.

Sequencing revealed mice fecal viromes were composed of approximately 56% bacteriophages, 3% eukaryotic viruses, and 41% currently unclassified sequences. Bacteriophages were highly diverse (Fig. 17E-H, and 18), with dominant phages belonging to the genera *Cellulophaga*, *Parabacteroides*, *Lactobacillus*, *Enterococcus*, *Bacillus*, and to the species *Enterobacteria Phage cdt1* (Fig. 19). Large changes within the community composition occurred during antibiotic treatment (day 14), which was distinct from pre-treatment at day 0 (Fig. 18 and 19). Interestingly, an increase in relative abundance in *Phage cdt1* was observed in most samples at this time (day 14), after which the relative abundance of this species was reduced (Fig. 19). Moreover, *Phage cdt1* was not detected at day 0. During the recovery phase, the viral community composition demonstrated huge variability within one week of antibiotic cessation (Fig. 19). However, no clear pattern of recovery over time or between the genotypes could be observed, with high inter-individual variation of viral community composition present throughout.

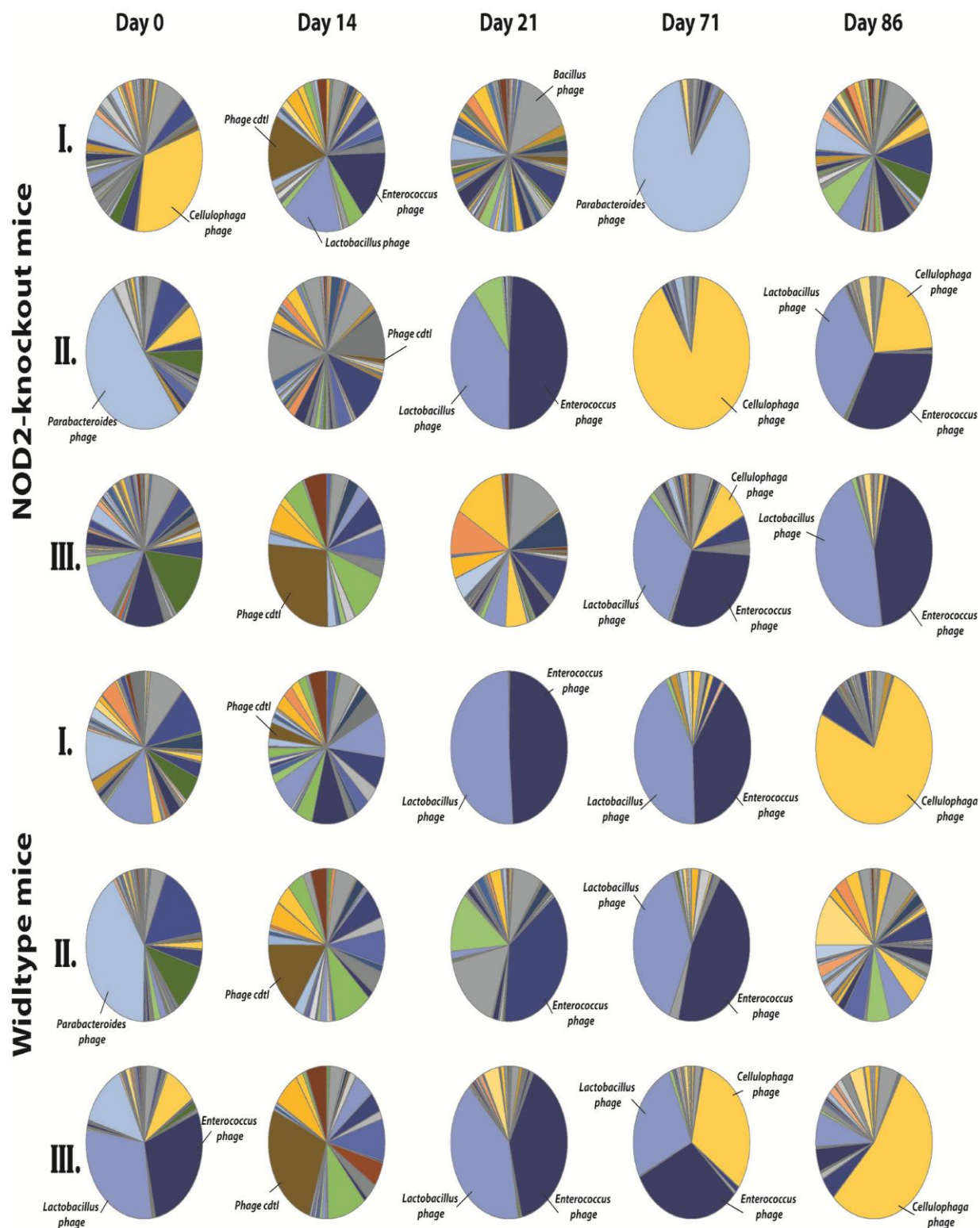


**Figure 19.** Viral community composition in WT and NOD2 KO mice. Roman numerals represent an individual mouse across time (in days). Bacteriophages were grouped by their corresponding bacterial host based on tblastx hit of the RefSeq viral sequence database.



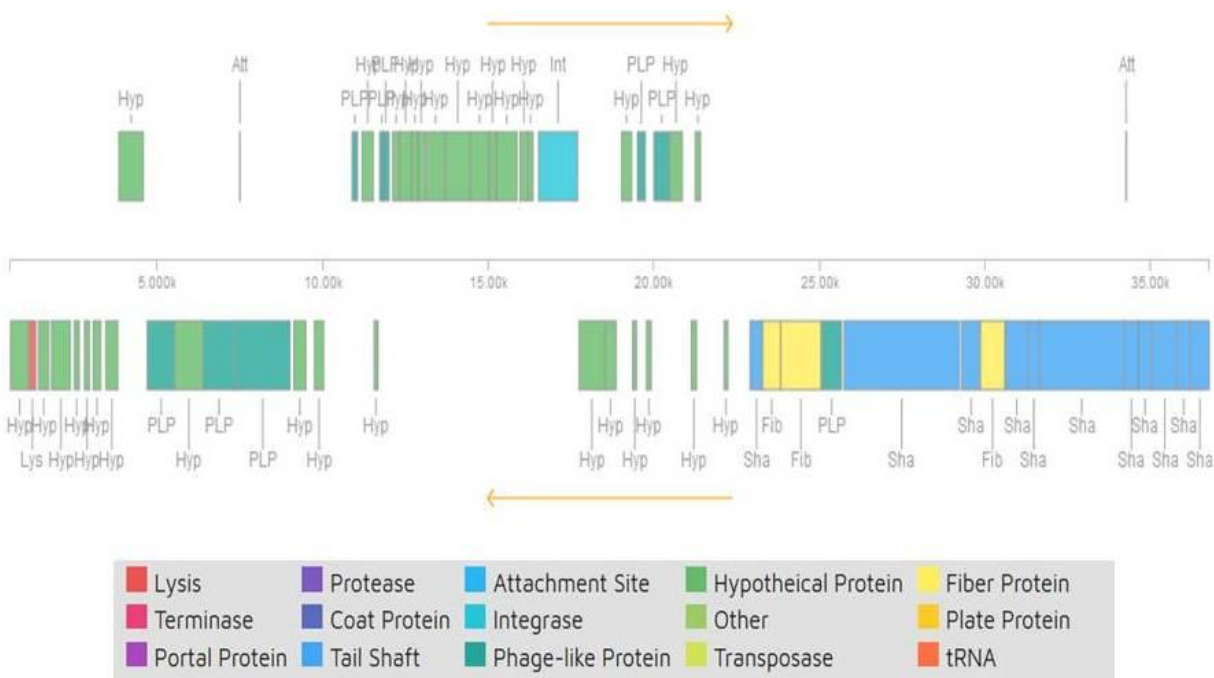


**Figure 21.** Genome of phage with high mapping similarity to *Phage cdt1*.

dissimilarity between day 0 and day 14 was explained by the higher relative abundance of *Phage cdt1* and the relative reduction of *Parabacterioides* phages and *Bacteroides* phages (Fig. 19 and Appendix 2 Table S5).

To verify the result of the tblastx prediction for *Phage cdt1*, the protein composition of the nucleotide sequence was analyzed to determine whether the sequence encoded components typical for a virus. *Phage cdt1* was confirmed to contain the typical properties of a bacteriophage, with a head (i.e. lysis and phage-like protein) and tail structure (i.e. tail shaft) (Fig. 21).

### 3.2. Fecal Transfer

A similar setup to study the dynamics of the viral community was used in a human case study. Fecal microbiota transplantation (FMT) is a highly effective therapy for RCDI; however, the therapy is also accompanied by potentially incalculable long-term risks largely due to the

transfer of living microorganisms. To reduce this risk in patients with limited eligibility for FMT, a study investigating sterile fecal filtrates, rather than intact microorganisms, was performed. Stool was collected from 5 patients with symptomatic chronic-relapsing CDI and 5 donors selected by the patients. Donor stool was sterile-filtered to remove small particles and bacteria, and transferred to the patients in a single administration (perturbation) via nasojunal tube.

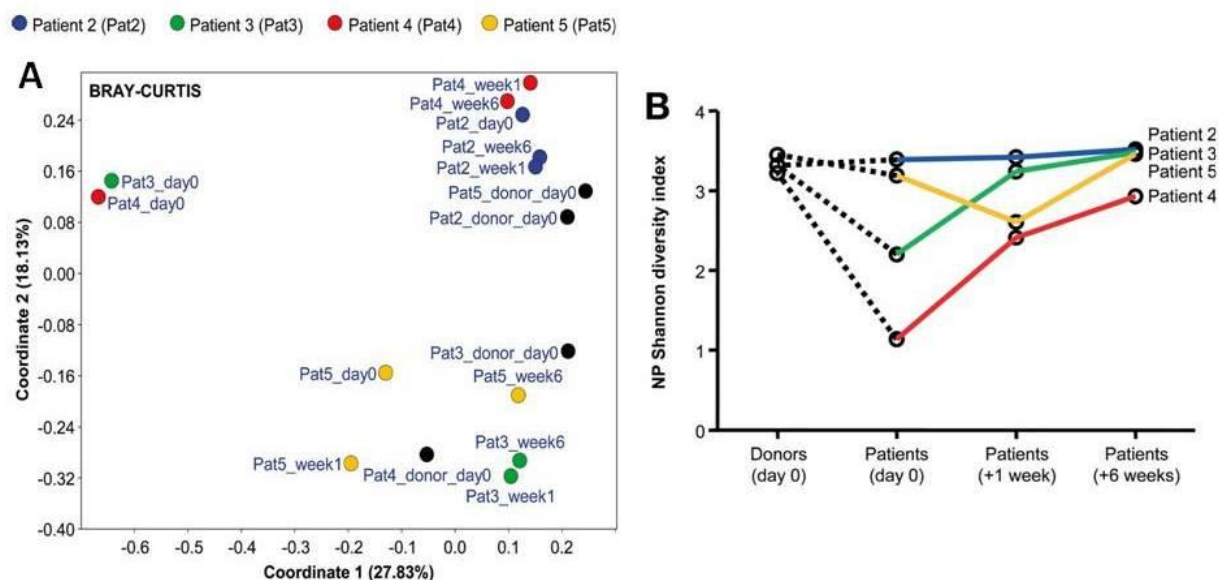


**Figure 22. (A)** Principle coordinate analysis (PCoA) of Bray-Curtis distances of the bacterial community in the donors and patients across time. **(B)** Shannon index of bacterial diversity, with patient's respective donor connected by dotted line.

Sterile fecal filtrate transfer (FFT) eliminated symptoms of CDI for at least 6 months in all five patients (Appendix 3 Table S1). Comparing patient samples from before, 1 week after, and 6 weeks after FFT demonstrated that FFT led to substantial bacterial community shifts (Fig. 22A). All patient samples after 6 weeks were found to cluster separately from their respective day 0 samples, with the greatest observable difference in patient 3 and 4 (Fig. 22A). Importantly, in contrast to conventional FMTs, FFT cannot be expected to establish a bacteriome similar to that of the donor in the respective recipient (Fig. 22A).

Shannon diversity was also found to have increased in all patients 6 weeks after FFT, with recipient samples resembling their donors more closely (Fig. 22B). However, patient 5 had

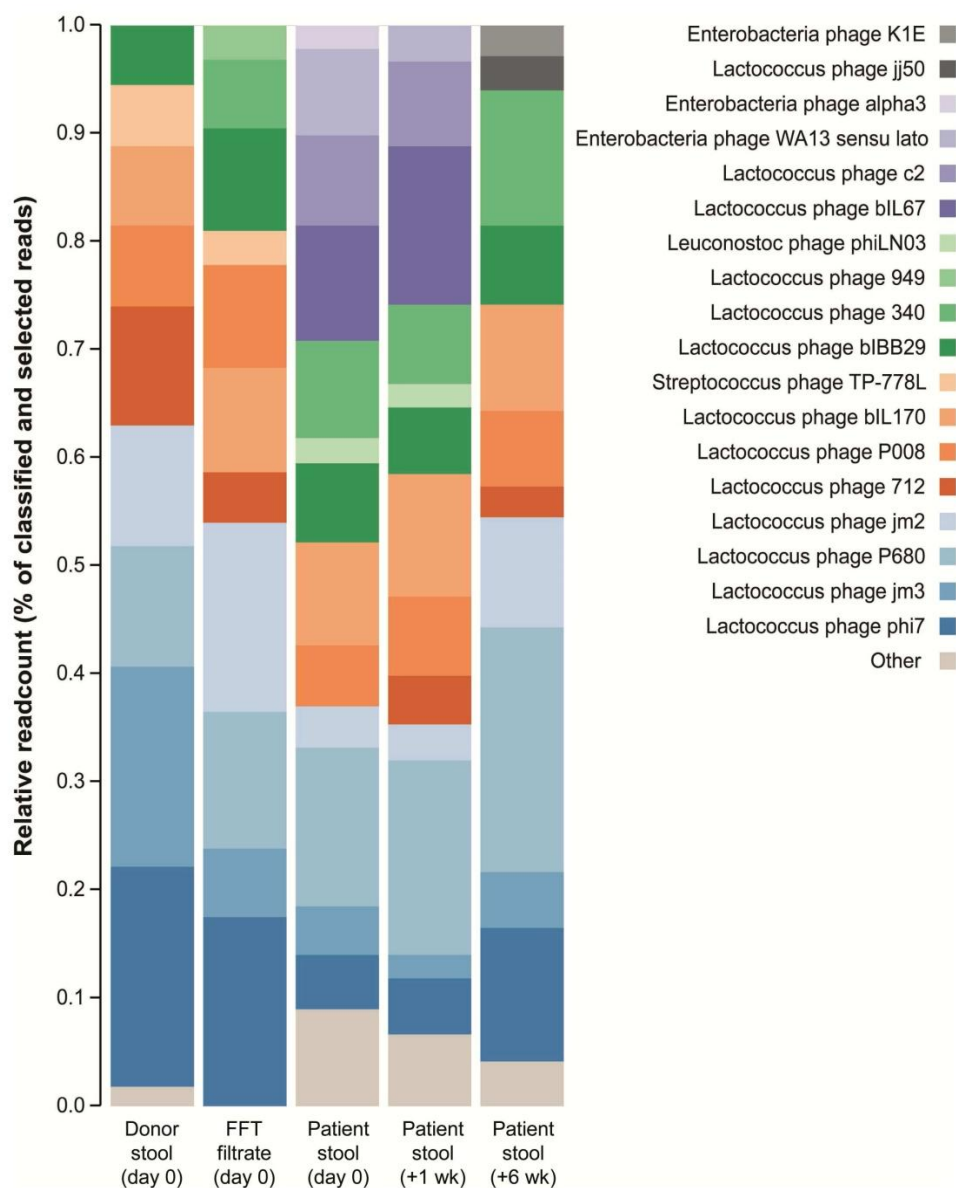


**Figure 23.** Virome composition of the donor (day 0), the FFT filtrate, and patient 4 samples before FFT treatment (day 0), and 1 and 6 weeks after treatment.

a loss of diversity 1 week after FFT, before also resembling the respective donor's level of diversity (Fig. 22B). Markedly, patient 4, which had the lowest diversity of all samples at day 0, demonstrated the largest increase in diversity in as little as 1 week.

The filtrate used for patient 4 was analyzed for virus-like particles (VLPs) and found to harbor a complex viral community primarily composed of bacteriophages (Fig. 23, patient 4). Additionally, longitudinal changes in the bacterial and viral community structures were observed in the patient's fecal samples after the sterile fecal filtrate transfer (Fig. 23 and Appendix 3 Fig. S1). Interestingly, patient 4, which had an expansion of the relative abundance Proteobacteria (attributed mostly to *Escherichia* species), had a significant community shift within 1 week after fecal filtrate transfer (FFT) (Appendix 3 Fig. S1A, B). Within the viral composition of patient 4, all samples, including those of the donor, were dominated by *Lactococcus* bacteriophages (Figure 23). Of note, immediately after FFT (patient stool day 0), an abundance of *Enterobacteria* phage was observed, which was still observable 1 week after FFT. This may in part explain the bacterial shift observed during this time. Moreover, the FFT substantially altered the virome of patient 4, and ultimately resembled that of the donor after 6 weeks (Figure 23).

### 3.3. Immunoglobulin A Levels

SIgA, or IgA, plays a key role at mucosal surfaces by binding to pathogens, and by regulating the commensal bacterial community. Moreover, low levels of IgA have been associated with an increase in gastrointestinal diseases. Yet, despite its importance, IgA levels have remained undetermined in many murine lines and wild mice. As such, fecal IgA levels were measured to determine whether a pattern of IgA levels could be established across different genotypes,

#### 3.3.1. IgA Levels in Wild Mice

In wild mice, no significant differences were observed when comparing IgA levels to gender, genotype, geography, haplogroup, population, or haplotype (Fig. 24). However, when

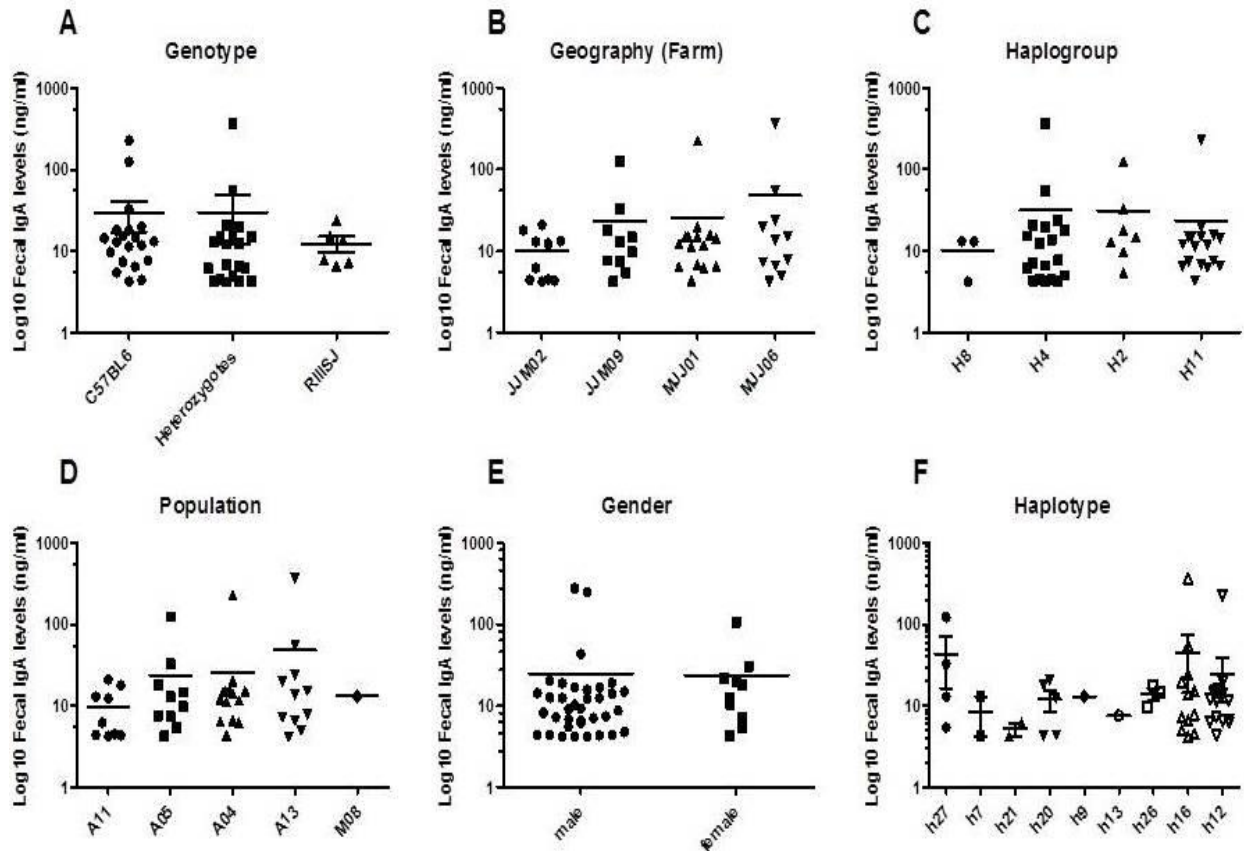


**Figure 24.** (A-F) Fecal IgA levels (ng/mL) from wild mice (in the area of Espelette, France). (C) Haplogroups were determined by the mitochondrial D-loop sequences and grouped from (F) haplotypes according to Bonhomme et al., 2011<sup>163</sup>.

comparing genotypes, heterozygotes appeared to divide into two groups of fecal IgA levels, where one group had a lower fecal IgA levels compared to the WT C57BL/6 and RIISJ genotypes (Fig. 24A). Seven different outliers with very high IgA levels were also identified. To determine whether high IgA levels were associated to gut inflammation, intestinal scores from histology were compared to all seven identified outliers (Appendix 4 Table S7A, B). Interestingly, all outliers had inflammation either in the ileum, cecum, proximal colon, or the distal colon, with most inflammation occurring in the cecum and proximal colon (Appendix 4 Table S3). However, inflammation was observed in all mice, independent of high IgA levels. Moreover, none of the mice with the highest intestinal scores were found to have high IgA.

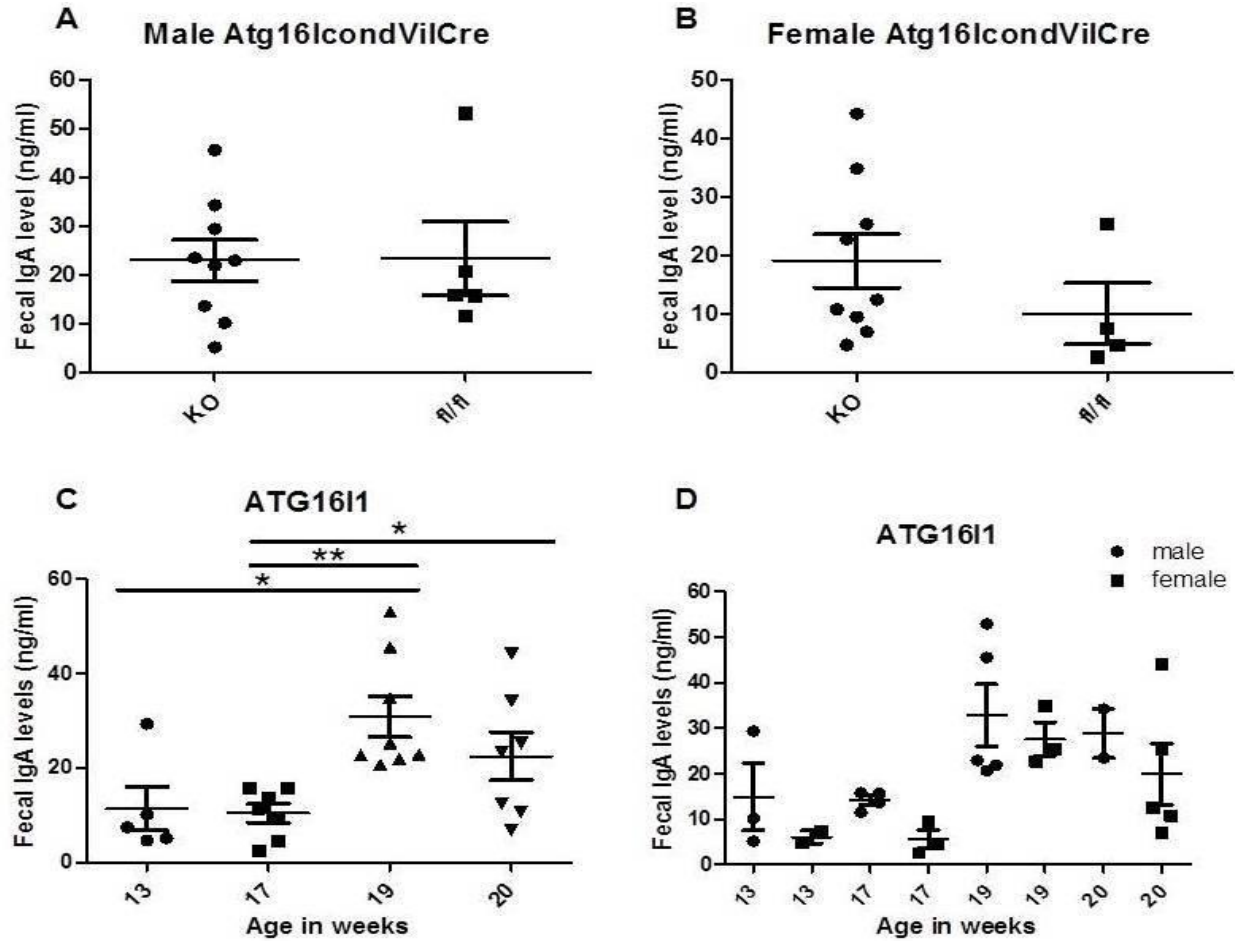


**Figure 25.** Fecal IgA levels (ng/mL) in ATG16L1 lab mice in (A) KO and fl/fl males, (B) KO and fl/fl females, and across time in weeks in (C) both genders, and (D) comparing both genders.

### 3.3.2. IgA Levels in Lab Mice

In ATG16L1 lab mice, a difference was observed between the genders, where female mice had lower fecal IgA levels compared to males (Figure 25). However, no significant difference was observed between the KO and fl/fl, or between the genders, although large individual variation was present. Interestingly, although not significant, a difference was observed between KO and fl/fl in females, which was not seen in males.

Comparing male C57BL/6 wild mice to lab mice revealed that wild mice had significantly higher fecal IgA levels (Fig. 26A,  $P=0.0023$ ). NOD2 KO mice did appear to have a higher serum IgA level compared to WT, although this difference was not significant and with large individual variation (Fig. 26B). Moreover, the mean serum IgA level in NOD2 KO was similar to the mean fecal IgA level of lab mice (Fig. 26A, B).

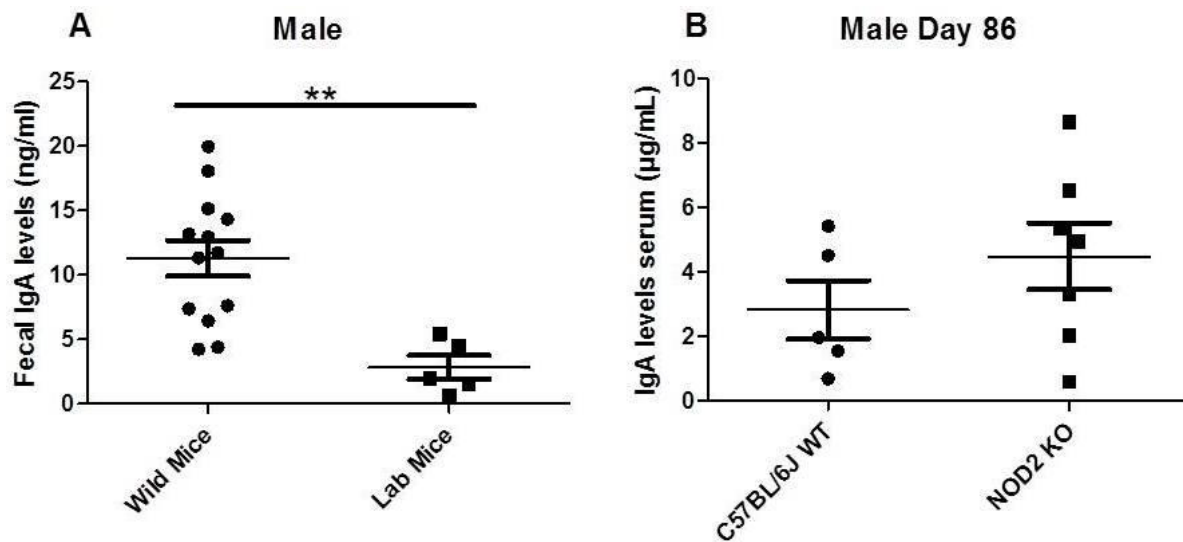


**Figure 26.** (A) Fecal IgA levels in male C57BL/6J wild mice and lab mice (t-test,  $P=0.0023$ ). (B) Serum IgA levels in male C57BL/6J and NOD2 KO mice at day 86 from the single pulse disturbance experiment.

## Chapter 4 – Discussion

### 4.1. NOD2

Here, we demonstrate a complex relationship between bacteria, fungi, and viruses in the gut, where an antibiotic perturbation creates significant community shifts, and a long-term increase in fungal diversity. We also observed an increase of antibiotic resistance genes in the gut bacteria of both genotypes. It is important to note that our study setup used targeted PCR assays, thus it is likely that more resistance genes are present, but could not be identified with the current set of assays. With the given panel of specific assays covering a number of important resistance genes; however, the observed pattern of antibiotic resistances was independent of the NOD2 deletion.

#### 4.1.1. Bacteriome

Contrary to some previous studies in mice and humans, including our own, we did neither observe an increase in Bacteroidetes at the phylum level in the KO, nor were KO and WT animals different at the  $\alpha$ -diversity level at the beginning of the experiment<sup>70,72,86,87,166–168</sup>. Several factors may serve as an explanation for these observations: (i) Three of the studies, including our own, demonstrated the strongest differences between NOD2<sup>-/-</sup> and WT communities in ileal content or in mucosal tissue samples. (ii) As our current experiment was performed in a different animal house compared to our previous study, we cannot fully exclude other complex influence factors, which are related to different standards of hygiene, food and bedding. (iii) The experiment was performed in middle-aged mice (52 weeks of age at the start of the experiment) in order to reflect a mature gut bacterial community. A previous study has shown that shifts in Bacteroidetes are an important part of the altered taxonomic composition of

the intestinal microbiota during ageing<sup>169</sup>. Thus, the effect of age may override the genotype effect.

A significant increase in the bacterial relative abundance of Proteobacteria, namely *E.coli/Shigella*, was observed during treatment. Interestingly, a significant association between the NOD2 risk allele and an increase in the relative abundance of Enterobacteriaceae has been previously reported<sup>170</sup>, with numerous studies supporting the observed increase in abundance, or even an expansion, of Proteobacteria and Enterobacteriaceae in IBD patients<sup>171–173</sup>. Notably, similar results were reported in a study where vancomycin alone was sufficient to induce these same changes<sup>174</sup>. Despite this, most NOD2 studies have been static and did not address the role of environmental perturbations<sup>172</sup>. In particular, vancomycin has been shown to cause distinct responses in the gut microbiome, promoting the expansion of Proteobacteria<sup>175–177</sup>, including Enterobacteriaceae or *E. coli*<sup>175</sup>. Vancomycin targets Gram-positive bacteria, and may have created niche availability to members of the Gram-negative phylum Proteobacteria, highlighting that antibiotics alone cause changes in the microbial community, regardless of genotype. This may be possible through antibiotic disruption of the gut microbial food web, which in turn may have led to an increase in microbiota liberated sugars, promoting the growth of opportunistic pathogens, such as members of the Enterobacteriaceae family<sup>178,179</sup>. Alternatively, the observed gut microbial shifts during the antibiotic perturbation may have also resulted from nutritional immunity, whereby the host innate defense sequesters essential nutrients from pathogens through the induction of calprotectin by neutrophils<sup>180</sup>. However, independent of genotype, *E. coli*, in addition to multiple Gram-negative bacteria, have the zinc uptake regulator/repressor Zur and a ZnuABCzinc transporter<sup>181</sup>, and thus allowing for growth in the inflamed gut<sup>180</sup>. It is tempting to speculate in such a scenario, since the bacterial shift was observed in both genotypes and

cessation of antibiotics lead to both a decrease and shift of *E.coli/Shigella*, and a partial recovery of the community by day 21. Taken together, this suggests that an observed enrichment of Enterobacteriaceae, is an important indicator of post-antibiotic dysbiosis, and is not unique to NOD2 deficiency.

Unsurprisingly, we observed a decrease in bacterial diversity in both genotypes during antibiotic administration. As seen in our results, low richness samples have often been described to be composed of, and or dominated by, Proteobacteria, including Enterobacteriaceae, compared to the high richness samples composed of Firmicutes, including Lachnospiraceae<sup>182</sup>. Studies have shown that when the resilience of a community is low, transitory changes to the structure occur, which may increase the community's susceptibility to invasion (by non-indigenous transient species), and thus cause functional changes. This change in function may be harmful if necessary for the health of the host, and in turn, may additionally lead to the colonization of (opportunistic) pathogens<sup>5</sup>. For instance, *Enterococcus faecalis* can disrupt the epithelial barrier, increasing inflammation in mice through the production of gelatinase, yet this only occurs when the host has a genetic susceptibility to inflammation (*i.e.* NOD2 deficiency)<sup>183</sup>. Moreover, in IBD, the intestinal microbiota plays a role in driving an inflammatory response<sup>109</sup>, and Enterobacteriaceae has been associated with low grade inflammation<sup>184</sup>. Hence, we expect low-grade inflammation likely occurred during the antibiotic period where an increase in Enterobacteriaceae and significant weight loss occurred (Fig. 1B and 3A,B). Intestinal inflammation may also result in an increase in intestinal permeability, leading to the translocation of microbial products, and at times translocation of viable bacteria, to extraintestinal tissues and organs, including the liver<sup>185</sup>. This may in part explain the significant

difference in liver weight between WT and KO, where KO liver weight was greater, even at the conclusion of the study, and long after antibiotic treatment.

#### **4.1.2. Mycobiome**

In mice, gut inflammation can also promote proliferation of fungi<sup>186</sup>, and overgrowth of fungi in the gut is additionally promoted through the use of antibiotics<sup>187,188</sup>. From the onset of antibiotics, we observed fungal community diversity significantly increased. Although perturbations from oral broad-spectrum antibiotics often lead to a reduction in commensal bacteria, allowing pathogen proliferation and the development of gastrointestinal inflammation<sup>178</sup>, another possibility for this observation is that loss of NOD2 leads to a faulty recognition of fungi causing certain taxa to dominate<sup>189</sup>. NOD2 is also responsible for chitin recognition, an essential component of the cell wall of all fungal pathogens, and together with the mannose receptor and TLR9, induces an anti-inflammatory response during fungal infection<sup>189</sup>. However, we observed an increase in fungal diversity in both genotypes, thus the loss of protective bacteria-bacteria interactions may be further driving this shift, where these interactions contribute to resistance against fungal infections<sup>190</sup>.

#### **4.1.3. Calprotectin Levels**

Calprotectin, a neutrophil protein, is essential for host defense against bacterial and fungal pathogens. Moreover, fecal calprotectin levels are used to evaluate the host inflammatory response in the gut, and is a useful biomarker for disease activity and diagnosis of IBD<sup>191,192</sup>. Recently, calprotectin has been shown to provide anti-fungal protection in a dose-dependent manner, where at low doses it functions as a reversible fungistatic (inhibitor of fungal growth), and at high doses it causes starvation and the killing of fungi<sup>193,194</sup>. In bacteria, calprotectin renders pathogens more sensitive to host immune effectors leading to a reduction in bacterial

growth<sup>180,195</sup>. However, some bacteria, such as *Escherichia coli* and *S. Typhimurium*, have been shown to be resistant to calprotectin's mediation of zinc sequestration (nutritional immunity), providing a competitive growth advantage and colonization of the gut during pro-inflammatory conditions<sup>180,196</sup>. It is possible that the observed greater relative abundance of *Escherichia coli/Shigella* during antibiotic administration is in part a result of the taxa's ability to overcome calprotectin-mediated metal sequestration (Fig. 7A and B).

Interestingly, results demonstrated a reduction in calprotectin levels during antibiotic administration in NOD2 KO mice from day 0 (pre-treatment) to day 14 (Fig. 15). One possibility for this observation is that in NOD2-deficient mice, the absence of spontaneous colitis can be attributed to the altered gut permeability caused by both the high mucosal cytokine production and the increased activity of myosin light chain kinase (MLCK). The microbiota, acting through MLCK-mediated effects on epithelial tight junctions, changes the permeability of the Peyer's patch epithelium in NOD2-deficient mice<sup>197,198</sup>. These changes in permeability lead to the dendritic cell exposure to TLR ligands, and changes within the microbiota. Studies in IBD patients have also shown similar results, where both increased permeability and an altered microbiota were associated with NOD2 polymorphisms with no inflammation<sup>85,199</sup>. Another possibility is that some fungi, including some *Candida* and *Penicillium* species, can inhibit intestinal inflammation through the dose dependent production of the metabolite gliotoxin<sup>200</sup>. Taken together, these results highlight the complexity of the gut polymicrobial communities.

#### **4.1.4. NOD2 Virome**

Here, the dynamics of the mouse gut virome during an antibiotic perturbation was demonstrated to be highly variable among individuals. This high inter-individual virome diversity has also been reported previously in the human gut virome<sup>33,201</sup>. Furthermore, similarly

to the human gut virome, the mouse gut virome was established to contain a large diversity of primarily bacteriophages, in addition to a much lower diversity of viral eukaryotes<sup>32,33,35</sup>. Additionally, consistent with previous reports, the most abundant viral taxa identified were bacteriophages of the order Caudovirales (i.e. *Phage cdt1* and *Cellulophaga* phage) and the family Microviridae (i.e. *Parabacteroides* phage)<sup>33,35,201</sup>. The presence of large viruses could not be established as a filtration step during sample processing removed all viruses larger than 0.45- $\mu\text{m}$ . Most studies to date have not reported the presence of large viruses as a result of filtering methods during isolation and extraction<sup>137</sup>. It is possible that these viruses are present more often than originally considered, though it remains to be seen what role they may play within the host. Furthermore, although antibiotics do not directly target viruses, our results demonstrated significant changes in the bacterial community, which in turn largely impacted the gut bacteriophage community. It is possible that the outgrowth of *E.coli/Shigella* during antibiotic treatment lead to the bloom of their respective bacteriophage (i.e. *Phage cdt1*) as expected in “kill-the-winner” dynamics<sup>37</sup>. Metagenomic analysis would help to elucidate these dynamics by detecting whether prophages are integrated within the respective genomes of the bacterial host, as the activation of latent prophages leads to the lysis of their hosts and ultimately impacts the ecology. Interestingly, the viral community appeared to have a delayed resilience, where the community was re-approaching a structure similar to day 0 (pre-treatment). However, contrary to a previous study in humans, no unique changes in the bacteriophage community occurred specific to the NOD2 KO<sup>201</sup>. Despite this, compositional shifts in the bacterial and viral communities were significantly correlated, where changes in the communities occurred in a similar direction and magnitude. This indicates that the virome may have a role in IBD through

interactions with the bacterial community, and further studies are needed to understand transkingdom interactions within the microbiome.

## 4.2. Fecal Transfer

Although the exact mechanism of action of FMTs is unknown, numerous studies have demonstrated its efficacy in treating RCDI<sup>112,113,118</sup>. Although FMTs have been shown to be safe, reducing the risk in immunocompromised patients would be highly beneficial. The results of this clinical case study showed that the transfer of sterile filtrates from donor stool is sufficient to restore normal stool habits and eliminate CDI symptoms (for at least for 6 months). This indicates that the viral community (largely composed of bacteriophages), antimicrobial compounds, metabolites, or bacterial components may be responsible for the successful treatment and recovery of patients, rather than the bacterial community as previously thought. Thus, sterile fecal transfers may be an effective alternative approach, particularly for immunocompromised patients, for which the risk of transferring unknown bacterial pathogens or undetectable functional properties within the living the living microbes to the recipient would be reduced<sup>118,201,202</sup>.

Taken together, perturbations led to substantial shifts in the viral communities of both mice and humans, further emphasizing the beneficial and detrimental effects viruses can have in response to environmental and host factors. In particular, the results presented here indicated that bacteriophage species may be playing an important role in either upregulating or downregulating the bacterial community. Restoring a healthy virome may therefore be a central goal of microbiota-targeted therapies, and highlights the importance of longitudinal studies to better understand factors contributing to resilience.

### 4.3. Immunoglobulin A Levels

Intestinal IgA is important in the regulation of the commensal bacterial populations and acts as an important first line of defense against ingested pathogens<sup>104,203</sup>. Interestingly, in the house mouse, a blood group-related glycosyltransferase, B4galnt2, displays cis-regulatory variation by directing tissue-specific expression<sup>204</sup>. In the wild-type allele (C57BL/6J strain), B4galnt2 drives intestinal epithelial expression, whereas RIIS/J inbred mice have a phenotype causing a switch in expression to a vascular endothelial pattern, similar to the human bleeding disorder Type 1 von Willebrand disease (VWD)<sup>205</sup>. It has been hypothesized that the prolonged bleeding in mice with the RIIS/J allele may be protective against gut pathogens<sup>204</sup>. As such, lower levels of fecal IgA were expected in these mice compared to WT mice. However, no significant difference was observed in fecal IgA levels between WT, heterozygotes, or RIIS/J mice (Fig. 24A). Noticeably, heterozygotes appeared to divide into two groups of fecal IgA levels, where one group had a lower fecal IgA levels compared to the WT C57BL/6 and RIIS/J genotypes (Fig. 24A). It is well established that individuals either heterozygous or homozygous for the RIIS/J haplotype display lower levels of plasma von Willebrand factor (VWF) levels compared to those that do not have the RIIS/J haplotype, and it has been postulated that low VWF levels may represent a fitness cost that is offset by the benefit associated to gastrointestinal pathogen resistance<sup>204,205</sup>. Heterozygotes are particularly interesting in this system as they express B4galnt2 in both the gastrointestinal tract and in the blood vessels. Thus, it is possible that the dichotomy observed in fecal IgA levels in heterozygotes may be reflecting this trade-off.

On the other hand, fecal IgA levels did not reveal any significant patterns for which strong associations between IgA levels and the different alleles, gender, population structure, or geographical distribution tested could be explained. This is in part due to the numerous factors

that could not be controlled, such as age, pathogen burden, diet, or co-habitation. In a previous study, little to no correspondence was identified where the observed allele frequencies were compared to the population structure across France and Germany<sup>206</sup>.

To determine whether differences in fecal IgA levels existed in lab mice, ATG16L1 mice were used due to their role in autophagy and the allele's known risk for CD<sup>207</sup>. ATG16L1 mice revealed a difference between the genders, where females had lower IgA levels compared to males, although no significant difference was observed (Fig. 25A, B). Comparing differences between KO and fl/fl, females appeared to demonstrate a phenotype, where fl/fl mice have lower IgA levels. Moreover, this pattern was not observed in males. However, these observations were not significant, and require further verification with a larger sampling size. Interestingly, ATG16L1 mice also showed a significant difference in fecal IgA levels across time, where weeks 19 and 20 had the highest levels in both genders compared to weeks 13 and 17 (Fig. 25C). Distinguishing between the genders further revealed that males had a slightly higher fecal IgA level compared to females (Fig. 25D).

Unsurprisingly, higher fecal IgA levels were observed in the wild mice compared to lab mice, likely a result of seasonal pathogen burden and diet. This was contrary to a recent study comparing lab mice to wild mice from the southern United Kingdom, where no significant difference was observed<sup>208</sup>. It remains to be determined whether a pattern can be established across other genotypes.

# Chapter 5 – Conclusions

## 5.1. Conclusions

Loss of NOD2 leads to a delayed or impaired resilience in the bacterial community. This delayed recovery may be playing a much more important role than previously known by providing a window of opportunity to potentially opportunistic pathogens, which may be driving inflammation and dysbiosis in genetically susceptible individuals. Furthermore, antibiotics also created a shift in both the fungal and viral composition to an alternative stable state, for which the consequences remain unclear. These results provide evidence of the role of NOD2 for controlling resilience of the intestinal microbiota, and suggest that uncontrolled dynamics of intestinal microbiota after perturbation could be involved in the etiology of IBD. Hence, NOD2 may serve as a key regulator of intestinal homeostasis. The resilience of microbial communities is a critical factor to host health and our results emphasize the need for more longitudinal studies in order to identify these dynamic shifts. Microbial resilience to antibiotic treatments can have considerable individual variation and is in part determined by the genotype of the respective host; consequently, perturbations and current treatments need further evaluation in individuals at genetic risk.

## 5.2. Future Perspectives

To further understand the effects of compounded perturbations, a new animal proposal is currently undergoing revisions for approval by the ethical committees of respective institutes. The proposal aims to investigate the bacterial and viral gut community response to multiple antibiotic pulse disturbance events. First, the study aims to investigate the resilience phenomenon

in C57BL/6J male mice (Figure 27). To determine the effects of multiple antibiotic disturbances on the microbiome, metagenome, and virome, a work flow composed of two antibiotic treatments, serving as two pulse disturbance events, will be administered to C57BL/6J mice. Two groups (A and B) composed of 20 mice each will be given a different antibiotic in the first round of treatment, where group (A) will receive ampicillin, and (B) ciprofloxacin. In each of the

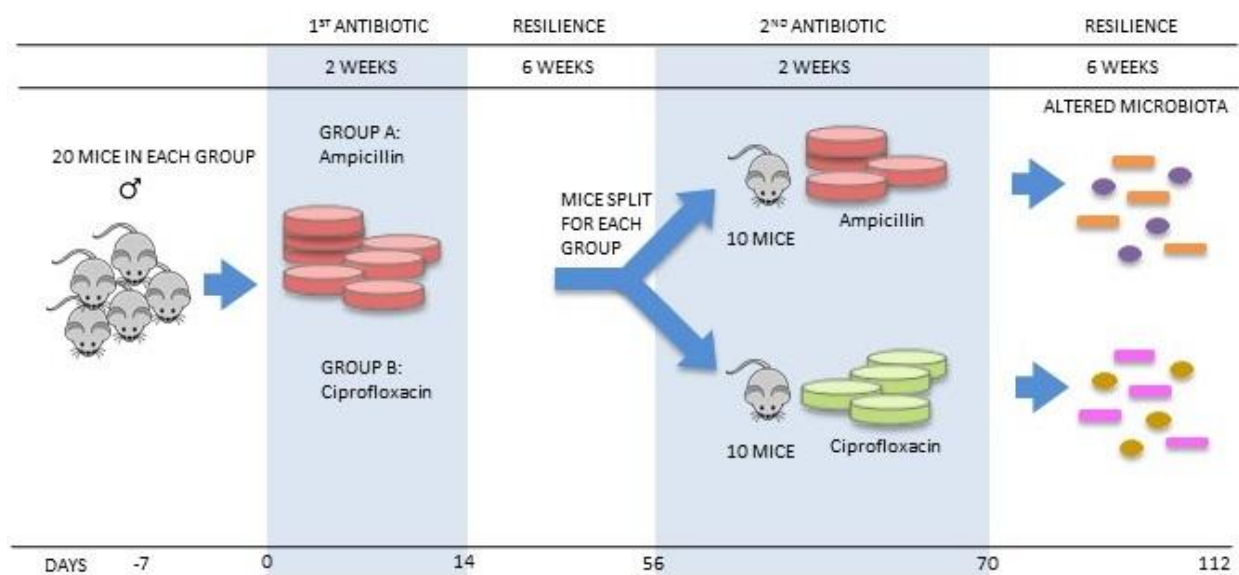


**Figure 27.** Experimental work flow demonstrating longitudinal study using C57BL/6J male mice. Two pulse disturbance events (antibiotic treatments) for 2 weeks each will take place, followed by a recovery period of 6 weeks each to study resilience. The first antibiotic treatment given to all mice will be dependent on the group, where group (A) will receive ampicillin, and (B) ciprofloxacin. Mice will then be split in both groups and the second antibiotic treatment will be ampicillin for half of the mice, whereas the other half will receive ciprofloxacin. Sampling to study the microbiome (16S),

two groups (A and B), mice will then be divided, where 10 mice will receive ampicillin, while the other 10 mice will be given ciprofloxacin. Mice will be split to observe cross-resistance, where microbes may have acquired resistance genes through direct exposure to the antibiotics. All control groups will receive only water. Each pulse event, including the resilience period, will take place over 8 weeks (56 days), for a total of 16 weeks. During this period, 2 weeks will serve

as the pulse event (antibiotic treatment), and the remaining 6 weeks as the resilience period. Secondly, the study aims to investigate the effect of genotypes on the resilience phenomenon, where NOD2 (KO) mice will be used instead of C57BL/6J.

Antibiotics were selected based on their use in previous studies, current laboratory use, and prevalence. In addition, antibiotics were selected based on their broad spectrum effect on both gram positive and gram negative bacteria. Ciprofloxacin acts by inhibiting DNA gyrase, a type II topoisomerase enzyme necessary to separate bacterial DNA, as well as topoisomerase IV, thus inhibiting cell division<sup>209</sup>. Moreover, ciprofloxacin is commonly used to treat Crohn's disease<sup>210,211</sup>. Alternatively, metronidazole is also commonly used, and unlike ampicillin or clindamycin, metronidazole is also used to treat *C. difficile* infections, serving as a possible alternative antibiotic of interest<sup>211,212</sup>. On the other hand, ampicillin acts as an irreversible inhibitor of the enzyme transpeptidase, which is needed by bacteria to develop their cell walls, thereby inhibiting the final stage of bacterial cell wall synthesis in binary fission, leading to cell lysis<sup>213</sup>. Interestingly, ampicillin is associated with the induction of *C. difficile* associated disease<sup>214</sup>. Clindamycin is also known as a high risk antibiotic and may additionally serve as an alternative antibiotic of use<sup>214</sup>. Due to their prevalence, widespread antibiotic resistance has emerged from the use of these antibiotics.

This study will serve as a basis for future research to answer questions regarding microbial diversity-function relationships. One such question is whether press and pulse disturbances select for different community members, and as such, have different effects on microbial resistance and resilience. Additionally, this study will serve as a foundation regarding the responses of the microbial community to combinations of both pulse and press antibiotic disturbances as seen in patients with IBD and *Clostridium difficile* infections. Finally, alternative

stable states may be detected and even predicted, which may have clinical use in patient management. Though the study uses a murine model, in the future, using human samples that have undergone antibiotic treatment would provide further insights into the resilience phenomenon. In particular, humans with the genes for disease susceptibility would be of interest.

## References

1. Dethlefsen, L. & Relman, D. A. Incomplete recovery and individualized responses of the human distal gut microbiota to repeated antibiotic perturbation. *Proc. Natl. Acad. Sci.* **108**, 4554–4561 (2011).
2. Jernberg, C., Löfmark, S., Edlund, C. & Jansson, J. K. Long-term ecological impacts of antibiotic administration on the human intestinal microbiota. *ISME J.* **1**, 56–66 (2007).
3. Keeney, K. M., Yurist-Doutsch, S., Arrieta, M.-C. & Finlay, B. B. Effects of Antibiotics on Human Microbiota and Subsequent Disease. *Annu. Rev. Microbiol.* **68**, 217–235 (2014).
4. Pimm, S. L. The complexity and stability of ecosystems. *Nat. Rev.* **307**, 321–326 (1984).
5. Shade, A. *et al.* Fundamentals of Microbial Community Resistance and Resilience. *Front. Microbiol.* **3**, (2012).
6. Holling, C. S. Resilience and stability of ecological systems. *Annu. Rev. Ecol. Syst.* **4**, 1–23 (1973).
7. Botton, S., van Heusden, M., Parsons, J. R., Smidt, H. & van Straalen, N. Resilience of Microbial Systems Towards Disturbances. *Crit. Rev. Microbiol.* **32**, 101–112 (2006).
8. Scheffer, M. & Carpenter, S. R. Catastrophic regime shifts in ecosystems: linking theory to observation. *Trends Ecol. Evol.* **18**, 648–656 (2003).
9. McNaughton, S. J. Diversity and Stability of Ecological Communities: A Comment on the Role of Empiricism in Ecology. *Am. Nat.* **111**, 515–525 (1977).
10. Naeem, S. & Li, S. Biodiversity enhances ecosystem reliability. *Nature* **390**, 507–509 (1997).
11. Sommer, F., Moltzau Anderson, J., Bharti, R., Raes, J. & Rosenstiel, P. The resilience of the intestinal microbiota influences health and disease. *Nat. Rev. Microbiol.* (2017).  
doi:10.1038/nrmicro.2017.58
12. Fleming, A. On the antibacterial action of cultures of a penicillium, with special reference to their use in the isolation of *B. influenzae*. *Br. J. Exp. Pathol.* **10**, 226 (1929).

13. Jakobsson, H. E. *et al.* Short-Term Antibiotic Treatment Has Differing Long-Term Impacts on the Human Throat and Gut Microbiome. *PLoS ONE* **5**, e9836 (2010).
14. Grice, E. A. & Segre, J. A. The Human Microbiome: Our Second Genome. *Annu. Rev. Genomics Hum. Genet.* **13**, 151–170 (2012).
15. Savage, D. C. Microbial ecology of the gastrointestinal tract. *Annu. Rev. Microbiol.* **31**, 107–133 (1977).
16. Sender, R., Fuchs, S. & Milo, R. Are we really vastly outnumbered? Revisiting the ratio of bacterial to host cells in humans. *Cell* **164**, 337–340 (2016).
17. Sidiq, T., Yoshihama, S., Downs, I. & Kobayashi, K. S. Nod2: A Critical Regulator of Ileal Microbiota and Crohn’s Disease. *Front. Immunol.* **7**, (2016).
18. Sommer, F. & Bäckhed, F. The gut microbiota — masters of host development and physiology. *Nat. Rev. Microbiol.* **11**, 227–238 (2013).
19. Abeles, S. R., Ly, M., Santiago-Rodriguez, T. M. & Pride, D. T. Effects of long term antibiotic therapy on human oral and fecal viromes. *PloS One* **10**, e0134941 (2015).
20. Filkins, L. M. & O’Toole, G. A. Cystic Fibrosis Lung Infections: Polymicrobial, Complex, and Hard to Treat. *PLOS Pathog.* **11**, e1005258 (2015).
21. Nguyen, L. D. N., Viscogliosi, E. & Delhaes, L. The lung mycobiome: an emerging field of the human respiratory microbiome. *Front. Microbiol.* **6**, (2015).
22. Kumamoto, C. A. The Fungal Mycobiota: Small Numbers, Large Impacts. *Cell Host Microbe* **19**, 750–751 (2016).
23. Huffnagle, G. B. & Noverr, M. C. The emerging world of the fungal microbiome. *Trends Microbiol.* **21**, 334–341 (2013).
24. Cui, L., Morris, A. & Ghedin, E. The human mycobiome in health and disease. *Genome Med.* **5**, 63 (2013).
25. Ott, S. J. *et al.* Fungi and inflammatory bowel diseases: Alterations of composition and diversity. *Scand. J. Gastroenterol.* **43**, 831–841 (2008).

26. Wheeler, M. L. *et al.* Immunological Consequences of Intestinal Fungal Dysbiosis. *Cell Host Microbe* **19**, 865–873 (2016).
27. Sharp, P. M. Origins of human virus diversity. *Cell* **108**, 305–312 (2002).
28. Popgeorgiev, N., Temmam, S., Raoult, D. & Desnues, C. Describing the Silent Human Virome with an Emphasis on Giant Viruses. *Intervirology* **56**, 395–412 (2013).
29. Colson, P. *et al.* Evidence of the megavirome in humans. *J. Clin. Virol.* **57**, 191–200 (2013).
30. Colson, P., La Scola, B., Levasseur, A., Caetano-Anoll's, G. & Raoult, D. Mimivirus: leading the way in the discovery of giant viruses of amoebae. *Nat. Rev. Microbiol.* **15**, 243–254 (2017).
31. Handley, S. A. The virome: a missing component of biological interaction networks in health and disease. *Genome Med.* **8**, (2016).
32. Minot, S. *et al.* Rapid evolution of the human gut virome. *Proc. Natl. Acad. Sci.* **110**, 12450–12455 (2013).
33. Reyes, A. *et al.* Viruses in the faecal microbiota of monozygotic twins and their mothers. *Nature* **466**, 334–338 (2010).
34. Reyes, A., Semenkovich, N. P., Whiteson, K., Rohwer, F. & Gordon, J. I. Going viral: next-generation sequencing applied to phage populations in the human gut. *Nat. Rev. Microbiol.* **10**, 607–617 (2012).
35. Minot, S. *et al.* The human gut virome: Inter-individual variation and dynamic response to diet. *Genome Res.* **21**, 1616–1625 (2011).
36. Belshaw, R. *et al.* Long-term reinfection of the human genome by endogenous retroviruses. *Proc. Natl. Acad. Sci. U. S. A.* **101**, 4894–4899 (2004).
37. Rodriguez-Valera, F. *et al.* Explaining microbial population genomics through phage predation. *Nat. Rev. Microbiol.* **7**, 828 (2009).
38. Schofield, D., Sharp, N. J. & Westwater, C. Phage-based platforms for the clinical detection of human bacterial pathogens. *Bacteriophage* **2**, 105–121 (2012).

39. Sell, T. L., Schaberg, D. R. & Fekety, F. R. Bacteriophage and bacteriocin typing scheme for *Clostridium difficile*. *J. Clin. Microbiol.* **17**, 1148–1152 (1983).
40. Duran-Pinedo, A. E. *et al.* Community-wide transcriptome of the oral microbiome in subjects with and without periodontitis. *ISME J.* **8**, 1659–1672 (2014).
41. Wargo, M. J. & Hogan, D. A. Fungal-bacterial interactions: a mixed bag of mingling microbes. *Curr. Opin. Microbiol.* **9**, 359–364 (2006).
42. Modi, S. R., Lee, H. H., Spina, C. S. & Collins, J. J. Antibiotic treatment expands the resistance reservoir and ecological network of the phage metagenome. *Nature* **499**, 219–222 (2013).
43. Allen, H. K. *et al.* Antibiotics in Feed Induce Prophages in Swine Fecal Microbiomes. *mBio* **2**, e00260-11-e00260-11 (2011).
44. Stanton, T. B., Humphrey, S. B., Sharma, V. K. & Zuerner, R. L. Collateral Effects of Antibiotics: Carbadox and Metronidazole Induce VSH-1 and Facilitate Gene Transfer among *Brachyspira hyodysenteriae* Strains. *Appl. Environ. Microbiol.* **74**, 2950–2956 (2008).
45. Kernbauer, E., Ding, Y. & Cadwell, K. An enteric virus can replace the beneficial function of commensal bacteria. *Nature* (2014). doi:10.1038/nature13960
46. Cadwell, K. *et al.* Virus-Plus-Susceptibility Gene Interaction Determines Crohn’s Disease Gene *Atg16L1* Phenotypes in Intestine. *Cell* **141**, 1135–1145 (2010).
47. Petnicki-Ocwieja, T. *et al.* *Nod2* is required for the regulation of commensal microbiota in the intestine. *Proc. Natl. Acad. Sci.* **106**, 15813–15818 (2009).
48. Lakshminarayanan, B., Stanton, C., O’Toole, P. W. & Ross, R. P. Compositional dynamics of the human intestinal microbiota with aging: Implications for health. *J. Nutr. Health Aging* **18**, 773–786 (2014).
49. Cox, L. M. & Blaser, M. J. Antibiotics in early life and obesity. *Nat. Rev. Endocrinol.* **11**, 182–190 (2014).
50. Xavier, R. J. & Podolsky, D. K. Unravelling the pathogenesis of inflammatory bowel disease. *Nature* **448**, 427–434 (2007).

51. Koenig, J. E. *et al.* Succession of microbial consortia in the developing infant gut microbiome. *Proc. Natl. Acad. Sci.* **108**, 4578–4585 (2011).
52. Fulde, M. & Hornef, M. Maturation of the enteric mucosal innate immune system during the postnatal period. *Immunol. Rev.* **260**, 21–34 (2014).
53. Günther, C., Josenhans, C. & Wehkamp, J. Crosstalk between microbiota, pathogens and the innate immune responses. *Int. J. Med. Microbiol.* **306**, 257–265 (2016).
54. Günther, C., Neumann, H., Neurath, M. F. & Becker, C. Apoptosis, necrosis and necroptosis: cell death regulation in the intestinal epithelium. *Gut* **62**, 1062–1071 (2013).
55. Wittkopf, N. *et al.* Cellular FLICE-Like Inhibitory Protein Secures Intestinal Epithelial Cell Survival and Immune Homeostasis by Regulating Caspase-8. *Gastroenterology* **145**, 1369–1379 (2013).
56. Takahashi, N. *et al.* RIPK1 ensures intestinal homeostasis by protecting the epithelium against apoptosis. *Nature* **513**, 95–99 (2014).
57. Kim, M. *et al.* Bacterial Interactions with the Host Epithelium. *Cell Host Microbe* **8**, 20–35 (2010).
58. Salzman, N. H. Paneth cell defensins and the regulation of the microbiome: Détente at mucosal surfaces. *Gut Microbes* **1**, 401–406 (2010).
59. Dupont, A., Heinbockel, L., Brandenburg, K. & Hornef, M. W. Antimicrobial peptides and the enteric mucus layer act in concert to protect the intestinal mucosa. *Gut Microbes* **5**, 761–765 (2014).
60. Ostaff, M. J., Stange, E. F. & Wehkamp, J. Antimicrobial peptides and gut microbiota in homeostasis and pathology: Homeostasis in the gut. *EMBO Mol. Med.* **5**, 1465–1483 (2013).
61. Schroeder, B. O. *et al.* Reduction of disulphide bonds unmasks potent antimicrobial activity of human  $\beta$ -defensin 1. *Nature* **469**, 419–423 (2011).
62. Wehkamp, J. *et al.* Reduced Paneth cell  $\alpha$ -defensins in ileal Crohn's disease. *Proc. Natl. Acad. Sci. U. S. A.* **102**, 18129–18134 (2005).
63. Bevins, C. L. Innate Immune Functions of  $\alpha$ -Defensins in the Small Intestine. *Dig. Dis.* **31**, 299–304 (2013).

64. Bevins, C. L., Strange, E. F. & Wehkamp, J. Decreased Paneth cell defensin expression in ileal Crohn's disease is independent of inflammation, but linked to the NOD2 1007fs genotype. *Gut* **58**, 882–883 (2009).
65. Dupont, A. *et al.* Intestinal mucus affinity and biological activity of an orally administered antibacterial and anti-inflammatory peptide. *Gut* **64**, 222–232 (2015).
66. Wlodarska, M., Kostic, A. D. & Xavier, R. J. An Integrative View of Microbiome-Host Interactions in Inflammatory Bowel Diseases. *Cell Host Microbe* **17**, 577–591 (2015).
67. Forbes, J. D., Van Domselaar, G. & Bernstein, C. N. Microbiome Survey of the Inflamed and Noninflamed Gut at Different Compartments Within the Gastrointestinal Tract of Inflammatory Bowel Disease Patients: *Inflamm. Bowel Dis.* **22**, 817–825 (2016).
68. Dicksved, J. *et al.* Molecular analysis of the gut microbiota of identical twins with Crohn's disease. *ISME J.* **2**, 716–727 (2008).
69. Baumgart, M. *et al.* Culture independent analysis of ileal mucosa reveals a selective increase in invasive *Escherichia coli* of novel phylogeny relative to depletion of Clostridiales in Crohn's disease involving the ileum. *ISME J.* **1**, 403–418 (2007).
70. Frank, D. N. *et al.* Molecular-phylogenetic characterization of microbial community imbalances in human inflammatory bowel diseases. *Proc. Natl. Acad. Sci.* **104**, 13780–13785 (2007).
71. Gophna, U., Sommerfeld, K., Gophna, S., Doolittle, W. F. & Veldhuyzen van Zanten, S. J. O. Differences between Tissue-Associated Intestinal Microfloras of Patients with Crohn's Disease and Ulcerative Colitis. *J. Clin. Microbiol.* **44**, 4136–4141 (2006).
72. Manichanh, C. Reduced diversity of faecal microbiota in Crohn's disease revealed by a metagenomic approach. *Gut* **55**, 205–211 (2006).
73. Patwa, L. G. *et al.* Chronic Intestinal Inflammation Induces Stress-Response Genes in Commensal *Escherichia coli*. *Gastroenterology* **141**, 1842–1851.e10 (2011).
74. Ellinghaus, D. *et al.* Analysis of five chronic inflammatory diseases identifies 27 new associations and highlights disease-specific patterns at shared loci. *Nat. Genet.* **48**, 510–518 (2016).

75. Chu, H. *et al.* Gene-microbiota interactions contribute to the pathogenesis of inflammatory bowel disease. *Science* **352**, 1116–1120 (2016).
76. Jostins, L. *et al.* Host-microbe interactions have shaped the genetic architecture of inflammatory bowel disease. *Nature* **491**, 119–124 (2012).
77. Hugot, J.-P. *et al.* Association of NOD2 leucine-rich repeat variants with susceptibility to Crohn's disease. *Nature* **411**, 599–603 (2001).
78. Ogura, Y. *et al.* A frameshift mutation in NOD2 associated with susceptibility to Crohn's disease. *Nature* **411**, 603–606 (2001).
79. Rosenstiel, P. *et al.* TNF-alpha and IFN-gamma regulate the expression of the NOD2 (CARD15) gene in human intestinal epithelial cells. *Gastroenterology* **124**, 1001–1009 (2003).
80. Lala, S. *et al.* Crohn's disease and the NOD2 gene: a role for paneth cells. *Gastroenterology* **125**, 47–57 (2003).
81. Inohara, N. *et al.* Host Recognition of Bacterial Muramyl Dipeptide Mediated through NOD2: IMPLICATIONS FOR CROHN'S DISEASE. *J. Biol. Chem.* **278**, 5509–5512 (2003).
82. Kobayashi, K. S. *et al.* Nod2-Dependent Regulation of Innate and Adaptive Immunity in the Intestinal Tract. *Science* **307**, 731–734 (2005).
83. Nakagome, S. *et al.* Crohn's Disease Risk Alleles on the NOD2 Locus Have Been Maintained by Natural Selection on Standing Variation. *Mol. Biol. Evol.* **29**, 1569–1585 (2012).
84. Swidsinski, A. *et al.* Mucosal flora in inflammatory bowel disease. *Gastroenterology* **122**, 44–54 (2002).
85. Frank, D. N. *et al.* Disease phenotype and genotype are associated with shifts in intestinal-associated microbiota in inflammatory bowel diseases. *Inflamm. Bowel Dis.* **17**, 179–184 (2011).
86. Rehman, A. *et al.* Nod2 is essential for temporal development of intestinal microbial communities. *Gut* **60**, 1354–1362 (2011).
87. Couturier-Maillard, A. *et al.* NOD2-mediated dysbiosis predisposes mice to transmissible colitis and colorectal cancer. *J. Clin. Invest.* **123**, 700–711 (2013).

88. Ghosh, S. & Almadi, M. Inflammatory bowel disease: A global disease. *Saudi J. Gastroenterol.* **19**, 1 (2013).
89. Underhill, D. & Braun, J. Current understanding of fungal microflora in inflammatory bowel disease pathogenesis: *Inflamm. Bowel Dis.* **14**, 1147–1153 (2008).
90. Molodecky, N. A. *et al.* Increasing Incidence and Prevalence of the Inflammatory Bowel Diseases With Time, Based on Systematic Review. *Gastroenterology* **142**, 46–54.e42 (2012).
91. Wilmanski, J. M., Petnicki-Ocwieja, T. & Kobayashi, K. S. NLR proteins: integral members of innate immunity and mediators of inflammatory diseases. *J. Leukoc. Biol.* **83**, 13–30 (2007).
92. Philpott, D. J., Sorbara, M. T., Robertson, S. J., Croitoru, K. & Girardin, S. E. NOD proteins: regulators of inflammation in health and disease. *Nat. Rev. Immunol.* **14**, 9–23 (2013).
93. Lesage, S. *et al.* CARD15/NOD2 mutational analysis and genotype-phenotype correlation in 612 patients with inflammatory bowel disease. *Am. J. Hum. Genet.* **70**, 845–857 (2002).
94. Gasche, C. *et al.* Evolution of Crohn's disease-associated Nod2 mutations. *Immunogenetics* **60**, 115–120 (2008).
95. Ayabe, T. *et al.* Secretion of microbicidal alpha-defensins by intestinal Paneth cells in response to bacteria. *Nat. Immunol.* **1**, 113–118 (2000).
96. Gutierrez, O. *et al.* Induction of Nod2 in Myelomonocytic and Intestinal Epithelial Cells via Nuclear Factor- $\kappa$ B Activation. *J. Biol. Chem.* **277**, 41701–41705 (2002).
97. Simms, L. A. *et al.* Reduced alpha-defensin expression is associated with inflammation and not NOD2 mutation status in ileal Crohn's disease. *Gut* **57**, 903–910 (2008).
98. Begue, B. *et al.* Microbial induction of CARD15 expression in intestinal epithelial cells via toll-like receptor 5 triggers an antibacterial response loop. *J. Cell. Physiol.* **209**, 241–252 (2006).
99. Naser, S. A. *et al.* Role of ATG16L, NOD2 and IL23R in Crohn's disease pathogenesis. *World J. Gastroenterol.* **18**, 412 (2012).
100. Travassos, L. H. *et al.* Nod1 and Nod2 direct autophagy by recruiting ATG16L1 to the plasma membrane at the site of bacterial entry. *Nat. Immunol.* **11**, 55–62 (2010).

101. Cooney, R. *et al.* NOD2 stimulation induces autophagy in dendritic cells influencing bacterial handling and antigen presentation. *Nat. Med.* **16**, 90–97 (2010).
102. Homer, C. R., Richmond, A. L., Rebert, N. A., Achkar, J. & McDonald, C. ATG16L1 and NOD2 Interact in an Autophagy-Dependent Antibacterial Pathway Implicated in Crohn's Disease Pathogenesis. *Gastroenterology* **139**, 1630–1641.e2 (2010).
103. Zhang, Q. *et al.* Commensal bacteria direct selective cargo sorting to promote symbiosis. *Nat. Immunol.* **16**, 918–926 (2015).
104. Blutt, S. E. & Conner, M. E. The Gastrointestinal Frontier: IgA and Viruses. *Front. Immunol.* **4**, (2013).
105. Corthésy, B. Multi-Faceted Functions of Secretory IgA at Mucosal Surfaces. *Front. Immunol.* **4**, (2013).
106. Perez-Lopez, A., Behnsen, J., Nuccio, S.-P. & Raffatellu, M. Mucosal immunity to pathogenic intestinal bacteria. *Nat. Rev. Immunol.* **16**, 135–148 (2016).
107. Hammarström, L., Vorechovsky, I. & Webster, D. Selective IgA deficiency (SIGAD) and common variable immunodeficiency (CVID). *Clin. Exp. Immunol.* **120**, 225–231 (1999).
108. Ludvigsson, J. F., Neovius, M. & Hammarström, L. Association Between IgA Deficiency & Other Autoimmune Conditions: A Population-Based Matched Cohort Study. *J. Clin. Immunol.* **34**, 444–451 (2014).
109. Palm, N. W. *et al.* Immunoglobulin A Coating Identifies Colitogenic Bacteria in Inflammatory Bowel Disease. *Cell* **158**, 1000–1010 (2014).
110. Moon, C. *et al.* Vertically transmitted faecal IgA levels determine extra-chromosomal phenotypic variation. *Nature* **521**, 90–93 (2015).
111. Li, S. S. *et al.* Durable coexistence of donor and recipient strains after fecal microbiota transplantation. *Science* **352**, 586–589 (2016).

112. Broecker, F., Klumpp, J. & Moelling, K. Long-term microbiota and virome in a Zürich patient after fecal transplantation against *Clostridium difficile* infection: *Clostridium difficile*, fecal transplant, and virome. *Ann. N. Y. Acad. Sci.* **1372**, 29–41 (2016).
113. Hamilton, M. J., Weingarden, A. R., Unno, T., Khoruts, A. & Sadowsky, M. J. High-throughput DNA sequence analysis reveals stable engraftment of gut microbiota following transplantation of previously frozen fecal bacteria. *Gut Microbes* **4**, 125–135 (2013).
114. Bojanova, D. P. & Bordenstein, S. R. Fecal Transplants: What Is Being Transferred? *PLOS Biol.* **14**, e1002503 (2016).
115. Jouhten, H., Mattila, E., Arkkila, P. & Satokari, R. Reduction of Antibiotic Resistance Genes in Intestinal Microbiota of Patients With Recurrent *Clostridium difficile* Infection After Fecal Microbiota Transplantation. *Clin. Infect. Dis.* **63**, 710–711 (2016).
116. Kumar, R. *et al.* Colonization potential to reconstitute a microbe community in patients detected early after fecal microbe transplant for recurrent *C. difficile*. *BMC Microbiol.* **16**, (2016).
117. Seekatz, A. M. *et al.* Recovery of the Gut Microbiome following Fecal Microbiota Transplantation. *mBio* **5**, e00893-14-e00893-14 (2014).
118. Ott, S. J. *et al.* Efficacy of Sterile Fecal Filtrate Transfer for Treating Patients With *Clostridium difficile* Infection. *Gastroenterology* **152**, 799–811.e7 (2017).
119. Fuentes, S. *et al.* Reset of a critically disturbed microbial ecosystem: faecal transplant in recurrent *Clostridium difficile* infection. *ISME J.* **8**, 1621–1633 (2014).
120. Chang, J. Y. *et al.* Decreased Diversity of the Fecal Microbiome in Recurrent *Clostridium difficile* – Associated Diarrhea. *J. Infect. Dis.* **197**, 435–438 (2008).
121. Khoruts, A., Dicksved, J., Jansson, J. K. & Sadowsky, M. J. Changes in the Composition of the Human Fecal Microbiome After Bacteriotherapy for Recurrent *Clostridium difficile*-associated Diarrhea. **44**, 354–360 (2010).
122. Manichanh, C. *et al.* Reshaping the gut microbiome with bacterial transplantation and antibiotic intake. *Genome Res.* **20**, 1411–1419 (2010).

123. Brandt, L. J. *et al.* Long-Term Follow-Up of Colonoscopic Fecal Microbiota Transplant for Recurrent *Clostridium difficile* Infection. *Am J Gastroenterol* **107**, 1079–1087 (2012).
124. Millan, B. *et al.* Fecal Microbial Transplants Reduce Antibiotic-resistant Genes in Patients With Recurrent *Clostridium difficile* Infection. *Clin. Infect. Dis.* **62**, 1479–1486 (2016).
125. Goodrich, J. K. *et al.* Human Genetics Shape the Gut Microbiome. *Cell* **159**, 789–799 (2014).
126. Blekhman, R. *et al.* Host genetic variation impacts microbiome composition across human body sites. *Genome Biol.* **16**, (2015).
127. Vijay-Kumar, M. *et al.* Metabolic Syndrome and Altered Gut Microbiota in Mice Lacking Toll-Like Receptor 5. *Science* **328**, 228–231 (2010).
128. Dasanayake, A. P., Li, Y., Wiener, H., Ruby, J. D. & Lee, M.-J. Salivary *Actinomyces naeslundii* genospecies 2 and *Lactobacillus casei* levels predict pregnancy outcomes. *J. Periodontol.* **76**, 171–177 (2005).
129. Aagaard, K. *et al.* The Placenta Harbors a Unique Microbiome. *Sci. Transl. Med.* **6**, 237ra65–237ra65 (2014).
130. Braniste, V. *et al.* The gut microbiota influences blood-brain barrier permeability in mice. *Sci. Transl. Med.* **6**, 263ra158–263ra158 (2014).
131. Bengtsson-Palme, J. *et al.* Improved software detection and extraction of ITS1 and ITS2 from ribosomal ITS sequences of fungi and other eukaryotes for analysis of environmental sequencing data. *Methods Ecol. Evol.* n/a–n/a (2013). doi:10.1111/2041-210X.12073
132. Op De Beeck, M. *et al.* Comparison and Validation of Some ITS Primer Pairs Useful for Fungal Metabarcoding Studies. *PLoS ONE* **9**, e97629 (2014).
133. Rooks, M. G. & Garrett, W. S. Gut microbiota, metabolites and host immunity. *Nat. Rev. Immunol.* **16**, 341–352 (2016).
134. Seifert, K. A. Progress towards DNA barcoding of fungi. *Mol. Ecol. Resour.* **9**, 83–89 (2009).
135. Schoch, C. L. *et al.* Nuclear ribosomal internal transcribed spacer (ITS) region as a universal DNA barcode marker for Fungi. *Proc. Natl. Acad. Sci.* **109**, 6241–6246 (2012).

136. Sachsenröder, J. *et al.* Simultaneous Identification of DNA and RNA Viruses Present in Pig Faeces Using Process-Controlled Deep Sequencing. *PLoS ONE* **7**, e34631 (2012).
137. Conceição-Neto, N. *et al.* Modular approach to customise sample preparation procedures for viral metagenomics: a reproducible protocol for virome analysis. *Sci. Rep.* **5**, (2015).
138. Thurber, R. V., Haynes, M., Breitbart, M., Wegley, L. & Rohwer, F. Laboratory procedures to generate viral metagenomes. *Nat. Protoc.* **4**, 470–483 (2009).
139. Philippe, N. *et al.* Pandoraviruses: Amoeba Viruses with Genomes Up to 2.5 Mb Reaching That of Parasitic Eukaryotes. *Science* **341**, 281–286 (2013).
140. Schloss, P. D. *et al.* Introducing mothur: Open-Source, Platform-Independent, Community-Supported Software for Describing and Comparing Microbial Communities. *Appl. Environ. Microbiol.* **75**, 7537–7541 (2009).
141. Oksanen, J. *et al.* vegan: Community Ecology Package, 2011. R package version; 1.17-11. (2011).
142. Hanley, J. A., Negassa, A., Edwardes, M. & Forrester, J. E. Statistical Analysis of Correlated Data Using Generalized Estimating Equations: An Orientation. *Am. J. Epidemiol.* **157**, 364–375 (2003).
143. Gardes, M. & Bruns, T. ITS primers with enhanced specificity for basidiomycetes--application to the identification of mycorrhizae and rusts. *Mol. Ecol.* **2**, 113–118 (1993).
144. White, T. J., Bruns, T., Lee, S. & Taylor, J. Amplification and direct sequencing of fungal ribosomal RNA genes for phylogenetics. in *PCR Protocols: A Guide to Methods and Applications* 315–322 (Academic Press, 1990).
145. Gweon, H. S. *et al.* PIPITS: an automated pipeline for analyses of fungal internal transcribed spacer sequences from the Illumina sequencing platform. *Methods Ecol. Evol.* **6**, 973–980 (2015).
146. Zhang, J., Kobert, K., Flouri, T. & Stamatakis, A. PEAR: a fast and accurate Illumina Paired-End reAd mergeR. *Bioinformatics* **30**, 614–620 (2014).
147. Nilsson, R. H. *et al.* A Comprehensive, Automatically Updated Fungal ITS Sequence Dataset for Reference-Based Chimera Control in Environmental Sequencing Efforts. *Microbes Environ.* **30**, 145–150 (2015).

148. Bolger, A. M., Lohse, M. & Usadel, B. Trimmomatic: a flexible trimmer for Illumina sequence data. *Bioinformatics* **30**, 2114–2120 (2014).
149. Bankevich, A. *et al.* SPAdes: A New Genome Assembly Algorithm and Its Applications to Single-Cell Sequencing. *J. Comput. Biol.* **19**, 455–477 (2012).
150. Langmead, B. & Salzberg, S. L. Fast gapped-read alignment with Bowtie 2. *Nat. Methods* **9**, 357–359 (2012).
151. Li, H. *et al.* The Sequence Alignment/Map format and SAMtools. *Bioinformatics* **25**, 2078–2079 (2009).
152. Roux, S. *et al.* Towards quantitative viromics for both double-stranded and single-stranded DNA viruses. *PeerJ* **4**, e2777 (2016).
153. Pruitt, K. D., Tatusova, T., Brown, G. R. & Maglott, D. R. NCBI Reference Sequences (RefSeq): current status, new features and genome annotation policy. *Nucleic Acids Res.* **40**, D130–D135 (2012).
154. Arndt, D. *et al.* PHASTER: a better, faster version of the PHAST phage search tool. *Nucleic Acids Res.* **44**, W16–W21 (2016).
155. Zhou, Y., Liang, Y., Lynch, K. H., Dennis, J. J. & Wishart, D. S. PHAST: A Fast Phage Search Tool. *Nucleic Acids Res.* **39**, W347–W352 (2011).
156. Clarke, R. K. & Gorley, R. N. PRIMER v7: User Manual/Tutorial. (2015).
157. CLARKE, K. R. Non-parametric multivariate analyses of changes in community structure. *Austral Ecol.* **18**, 117–143 (1993).
158. Nurk, S. *et al.* Assembling Single-Cell Genomes and Mini-Metagenomes From Chimeric MDA Products. *J. Comput. Biol.* **20**, 714–737 (2013).
159. Minot, S. S., Krumm, N. & Greenfield, N. B. One Codex: A Sensitive and Accurate Data Platform for Genomic Microbial Identification. *bioRxiv* (2015). doi:10.1101/027607
160. Anderson, J. M., Gorley, R. N. & Clarke, R. K. *PERMANOVA+ for primer: Guide to software and statistical methods.* (2008).

161. Anderson, M. J. A new method for non-parametric multivariate analysis of variance. *Austral Ecol.* **26**, 32–46 (2001).
162. McArdle, B. H. & Anderson, M. J. Fitting Multivariate Models to Community Data: A Comment on Distance-Based Redundancy Analysis. *Ecology* **82**, 290 (2001).
163. Livak, K. J. & Schmittgen, T. D. Analysis of Relative Gene Expression Data Using Real-Time Quantitative PCR and the 2-DDCT Method. *Methods* **25**, 402–408 (2001).
164. Bonhomme, F. *et al.* Genetic differentiation of the house mouse around the Mediterranean basin: matrilineal footprints of early and late colonization. *Proc. R. Soc. B Biol. Sci.* **278**, 1034–1043 (2011).
165. Bradley, D. E. Ultrastructure of bacteriophage and bacteriocins. *Bacteriol. Rev.* **31**, 230–314 (1967).
166. Mondot, S. *et al.* Altered gut microbiota composition in immune-impaired Nod2<sup>-/-</sup> mice. *Gut* **61**, 634–635 (2012).
167. Scanlan, P. D., Shanahan, F., O’Mahony, C. & Marchesi, J. R. Culture-Independent Analyses of Temporal Variation of the Dominant Fecal Microbiota and Targeted Bacterial Subgroups in Crohn’s Disease. *J. Clin. Microbiol.* **44**, 3980–3988 (2006).
168. Ramanan, D., Tang, M. S., Bowcutt, R., Loke, P. & Cadwell, K. Bacterial Sensor Nod2 Prevents Inflammation of the Small Intestine by Restricting the Expansion of the Commensal *Bacteroides vulgatus*. *Immunity* **41**, 311–324 (2014).
169. Langille, M. G. *et al.* Microbial shifts in the aging mouse gut. *Microbiome* **2**, 50 (2014).
170. Knights, D. *et al.* Complex host genetics influence the microbiome in inflammatory bowel disease. *Genome Med.* **6**, 107 (2014).
171. Garrett, W. S. *et al.* Communicable ulcerative colitis induced by T-bet deficiency in the innate immune system. *Cell* **131**, 33–45 (2007).
172. Gevers, D. *et al.* The Treatment-Naive Microbiome in New-Onset Crohn’s Disease. *Cell Host Microbe* **15**, 382–392 (2014).

173. Morgan, X. C. *et al.* Dysfunction of the intestinal microbiome in inflammatory bowel disease and treatment. *Genome Biol.* **13**, R79 (2012).
174. Nagalingam, N. A. *et al.* The effects of intestinal microbial community structure on disease manifestation in IL-10<sup>-/-</sup>-mice infected with *Helicobacter hepaticus*. *Microbiome* **1**, 15 (2013).
175. Rooks, M. G. *et al.* Gut microbiome composition and function in experimental colitis during active disease and treatment-induced remission. *ISME J.* **8**, 1403–1417 (2014).
176. Carvalho, F. *et al.* Transient Inability to Manage Proteobacteria Promotes Chronic Gut Inflammation in TLR5-Deficient Mice. *Cell Host Microbe* **12**, 139–152 (2012).
177. Ubeda, C. & Pamer, E. G. Antibiotics, microbiota, and immune defense. *Trends Immunol.* **33**, 459–466 (2012).
178. Faber, F. *et al.* Host-mediated sugar oxidation promotes post-antibiotic pathogen expansion. *Nature* **534**, 697–699 (2016).
179. Bohnhoff, M., Drake, B. L. & Miller, C. P. Effect of Streptomycin on Susceptibility of Intestinal Tract to Experimental Salmonella Infection. *Exp. Biol. Med.* **86**, 132–137 (1954).
180. Liu, J. Z. *et al.* Zinc Sequestration by the Neutrophil Protein Calprotectin Enhances Salmonella Growth in the Inflamed Gut. *Cell Host Microbe* **11**, 227–239 (2012).
181. Hantke, K. Bacterial zinc transporters and regulators. in *Zinc Biochemistry, Physiology, and Homeostasis* 53–63 (Springer, 2001).
182. Hildebrand, F. *et al.* Inflammation-associated enterotypes, host genotype, cage and inter-individual effects drive gut microbiota variation in common laboratory mice. *Genome Biol.* **14**, R4 (2013).
183. Steck, N., Mueller, K., Schemann, M. & Haller, D. Bacterial proteases in IBD and IBS. *Gut* **61**, 1610–1618 (2012).
184. Maes, M., Mihaylova, I. & Leunis, J.-C. Increased serum IgA and IgM against LPS of enterobacteria in chronic fatigue syndrome (CFS): Indication for the involvement of gram-negative enterobacteria in the etiology of CFS and for the presence of an increased gut–intestinal permeability. *J. Affect. Disord.* **99**, 237–240 (2007).

185. Llorente, C. & Schnabl, B. The gut microbiota and liver disease. *CMGH Cell. Mol. Gastroenterol. Hepatol.* **1**, 275–284 (2015).
186. Jawhara, S. *et al.* Colonization of Mice by *Candida albicans* Is Promoted by Chemically Induced Colitis and Augments Inflammatory Responses through Galectin-3. *J. Infect. Dis.* **197**, 972–980 (2008).
187. Dollive, S. *et al.* Fungi of the Murine Gut: Episodic Variation and Proliferation during Antibiotic Treatment. *PLoS ONE* **8**, e71806 (2013).
188. Noverr, M. C., Noggle, R. M., Toews, G. B. & Huffnagle, G. B. Role of Antibiotics and Fungal Microbiota in Driving Pulmonary Allergic Responses. *Infect. Immun.* **72**, 4996–5003 (2004).
189. Wagener, J. *et al.* Fungal Chitin Dampens Inflammation through IL-10 Induction Mediated by NOD2 and TLR9 Activation. *PLoS Pathog.* **10**, e1004050 (2014).
190. Fraune, S. *et al.* Bacteria–bacteria interactions within the microbiota of the ancestral metazoan Hydra contribute to fungal resistance. *ISME J.* **9**, 1543–1556 (2015).
191. De Jong, H. K. *et al.* Expression and Function of S100A8/A9 (Calprotectin) in Human Typhoid Fever and the Murine Salmonella Model. *PLoS Negl. Trop. Dis.* **9**, e0003663 (2015).
192. Konikoff, M. R. & Denson, L. A. Role of fecal calprotectin as a biomarker of intestinal inflammation in inflammatory bowel disease. *Inflamm. Bowel Dis.* **12**, (2010).
193. Branzk, N. & Papayannopoulos, V. Molecular mechanisms regulating NETosis in infection and disease. *Semin. Immunopathol.* **35**, 513–530 (2013).
194. Bianchi, M., Niemiec, M. J., Siler, U., Urban, C. F. & Reichenbach, J. Restoration of anti-*Aspergillus* defense by neutrophil extracellular traps in human chronic granulomatous disease after gene therapy is calprotectin-dependent. *J. Allergy Clin. Immunol.* **127**, 1243–1252.e7 (2011).
195. Kehl-Fie, T. E. *et al.* Nutrient Metal Sequestration by Calprotectin Inhibits Bacterial Superoxide Defense, Enhancing Neutrophil Killing of *Staphylococcus aureus*. *Cell Host Microbe* **10**, 158–164 (2011).

196. Kehl-Fie, T. E. & Skaar, E. P. Nutritional immunity beyond iron: a role for manganese and zinc. *Curr. Opin. Chem. Biol.* **14**, 218–224 (2010).
197. Amendola, A., Butera, A., Sanchez, M., Strober, W. & Boirivant, M. Nod2 deficiency is associated with an increased mucosal immunoregulatory response to commensal microorganisms. *Mucosal Immunol.* **7**, 391–404 (2014).
198. Barreau, F. *et al.* Nod2 regulates the host response towards microflora by modulating T cell function and epithelial permeability in mouse Peyer's patches. *Gut* **59**, 207–217 (2010).
199. D'Inca, R. *et al.* Increased intestinal permeability and NOD2 variants in familial and sporadic Crohn's disease. *Aliment. Pharmacol. Ther.* **23**, 1455–1461 (2006).
200. Herfarth, H. *et al.* Nuclear factor- $\kappa$ B activity and intestinal inflammation in dextran sulphate sodium (DSS)-induced colitis in mice is suppressed by gliotoxin. *Clin. Exp. Immunol.* **120**, 59–65 (2000).
201. Norman, J. M. *et al.* Disease-Specific Alterations in the Enteric Virome in Inflammatory Bowel Disease. *Cell* **160**, 447–460 (2015).
202. Alang, N. & Kelly, C. R. Weight Gain After Fecal Microbiota Transplantation. *Open Forum Infect. Dis.* **2**, ofv004-ofv004 (2015).
203. Bidgood, S. R., Tam, J. C. H., McEwan, W. A., Mallery, D. L. & James, L. C. Translocalized IgA mediates neutralization and stimulates innate immunity inside infected cells. *Proc. Natl. Acad. Sci.* **111**, 13463–13468 (2014).
204. Vallier, M. *et al.* Evaluating the maintenance of disease-associated variation at the blood group-related gene B4galnt2 in house mice. *BMC Evol. Biol.* **17**, (2017).
205. Johnsen, J. M. *et al.* Selection on cis-regulatory variation at B4galnt2 and its influence on von Willebrand factor in house mice. *Mol. Biol. Evol.* **26**, 567–578 (2009).
206. Linnenbrink, M. *et al.* The role of biogeography in shaping diversity of the intestinal microbiota in house mice. *Mol. Ecol.* **22**, 1904–1916 (2013).
207. Cadwell, K. *et al.* A key role for autophagy and the autophagy gene Atg16l1 in mouse and human intestinal Paneth cells. *Nature* **456**, 259–263 (2008).

208. Abolins, S. *et al.* The comparative immunology of wild and laboratory mice, *Mus musculus domesticus*. *Nat. Commun.* **8**, 14811 (2017).
209. Collin, F., Karkare, S. & Maxwell, A. Exploiting bacterial DNA gyrase as a drug target: current state and perspectives. *Appl. Microbiol. Biotechnol.* **92**, 479–497 (2011).
210. Wu, X.-W., Ji, H.-Z. & Wang, F.-Y. Meta-analysis of ciprofloxacin in treatment of Crohn’s disease. *Biomed. Rep.* **3**, 70–74 (2015).
211. Lal, S. & Steinhart, A. H. Antibiotic therapy for Crohn’s disease: a review. *Can. J. Gastroenterol. Hepatol.* **20**, 651–655 (2006).
212. Shen, E. P. & Surawicz, C. M. Current Treatment Options for Severe *Clostridium difficile*-associated Disease. *Gastroenterol. Hepatol.* **4**, 134 (2008).
213. Kohanski, M. A., Dwyer, D. J. & Collins, J. J. How antibiotics kill bacteria: from targets to networks. *Nat. Rev. Microbiol.* **8**, 423–435 (2010).
214. Deneve, C., Delomenie, C., Barc, M.-C., Collignon, A. & Janoir, C. Antibiotics involved in *Clostridium difficile*-associated disease increase colonization factor gene expression. *J. Med. Microbiol.* **57**, 732–738 (2008).
1. Dethlefsen, L. & Relman, D. A. Incomplete recovery and individualized responses of the human distal gut microbiota to repeated antibiotic perturbation. *Proc. Natl. Acad. Sci.* **108**, 4554–4561 (2011).
  2. Jernberg, C., Löfmark, S., Edlund, C. & Jansson, J. K. Long-term ecological impacts of antibiotic administration on the human intestinal microbiota. *ISME J.* **1**, 56–66 (2007).
  3. Keeney, K. M., Yurist-Doutsch, S., Arrieta, M.-C. & Finlay, B. B. Effects of Antibiotics on Human Microbiota and Subsequent Disease. *Annu. Rev. Microbiol.* **68**, 217–235 (2014).
  4. Pimm, S. L. The complexity and stability of ecosystems. *Nat. Rev.* **307**, 321–326 (1984).
  5. Shade, A. *et al.* Fundamentals of Microbial Community Resistance and Resilience. *Front. Microbiol.* **3**, (2012).
  6. Holling, C. S. Resilience and stability of ecological systems. *Annu. Rev. Ecol. Syst.* **4**, 1–23 (1973).

7. Botton, S., van Heusden, M., Parsons, J. R., Smidt, H. & van Straalen, N. Resilience of Microbial Systems Towards Disturbances. *Crit. Rev. Microbiol.* **32**, 101–112 (2006).
8. Scheffer, M. & Carpenter, S. R. Catastrophic regime shifts in ecosystems: linking theory to observation. *Trends Ecol. Evol.* **18**, 648–656 (2003).
9. McNaughton, S. J. Diversity and Stability of Ecological Communities: A Comment on the Role of Empiricism in Ecology. *Am. Nat.* **111**, 515–525 (1977).
10. Naeem, S. & Li, S. Biodiversity enhances ecosystem reliability. *Nature* **390**, 507–509 (1997).
11. Sommer, F., Moltzau Anderson, J., Bharti, R., Raes, J. & Rosenstiel, P. The resilience of the intestinal microbiota influences health and disease. *Nat. Rev. Microbiol.* (2017).  
doi:10.1038/nrmicro.2017.58
12. Fleming, A. On the antibacterial action of cultures of a penicillium, with special reference to their use in the isolation of *B. influenzae*. *Br. J. Exp. Pathol.* **10**, 226 (1929).
13. Jakobsson, H. E. *et al.* Short-Term Antibiotic Treatment Has Differing Long-Term Impacts on the Human Throat and Gut Microbiome. *PLoS ONE* **5**, e9836 (2010).
14. Grice, E. A. & Segre, J. A. The Human Microbiome: Our Second Genome. *Annu. Rev. Genomics Hum. Genet.* **13**, 151–170 (2012).
15. Savage, D. C. Microbial ecology of the gastrointestinal tract. *Annu. Rev. Microbiol.* **31**, 107–133 (1977).
16. Sender, R., Fuchs, S. & Milo, R. Are we really vastly outnumbered? Revisiting the ratio of bacterial to host cells in humans. *Cell* **164**, 337–340 (2016).
17. Sidiq, T., Yoshihama, S., Downs, I. & Kobayashi, K. S. Nod2: A Critical Regulator of Ileal Microbiota and Crohn's Disease. *Front. Immunol.* **7**, (2016).
18. Sommer, F. & Bäckhed, F. The gut microbiota — masters of host development and physiology. *Nat. Rev. Microbiol.* **11**, 227–238 (2013).
19. Abeles, S. R., Ly, M., Santiago-Rodriguez, T. M. & Pride, D. T. Effects of long term antibiotic therapy on human oral and fecal viromes. *PloS One* **10**, e0134941 (2015).

20. Filkins, L. M. & O'Toole, G. A. Cystic Fibrosis Lung Infections: Polymicrobial, Complex, and Hard to Treat. *PLOS Pathog.* **11**, e1005258 (2015).
21. Nguyen, L. D. N., Viscogliosi, E. & Delhaes, L. The lung mycobiome: an emerging field of the human respiratory microbiome. *Front. Microbiol.* **6**, (2015).
22. Kumamoto, C. A. The Fungal Mycobiota: Small Numbers, Large Impacts. *Cell Host Microbe* **19**, 750–751 (2016).
23. Huffnagle, G. B. & Noverr, M. C. The emerging world of the fungal microbiome. *Trends Microbiol.* **21**, 334–341 (2013).
24. Cui, L., Morris, A. & Ghedin, E. The human mycobiome in health and disease. *Genome Med.* **5**, 63 (2013).
25. Ott, S. J. *et al.* Fungi and inflammatory bowel diseases: Alterations of composition and diversity. *Scand. J. Gastroenterol.* **43**, 831–841 (2008).
26. Wheeler, M. L. *et al.* Immunological Consequences of Intestinal Fungal Dysbiosis. *Cell Host Microbe* **19**, 865–873 (2016).
27. Sharp, P. M. Origins of human virus diversity. *Cell* **108**, 305–312 (2002).
28. Popgeorgiev, N., Temmam, S., Raoult, D. & Desnues, C. Describing the Silent Human Virome with an Emphasis on Giant Viruses. *Intervirology* **56**, 395–412 (2013).
29. Colson, P. *et al.* Evidence of the megavirome in humans. *J. Clin. Virol.* **57**, 191–200 (2013).
30. Colson, P., La Scola, B., Levasseur, A., Caetano-Anoll's, G. & Raoult, D. Mimivirus: leading the way in the discovery of giant viruses of amoebae. *Nat. Rev. Microbiol.* **15**, 243–254 (2017).
31. Handley, S. A. The virome: a missing component of biological interaction networks in health and disease. *Genome Med.* **8**, (2016).
32. Minot, S. *et al.* Rapid evolution of the human gut virome. *Proc. Natl. Acad. Sci.* **110**, 12450–12455 (2013).
33. Reyes, A. *et al.* Viruses in the faecal microbiota of monozygotic twins and their mothers. *Nature* **466**, 334–338 (2010).

34. Reyes, A., Semenkovich, N. P., Whiteson, K., Rohwer, F. & Gordon, J. I. Going viral: next-generation sequencing applied to phage populations in the human gut. *Nat. Rev. Microbiol.* **10**, 607–617 (2012).
35. Minot, S. *et al.* The human gut virome: Inter-individual variation and dynamic response to diet. *Genome Res.* **21**, 1616–1625 (2011).
36. Belshaw, R. *et al.* Long-term reinfection of the human genome by endogenous retroviruses. *Proc. Natl. Acad. Sci. U. S. A.* **101**, 4894–4899 (2004).
37. Rodriguez-Valera, F. *et al.* Explaining microbial population genomics through phage predation. *Nat. Rev. Microbiol.* **7**, 828 (2009).
38. Schofield, D., Sharp, N. J. & Westwater, C. Phage-based platforms for the clinical detection of human bacterial pathogens. *Bacteriophage* **2**, 105–121 (2012).
39. Sell, T. L., Schaberg, D. R. & Fekety, F. R. Bacteriophage and bacteriocin typing scheme for *Clostridium difficile*. *J. Clin. Microbiol.* **17**, 1148–1152 (1983).
40. Duran-Pinedo, A. E. *et al.* Community-wide transcriptome of the oral microbiome in subjects with and without periodontitis. *ISME J.* **8**, 1659–1672 (2014).
41. Wargo, M. J. & Hogan, D. A. Fungal-bacterial interactions: a mixed bag of mingling microbes. *Curr. Opin. Microbiol.* **9**, 359–364 (2006).
42. Modi, S. R., Lee, H. H., Spina, C. S. & Collins, J. J. Antibiotic treatment expands the resistance reservoir and ecological network of the phage metagenome. *Nature* **499**, 219–222 (2013).
43. Allen, H. K. *et al.* Antibiotics in Feed Induce Prophages in Swine Fecal Microbiomes. *mBio* **2**, e00260-11-e00260-11 (2011).
44. Stanton, T. B., Humphrey, S. B., Sharma, V. K. & Zuerner, R. L. Collateral Effects of Antibiotics: Carbadox and Metronidazole Induce VSH-1 and Facilitate Gene Transfer among *Brachyspira hyodysenteriae* Strains. *Appl. Environ. Microbiol.* **74**, 2950–2956 (2008).
45. Kernbauer, E., Ding, Y. & Cadwell, K. An enteric virus can replace the beneficial function of commensal bacteria. *Nature* (2014). doi:10.1038/nature13960

46. Cadwell, K. *et al.* Virus-Plus-Susceptibility Gene Interaction Determines Crohn's Disease Gene Atg16L1 Phenotypes in Intestine. *Cell* **141**, 1135–1145 (2010).
47. Petnicki-Ocwieja, T. *et al.* Nod2 is required for the regulation of commensal microbiota in the intestine. *Proc. Natl. Acad. Sci.* **106**, 15813–15818 (2009).
48. Lakshminarayanan, B., Stanton, C., O'Toole, P. W. & Ross, R. P. Compositional dynamics of the human intestinal microbiota with aging: Implications for health. *J. Nutr. Health Aging* **18**, 773–786 (2014).
49. Cox, L. M. & Blaser, M. J. Antibiotics in early life and obesity. *Nat. Rev. Endocrinol.* **11**, 182–190 (2014).
50. Xavier, R. J. & Podolsky, D. K. Unravelling the pathogenesis of inflammatory bowel disease. *Nature* **448**, 427–434 (2007).
51. Koenig, J. E. *et al.* Succession of microbial consortia in the developing infant gut microbiome. *Proc. Natl. Acad. Sci.* **108**, 4578–4585 (2011).
52. Fulde, M. & Hornef, M. Maturation of the enteric mucosal innate immune system during the postnatal period. *Immunol. Rev.* **260**, 21–34 (2014).
53. Günther, C., Josenhans, C. & Wehkamp, J. Crosstalk between microbiota, pathogens and the innate immune responses. *Int. J. Med. Microbiol.* **306**, 257–265 (2016).
54. Günther, C., Neumann, H., Neurath, M. F. & Becker, C. Apoptosis, necrosis and necroptosis: cell death regulation in the intestinal epithelium. *Gut* **62**, 1062–1071 (2013).
55. Wittkopf, N. *et al.* Cellular FLICE-Like Inhibitory Protein Secures Intestinal Epithelial Cell Survival and Immune Homeostasis by Regulating Caspase-8. *Gastroenterology* **145**, 1369–1379 (2013).
56. Takahashi, N. *et al.* RIPK1 ensures intestinal homeostasis by protecting the epithelium against apoptosis. *Nature* **513**, 95–99 (2014).
57. Kim, M. *et al.* Bacterial Interactions with the Host Epithelium. *Cell Host Microbe* **8**, 20–35 (2010).

58. Salzman, N. H. Paneth cell defensins and the regulation of the microbiome: Détente at mucosal surfaces. *Gut Microbes* **1**, 401–406 (2010).
59. Dupont, A., Heinbockel, L., Brandenburg, K. & Hornef, M. W. Antimicrobial peptides and the enteric mucus layer act in concert to protect the intestinal mucosa. *Gut Microbes* **5**, 761–765 (2014).
60. Ostaff, M. J., Stange, E. F. & Wehkamp, J. Antimicrobial peptides and gut microbiota in homeostasis and pathology: Homeostasis in the gut. *EMBO Mol. Med.* **5**, 1465–1483 (2013).
61. Schroeder, B. O. *et al.* Reduction of disulphide bonds unmasks potent antimicrobial activity of human  $\beta$ -defensin 1. *Nature* **469**, 419–423 (2011).
62. Wehkamp, J. *et al.* Reduced Paneth cell  $\alpha$ -defensins in ileal Crohn's disease. *Proc. Natl. Acad. Sci. U. S. A.* **102**, 18129–18134 (2005).
63. Bevins, C. L. Innate Immune Functions of  $\alpha$ -Defensins in the Small Intestine. *Dig. Dis.* **31**, 299–304 (2013).
64. Bevins, C. L., Strange, E. F. & Wehkamp, J. Decreased Paneth cell defensin expression in ileal Crohn's disease is independent of inflammation, but linked to the NOD2 1007fs genotype. *Gut* **58**, 882–883 (2009).
65. Dupont, A. *et al.* Intestinal mucus affinity and biological activity of an orally administered antibacterial and anti-inflammatory peptide. *Gut* **64**, 222–232 (2015).
66. Wlodarska, M., Kostic, A. D. & Xavier, R. J. An Integrative View of Microbiome-Host Interactions in Inflammatory Bowel Diseases. *Cell Host Microbe* **17**, 577–591 (2015).
67. Forbes, J. D., Van Domselaar, G. & Bernstein, C. N. Microbiome Survey of the Inflamed and Noninflamed Gut at Different Compartments Within the Gastrointestinal Tract of Inflammatory Bowel Disease Patients: *Inflamm. Bowel Dis.* **22**, 817–825 (2016).
68. Dicksved, J. *et al.* Molecular analysis of the gut microbiota of identical twins with Crohn's disease. *ISME J.* **2**, 716–727 (2008).

69. Baumgart, M. *et al.* Culture independent analysis of ileal mucosa reveals a selective increase in invasive *Escherichia coli* of novel phylogeny relative to depletion of Clostridiales in Crohn's disease involving the ileum. *ISME J.* **1**, 403–418 (2007).
70. Frank, D. N. *et al.* Molecular-phylogenetic characterization of microbial community imbalances in human inflammatory bowel diseases. *Proc. Natl. Acad. Sci.* **104**, 13780–13785 (2007).
71. Gophna, U., Sommerfeld, K., Gophna, S., Doolittle, W. F. & Veldhuyzen van Zanten, S. J. O. Differences between Tissue-Associated Intestinal Microfloras of Patients with Crohn's Disease and Ulcerative Colitis. *J. Clin. Microbiol.* **44**, 4136–4141 (2006).
72. Manichanh, C. Reduced diversity of faecal microbiota in Crohn's disease revealed by a metagenomic approach. *Gut* **55**, 205–211 (2006).
73. Patwa, L. G. *et al.* Chronic Intestinal Inflammation Induces Stress-Response Genes in Commensal *Escherichia coli*. *Gastroenterology* **141**, 1842–1851.e10 (2011).
74. Ellinghaus, D. *et al.* Analysis of five chronic inflammatory diseases identifies 27 new associations and highlights disease-specific patterns at shared loci. *Nat. Genet.* **48**, 510–518 (2016).
75. Chu, H. *et al.* Gene-microbiota interactions contribute to the pathogenesis of inflammatory bowel disease. *Science* **352**, 1116–1120 (2016).
76. Jostins, L. *et al.* Host-microbe interactions have shaped the genetic architecture of inflammatory bowel disease. *Nature* **491**, 119–124 (2012).
77. Hugot, J.-P. *et al.* Association of NOD2 leucine-rich repeat variants with susceptibility to Crohn's disease. *Nature* **411**, 599–603 (2001).
78. Ogura, Y. *et al.* A frameshift mutation in NOD2 associated with susceptibility to Crohn's disease. *Nature* **411**, 603–606 (2001).
79. Rosenstiel, P. *et al.* TNF-alpha and IFN-gamma regulate the expression of the NOD2 (CARD15) gene in human intestinal epithelial cells. *Gastroenterology* **124**, 1001–1009 (2003).
80. Lala, S. *et al.* Crohn's disease and the NOD2 gene: a role for paneth cells. *Gastroenterology* **125**, 47–57 (2003).

81. Inohara, N. *et al.* Host Recognition of Bacterial Muramyl Dipeptide Mediated through NOD2: IMPLICATIONS FOR CROHN'S DISEASE. *J. Biol. Chem.* **278**, 5509–5512 (2003).
82. Kobayashi, K. S. *et al.* Nod2-Dependent Regulation of Innate and Adaptive Immunity in the Intestinal Tract. *Science* **307**, 731–734 (2005).
83. Nakagome, S. *et al.* Crohn's Disease Risk Alleles on the NOD2 Locus Have Been Maintained by Natural Selection on Standing Variation. *Mol. Biol. Evol.* **29**, 1569–1585 (2012).
84. Swidsinski, A. *et al.* Mucosal flora in inflammatory bowel disease. *Gastroenterology* **122**, 44–54 (2002).
85. Frank, D. N. *et al.* Disease phenotype and genotype are associated with shifts in intestinal-associated microbiota in inflammatory bowel diseases: *Inflamm. Bowel Dis.* **17**, 179–184 (2011).
86. Rehman, A. *et al.* Nod2 is essential for temporal development of intestinal microbial communities. *Gut* **60**, 1354–1362 (2011).
87. Couturier-Maillard, A. *et al.* NOD2-mediated dysbiosis predisposes mice to transmissible colitis and colorectal cancer. *J. Clin. Invest.* **123**, 700–711 (2013).
88. Ghosh, S. & Almadi, M. Inflammatory bowel disease: A global disease. *Saudi J. Gastroenterol.* **19**, 1 (2013).
89. Underhill, D. & Braun, J. Current understanding of fungal microflora in inflammatory bowel disease pathogenesis: *Inflamm. Bowel Dis.* **14**, 1147–1153 (2008).
90. Molodecky, N. A. *et al.* Increasing Incidence and Prevalence of the Inflammatory Bowel Diseases With Time, Based on Systematic Review. *Gastroenterology* **142**, 46–54.e42 (2012).
91. Wilmanski, J. M., Petnicki-Ocwieja, T. & Kobayashi, K. S. NLR proteins: integral members of innate immunity and mediators of inflammatory diseases. *J. Leukoc. Biol.* **83**, 13–30 (2007).
92. Philpott, D. J., Sorbara, M. T., Robertson, S. J., Croitoru, K. & Girardin, S. E. NOD proteins: regulators of inflammation in health and disease. *Nat. Rev. Immunol.* **14**, 9–23 (2013).
93. Lesage, S. *et al.* CARD15/NOD2 mutational analysis and genotype-phenotype correlation in 612 patients with inflammatory bowel disease. *Am. J. Hum. Genet.* **70**, 845–857 (2002).

94. Gasche, C. *et al.* Evolution of Crohn's disease-associated Nod2 mutations. *Immunogenetics* **60**, 115–120 (2008).
95. Ayabe, T. *et al.* Secretion of microbicidal alpha-defensins by intestinal Paneth cells in response to bacteria. *Nat. Immunol.* **1**, 113–118 (2000).
96. Gutierrez, O. *et al.* Induction of Nod2 in Myelomonocytic and Intestinal Epithelial Cells via Nuclear Factor- $\kappa$ B Activation. *J. Biol. Chem.* **277**, 41701–41705 (2002).
97. Simms, L. A. *et al.* Reduced alpha-defensin expression is associated with inflammation and not NOD2 mutation status in ileal Crohn's disease. *Gut* **57**, 903–910 (2008).
98. Begue, B. *et al.* Microbial induction of CARD15 expression in intestinal epithelial cells via toll-like receptor 5 triggers an antibacterial response loop. *J. Cell. Physiol.* **209**, 241–252 (2006).
99. Naser, S. A. *et al.* Role of ATG16L , NOD2 and IL23R in Crohn's disease pathogenesis. *World J. Gastroenterol.* **18**, 412 (2012).
100. Travassos, L. H. *et al.* Nod1 and Nod2 direct autophagy by recruiting ATG16L1 to the plasma membrane at the site of bacterial entry. *Nat. Immunol.* **11**, 55–62 (2010).
101. Cooney, R. *et al.* NOD2 stimulation induces autophagy in dendritic cells influencing bacterial handling and antigen presentation. *Nat. Med.* **16**, 90–97 (2010).
102. Homer, C. R., Richmond, A. L., Rebert, N. A., Achkar, J. & McDonald, C. ATG16L1 and NOD2 Interact in an Autophagy-Dependent Antibacterial Pathway Implicated in Crohn's Disease Pathogenesis. *Gastroenterology* **139**, 1630–1641.e2 (2010).
103. Zhang, Q. *et al.* Commensal bacteria direct selective cargo sorting to promote symbiosis. *Nat. Immunol.* **16**, 918–926 (2015).
104. Blutt, S. E. & Conner, M. E. The Gastrointestinal Frontier: IgA and Viruses. *Front. Immunol.* **4**, (2013).
105. Corthésy, B. Multi-Faceted Functions of Secretory IgA at Mucosal Surfaces. *Front. Immunol.* **4**, (2013).

106. Perez-Lopez, A., Behnsen, J., Nuccio, S.-P. & Raffatellu, M. Mucosal immunity to pathogenic intestinal bacteria. *Nat. Rev. Immunol.* **16**, 135–148 (2016).
107. Hammarström, L., Vorechovsky, I. & Webster, D. Selective IgA deficiency (SIgAD) and common variable immunodeficiency (CVID). *Clin. Exp. Immunol.* **120**, 225–231 (1999).
108. Ludvigsson, J. F., Neovius, M. & Hammarström, L. Association Between IgA Deficiency & Other Autoimmune Conditions: A Population-Based Matched Cohort Study. *J. Clin. Immunol.* **34**, 444–451 (2014).
109. Palm, N. W. *et al.* Immunoglobulin A Coating Identifies Colitogenic Bacteria in Inflammatory Bowel Disease. *Cell* **158**, 1000–1010 (2014).
110. Moon, C. *et al.* Vertically transmitted faecal IgA levels determine extra-chromosomal phenotypic variation. *Nature* **521**, 90–93 (2015).
111. Li, S. S. *et al.* Durable coexistence of donor and recipient strains after fecal microbiota transplantation. *Science* **352**, 586–589 (2016).
112. Broecker, F., Klumpp, J. & Moelling, K. Long-term microbiota and virome in a Zürich patient after fecal transplantation against *Clostridium difficile* infection: *Clostridium difficile*, fecal transplant, and virome. *Ann. N. Y. Acad. Sci.* **1372**, 29–41 (2016).
113. Hamilton, M. J., Weingarden, A. R., Unno, T., Khoruts, A. & Sadowsky, M. J. High-throughput DNA sequence analysis reveals stable engraftment of gut microbiota following transplantation of previously frozen fecal bacteria. *Gut Microbes* **4**, 125–135 (2013).
114. Bojanova, D. P. & Bordenstein, S. R. Fecal Transplants: What Is Being Transferred? *PLOS Biol.* **14**, e1002503 (2016).
115. Jouhten, H., Mattila, E., Arkkila, P. & Satokari, R. Reduction of Antibiotic Resistance Genes in Intestinal Microbiota of Patients With Recurrent *Clostridium difficile* Infection After Fecal Microbiota Transplantation. *Clin. Infect. Dis.* **63**, 710–711 (2016).
116. Kumar, R. *et al.* Colonization potential to reconstitute a microbe community in patients detected early after fecal microbe transplant for recurrent *C. difficile*. *BMC Microbiol.* **16**, (2016).

117. Seekatz, A. M. *et al.* Recovery of the Gut Microbiome following Fecal Microbiota Transplantation. *mBio* **5**, e00893-14-e00893-14 (2014).
118. Ott, S. J. *et al.* Efficacy of Sterile Fecal Filtrate Transfer for Treating Patients With *Clostridium difficile* Infection. *Gastroenterology* **152**, 799–811.e7 (2017).
119. Fuentes, S. *et al.* Reset of a critically disturbed microbial ecosystem: faecal transplant in recurrent *Clostridium difficile* infection. *ISME J.* **8**, 1621–1633 (2014).
120. Chang, J. Y. *et al.* Decreased Diversity of the Fecal Microbiome in Recurrent *Clostridium difficile* – Associated Diarrhea. *J. Infect. Dis.* **197**, 435–438 (2008).
121. Khoruts, A., Dicksved, J., Jansson, J. K. & Sadowsky, M. J. Changes in the Composition of the Human Fecal Microbiome After Bacteriotherapy for Recurrent *Clostridium difficile*-associated Diarrhea. **44**, 354–360 (2010).
122. Manichanh, C. *et al.* Reshaping the gut microbiome with bacterial transplantation and antibiotic intake. *Genome Res.* **20**, 1411–1419 (2010).
123. Brandt, L. J. *et al.* Long-Term Follow-Up of Colonoscopic Fecal Microbiota Transplant for Recurrent *Clostridium difficile* Infection. *Am J Gastroenterol* **107**, 1079–1087 (2012).
124. Millan, B. *et al.* Fecal Microbial Transplants Reduce Antibiotic-resistant Genes in Patients With Recurrent *Clostridium difficile* Infection. *Clin. Infect. Dis.* **62**, 1479–1486 (2016).
125. Goodrich, J. K. *et al.* Human Genetics Shape the Gut Microbiome. *Cell* **159**, 789–799 (2014).
126. Blekhman, R. *et al.* Host genetic variation impacts microbiome composition across human body sites. *Genome Biol.* **16**, (2015).
127. Vijay-Kumar, M. *et al.* Metabolic Syndrome and Altered Gut Microbiota in Mice Lacking Toll-Like Receptor 5. *Science* **328**, 228–231 (2010).
128. Dasanayake, A. P., Li, Y., Wiener, H., Ruby, J. D. & Lee, M.-J. Salivary *Actinomyces naeslundii* genospecies 2 and *Lactobacillus casei* levels predict pregnancy outcomes. *J. Periodontol.* **76**, 171–177 (2005).

129. Aagaard, K. *et al.* The Placenta Harbors a Unique Microbiome. *Sci. Transl. Med.* **6**, 237ra65-237ra65 (2014).
130. Braniste, V. *et al.* The gut microbiota influences blood-brain barrier permeability in mice. *Sci. Transl. Med.* **6**, 263ra158-263ra158 (2014).
131. Bengtsson-Palme, J. *et al.* Improved software detection and extraction of ITS1 and ITS2 from ribosomal ITS sequences of fungi and other eukaryotes for analysis of environmental sequencing data. *Methods Ecol. Evol.* n/a-n/a (2013). doi:10.1111/2041-210X.12073
132. Op De Beeck, M. *et al.* Comparison and Validation of Some ITS Primer Pairs Useful for Fungal Metabarcoding Studies. *PLoS ONE* **9**, e97629 (2014).
133. Rooks, M. G. & Garrett, W. S. Gut microbiota, metabolites and host immunity. *Nat. Rev. Immunol.* **16**, 341–352 (2016).
134. Seifert, K. A. Progress towards DNA barcoding of fungi. *Mol. Ecol. Resour.* **9**, 83–89 (2009).
135. Schoch, C. L. *et al.* Nuclear ribosomal internal transcribed spacer (ITS) region as a universal DNA barcode marker for Fungi. *Proc. Natl. Acad. Sci.* **109**, 6241–6246 (2012).
136. Sachsenröder, J. *et al.* Simultaneous Identification of DNA and RNA Viruses Present in Pig Faeces Using Process-Controlled Deep Sequencing. *PLoS ONE* **7**, e34631 (2012).
137. Conceição-Neto, N. *et al.* Modular approach to customise sample preparation procedures for viral metagenomics: a reproducible protocol for virome analysis. *Sci. Rep.* **5**, (2015).
138. Thurber, R. V., Haynes, M., Breitbart, M., Wegley, L. & Rohwer, F. Laboratory procedures to generate viral metagenomes. *Nat. Protoc.* **4**, 470–483 (2009).
139. Philippe, N. *et al.* Pandoraviruses: Amoeba Viruses with Genomes Up to 2.5 Mb Reaching That of Parasitic Eukaryotes. *Science* **341**, 281–286 (2013).
140. Schloss, P. D. *et al.* Introducing mothur: Open-Source, Platform-Independent, Community-Supported Software for Describing and Comparing Microbial Communities. *Appl. Environ. Microbiol.* **75**, 7537–7541 (2009).
141. Oksanen, J. *et al.* vegan: Community Ecology Package, 2011. R package version; 1.17-11. (2011).

142. Hanley, J. A., Negassa, A., Edwardes, M. & Forrester, J. E. Statistical Analysis of Correlated Data Using Generalized Estimating Equations: An Orientation. *Am. J. Epidemiol.* **157**, 364–375 (2003).
143. Gardes, M. & Bruns, T. ITS primers with enhanced specificity for basidiomycetes--application to the identification of mycorrhizae and rusts. *Mol. Ecol.* **2**, 113–118 (1993).
144. White, T. J., Bruns, T., Lee, S. & Taylor, J. Amplification and direct sequencing of fungal ribosomal RNA genes for phylogenetics. in *PCR Protocols: A Guide to Methods and Applications* 315–322 (Academic Press, 1990).
145. Gweon, H. S. *et al.* PIPITS: an automated pipeline for analyses of fungal internal transcribed spacer sequences from the Illumina sequencing platform. *Methods Ecol. Evol.* **6**, 973–980 (2015).
146. Zhang, J., Kobert, K., Flouri, T. & Stamatakis, A. PEAR: a fast and accurate Illumina Paired-End reAd mergeR. *Bioinformatics* **30**, 614–620 (2014).
147. Nilsson, R. H. *et al.* A Comprehensive, Automatically Updated Fungal ITS Sequence Dataset for Reference-Based Chimera Control in Environmental Sequencing Efforts. *Microbes Environ.* **30**, 145–150 (2015).
148. Bolger, A. M., Lohse, M. & Usadel, B. Trimmomatic: a flexible trimmer for Illumina sequence data. *Bioinformatics* **30**, 2114–2120 (2014).
149. Bankevich, A. *et al.* SPAdes: A New Genome Assembly Algorithm and Its Applications to Single-Cell Sequencing. *J. Comput. Biol.* **19**, 455–477 (2012).
150. Langmead, B. & Salzberg, S. L. Fast gapped-read alignment with Bowtie 2. *Nat. Methods* **9**, 357–359 (2012).
151. Li, H. *et al.* The Sequence Alignment/Map format and SAMtools. *Bioinformatics* **25**, 2078–2079 (2009).
152. Roux, S. *et al.* Towards quantitative viromics for both double-stranded and single-stranded DNA viruses. *PeerJ* **4**, e2777 (2016).

153. Pruitt, K. D., Tatusova, T., Brown, G. R. & Maglott, D. R. NCBI Reference Sequences (RefSeq): current status, new features and genome annotation policy. *Nucleic Acids Res.* **40**, D130–D135 (2012).
154. Arndt, D. *et al.* PHASTER: a better, faster version of the PHAST phage search tool. *Nucleic Acids Res.* **44**, W16–W21 (2016).
155. Zhou, Y., Liang, Y., Lynch, K. H., Dennis, J. J. & Wishart, D. S. PHAST: A Fast Phage Search Tool. *Nucleic Acids Res.* **39**, W347–W352 (2011).
156. Clarke, R. K. & Gorley, R. N. PRIMER v7: User Manual/Tutorial. (2015).
157. CLARKE, K. R. Non-parametric multivariate analyses of changes in community structure. *Austral Ecol.* **18**, 117–143 (1993).
158. Nurk, S. *et al.* Assembling Single-Cell Genomes and Mini-Metagenomes From Chimeric MDA Products. *J. Comput. Biol.* **20**, 714–737 (2013).
159. Minot, S. S., Krumm, N. & Greenfield, N. B. One Codex: A Sensitive and Accurate Data Platform for Genomic Microbial Identification. *bioRxiv* (2015). doi:10.1101/027607
160. Anderson, J. M., Gorley, R. N. & Clarke, R. K. *PERMANOVA+ for primer: Guide to software and statistical methods.* (2008).
161. Anderson, M. J. A new method for non-parametric multivariate analysis of variance. *Austral Ecol.* **26**, 32–46 (2001).
162. McArdle, B. H. & Anderson, M. J. Fitting Multivariate Models to Community Data: A Comment on Distance-Based Redundancy Analysis. *Ecology* **82**, 290 (2001).
163. Livak, K. J. & Schmittgen, T. D. Analysis of Relative Gene Expression Data Using Real-Time Quantitative PCR and the 2-DDCT Method. *Methods* **25**, 402–408 (2001).
164. Bonhomme, F. *et al.* Genetic differentiation of the house mouse around the Mediterranean basin: matrilineal footprints of early and late colonization. *Proc. R. Soc. B Biol. Sci.* **278**, 1034–1043 (2011).
165. Bradley, D. E. Ultrastructure of bacteriophage and bacteriocins. *Bacteriol. Rev.* **31**, 230–314 (1967).

166. Mondot, S. *et al.* Altered gut microbiota composition in immune-impaired Nod2<sup>-/-</sup> mice. *Gut* **61**, 634–635 (2012).
167. Scanlan, P. D., Shanahan, F., O'Mahony, C. & Marchesi, J. R. Culture-Independent Analyses of Temporal Variation of the Dominant Fecal Microbiota and Targeted Bacterial Subgroups in Crohn's Disease. *J. Clin. Microbiol.* **44**, 3980–3988 (2006).
168. Ramanan, D., Tang, M. S., Bowcutt, R., Loke, P. & Cadwell, K. Bacterial Sensor Nod2 Prevents Inflammation of the Small Intestine by Restricting the Expansion of the Commensal *Bacteroides vulgatus*. *Immunity* **41**, 311–324 (2014).
169. Langille, M. G. *et al.* Microbial shifts in the aging mouse gut. *Microbiome* **2**, 50 (2014).
170. Knights, D. *et al.* Complex host genetics influence the microbiome in inflammatory bowel disease. *Genome Med.* **6**, 107 (2014).
171. Garrett, W. S. *et al.* Communicable ulcerative colitis induced by T-bet deficiency in the innate immune system. *Cell* **131**, 33–45 (2007).
172. Gevers, D. *et al.* The Treatment-Naive Microbiome in New-Onset Crohn's Disease. *Cell Host Microbe* **15**, 382–392 (2014).
173. Morgan, X. C. *et al.* Dysfunction of the intestinal microbiome in inflammatory bowel disease and treatment. *Genome Biol.* **13**, R79 (2012).
174. Nagalingam, N. A. *et al.* The effects of intestinal microbial community structure on disease manifestation in IL-10<sup>-/-</sup> mice infected with *Helicobacter hepaticus*. *Microbiome* **1**, 15 (2013).
175. Rooks, M. G. *et al.* Gut microbiome composition and function in experimental colitis during active disease and treatment-induced remission. *ISME J.* **8**, 1403–1417 (2014).
176. Carvalho, F. *et al.* Transient Inability to Manage Proteobacteria Promotes Chronic Gut Inflammation in TLR5-Deficient Mice. *Cell Host Microbe* **12**, 139–152 (2012).
177. Ubeda, C. & Pamer, E. G. Antibiotics, microbiota, and immune defense. *Trends Immunol.* **33**, 459–466 (2012).

178. Faber, F. *et al.* Host-mediated sugar oxidation promotes post-antibiotic pathogen expansion. *Nature* **534**, 697–699 (2016).
179. Bohnhoff, M., Drake, B. L. & Miller, C. P. Effect of Streptomycin on Susceptibility of Intestinal Tract to Experimental Salmonella Infection. *Exp. Biol. Med.* **86**, 132–137 (1954).
180. Liu, J. Z. *et al.* Zinc Sequestration by the Neutrophil Protein Calprotectin Enhances Salmonella Growth in the Inflamed Gut. *Cell Host Microbe* **11**, 227–239 (2012).
181. Hantke, K. Bacterial zinc transporters and regulators. in *Zinc Biochemistry, Physiology, and Homeostasis* 53–63 (Springer, 2001).
182. Hildebrand, F. *et al.* Inflammation-associated enterotypes, host genotype, cage and inter-individual effects drive gut microbiota variation in common laboratory mice. *Genome Biol.* **14**, R4 (2013).
183. Steck, N., Mueller, K., Schemann, M. & Haller, D. Bacterial proteases in IBD and IBS. *Gut* **61**, 1610–1618 (2012).
184. Maes, M., Mihaylova, I. & Leunis, J.-C. Increased serum IgA and IgM against LPS of enterobacteria in chronic fatigue syndrome (CFS): Indication for the involvement of gram-negative enterobacteria in the etiology of CFS and for the presence of an increased gut–intestinal permeability. *J. Affect. Disord.* **99**, 237–240 (2007).
185. Llorente, C. & Schnabl, B. The gut microbiota and liver disease. *CMGH Cell. Mol. Gastroenterol. Hepatol.* **1**, 275–284 (2015).
186. Jawhara, S. *et al.* Colonization of Mice by *Candida albicans* Is Promoted by Chemically Induced Colitis and Augments Inflammatory Responses through Galectin-3. *J. Infect. Dis.* **197**, 972–980 (2008).
187. Dollive, S. *et al.* Fungi of the Murine Gut: Episodic Variation and Proliferation during Antibiotic Treatment. *PLoS ONE* **8**, e71806 (2013).
188. Noverr, M. C., Noggle, R. M., Toews, G. B. & Huffnagle, G. B. Role of Antibiotics and Fungal Microbiota in Driving Pulmonary Allergic Responses. *Infect. Immun.* **72**, 4996–5003 (2004).

189. Wagener, J. *et al.* Fungal Chitin Dampens Inflammation through IL-10 Induction Mediated by NOD2 and TLR9 Activation. *PLoS Pathog.* **10**, e1004050 (2014).
190. Fraune, S. *et al.* Bacteria–bacteria interactions within the microbiota of the ancestral metazoan Hydra contribute to fungal resistance. *ISME J.* **9**, 1543–1556 (2015).
191. De Jong, H. K. *et al.* Expression and Function of S100A8/A9 (Calprotectin) in Human Typhoid Fever and the Murine Salmonella Model. *PLoS Negl. Trop. Dis.* **9**, e0003663 (2015).
192. Konikoff, M. R. & Denson, L. A. Role of fecal calprotectin as a biomarker of intestinal inflammation in inflammatory bowel disease. *Inflamm. Bowel Dis.* **12**, (2010).
193. Branzk, N. & Papayannopoulos, V. Molecular mechanisms regulating NETosis in infection and disease. *Semin. Immunopathol.* **35**, 513–530 (2013).
194. Bianchi, M., Niemiec, M. J., Siler, U., Urban, C. F. & Reichenbach, J. Restoration of anti-Aspergillus defense by neutrophil extracellular traps in human chronic granulomatous disease after gene therapy is calprotectin-dependent. *J. Allergy Clin. Immunol.* **127**, 1243–1252.e7 (2011).
195. Kehl-Fie, T. E. *et al.* Nutrient Metal Sequestration by Calprotectin Inhibits Bacterial Superoxide Defense, Enhancing Neutrophil Killing of Staphylococcus aureus. *Cell Host Microbe* **10**, 158–164 (2011).
196. Kehl-Fie, T. E. & Skaar, E. P. Nutritional immunity beyond iron: a role for manganese and zinc. *Curr. Opin. Chem. Biol.* **14**, 218–224 (2010).
197. Amendola, A., Butera, A., Sanchez, M., Strober, W. & Boirivant, M. Nod2 deficiency is associated with an increased mucosal immunoregulatory response to commensal microorganisms. *Mucosal Immunol.* **7**, 391–404 (2014).
198. Barreau, F. *et al.* Nod2 regulates the host response towards microflora by modulating T cell function and epithelial permeability in mouse Peyer’s patches. *Gut* **59**, 207–217 (2010).
199. D’Inca, R. *et al.* Increased intestinal permeability and NOD2 variants in familial and sporadic Crohn’s disease. *Aliment. Pharmacol. Ther.* **23**, 1455–1461 (2006).

200. Herfarth, H. *et al.* Nuclear factor- $\kappa$ B activity and intestinal inflammation in dextran sulphate sodium (DSS)-induced colitis in mice is suppressed by gliotoxin. *Clin. Exp. Immunol.* **120**, 59–65 (2000).
201. Norman, J. M. *et al.* Disease-Specific Alterations in the Enteric Virome in Inflammatory Bowel Disease. *Cell* **160**, 447–460 (2015).
202. Alang, N. & Kelly, C. R. Weight Gain After Fecal Microbiota Transplantation. *Open Forum Infect. Dis.* **2**, ofv004-ofv004 (2015).
203. Bidgood, S. R., Tam, J. C. H., McEwan, W. A., Mallery, D. L. & James, L. C. Translocalized IgA mediates neutralization and stimulates innate immunity inside infected cells. *Proc. Natl. Acad. Sci.* **111**, 13463–13468 (2014).
204. Vallier, M. *et al.* Evaluating the maintenance of disease-associated variation at the blood group-related gene B4galnt2 in house mice. *BMC Evol. Biol.* **17**, (2017).
205. Johnsen, J. M. *et al.* Selection on cis-regulatory variation at B4galnt2 and its influence on von Willebrand factor in house mice. *Mol. Biol. Evol.* **26**, 567–578 (2009).
206. Linnenbrink, M. *et al.* The role of biogeography in shaping diversity of the intestinal microbiota in house mice. *Mol. Ecol.* **22**, 1904–1916 (2013).
207. Cadwell, K. *et al.* A key role for autophagy and the autophagy gene Atg16l1 in mouse and human intestinal Paneth cells. *Nature* **456**, 259–263 (2008).
208. Abolins, S. *et al.* The comparative immunology of wild and laboratory mice, *Mus musculus domesticus*. *Nat. Commun.* **8**, 14811 (2017).
209. Collin, F., Karkare, S. & Maxwell, A. Exploiting bacterial DNA gyrase as a drug target: current state and perspectives. *Appl. Microbiol. Biotechnol.* **92**, 479–497 (2011).
210. Wu, X.-W., Ji, H.-Z. & Wang, F.-Y. Meta-analysis of ciprofloxacin in treatment of Crohn’s disease. *Biomed. Rep.* **3**, 70–74 (2015).
211. Lal, S. & Steinhart, A. H. Antibiotic therapy for Crohn’s disease: a review. *Can. J. Gastroenterol. Hepatol.* **20**, 651–655 (2006).

212. Shen, E. P. & Surawicz, C. M. Current Treatment Options for Severe Clostridium difficile-associated Disease. *Gastroenterol. Hepatol.* **4**, 134 (2008).
213. Kohanski, M. A., Dwyer, D. J. & Collins, J. J. How antibiotics kill bacteria: from targets to networks. *Nat. Rev. Microbiol.* **8**, 423–435 (2010).
214. Deneve, C., Delomenie, C., Barc, M.-C., Collignon, A. & Janoir, C. Antibiotics involved in Clostridium difficile-associated disease increase colonization factor gene expression. *J. Med. Microbiol.* **57**, 732–738 (2008).

# Appendix

## Appendix 1 – Online Material

Raw FASTQ reads generated from the study, “NOD2 influences intestinal microbial resilience after antibiotic perturbation”, were uploaded to EBI's ENA under the Accession Number PRJEB21817 (<http://www.ebi.ac.uk/ena/data/view/PRJEB21817>). Metadata associated to all samples used in this study, and the OUT tables for bacteria and fungi, with corresponding taxonomic classifications, have all been included in the manuscript as Additional files 10, 11, and 12, respectively.

## Appendix 2 – NOD2

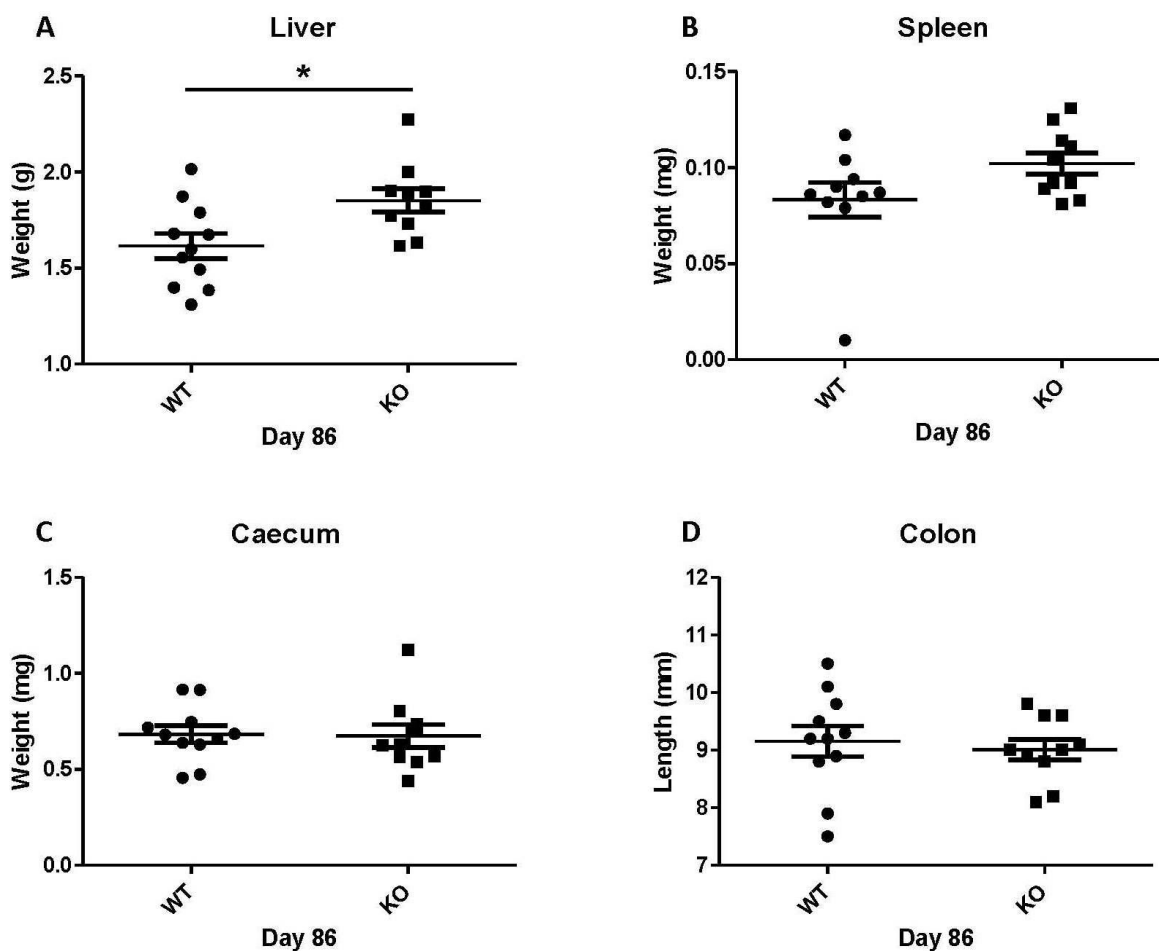


**Figure S1.** WT and KO mice mean weights of (A) liver, (B) spleen, (C) caecum, and (D) colon length. (Mann-Whitney test, \*P < 0.05).

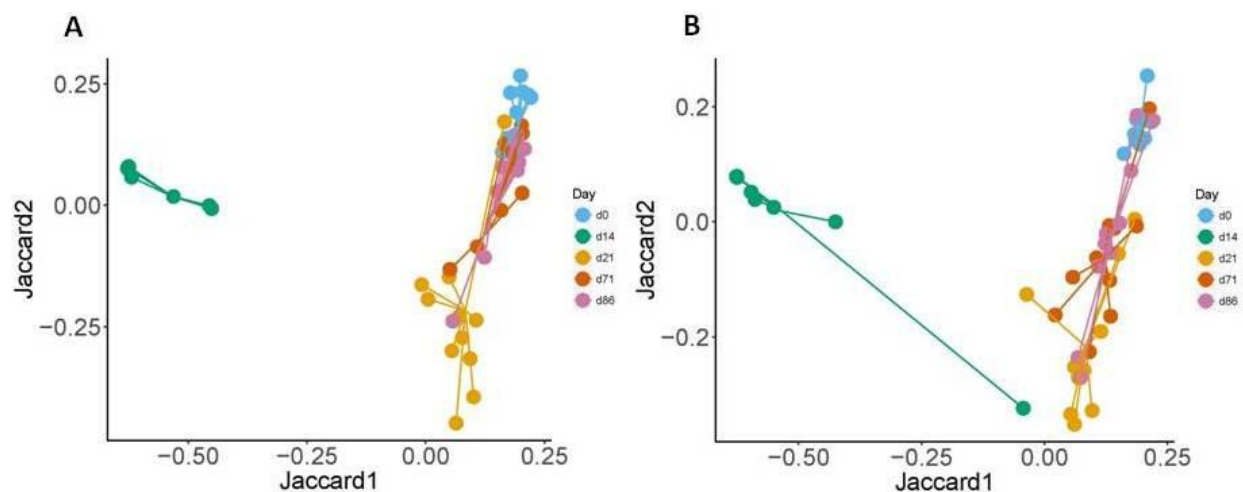


**Figure S2.** Principle coordinate analysis (PCoA) based on Jaccard of (A) WT, and (B) KO at day 0 (brown), day 14 (red), day 21 (orange), and day 86 (pink).

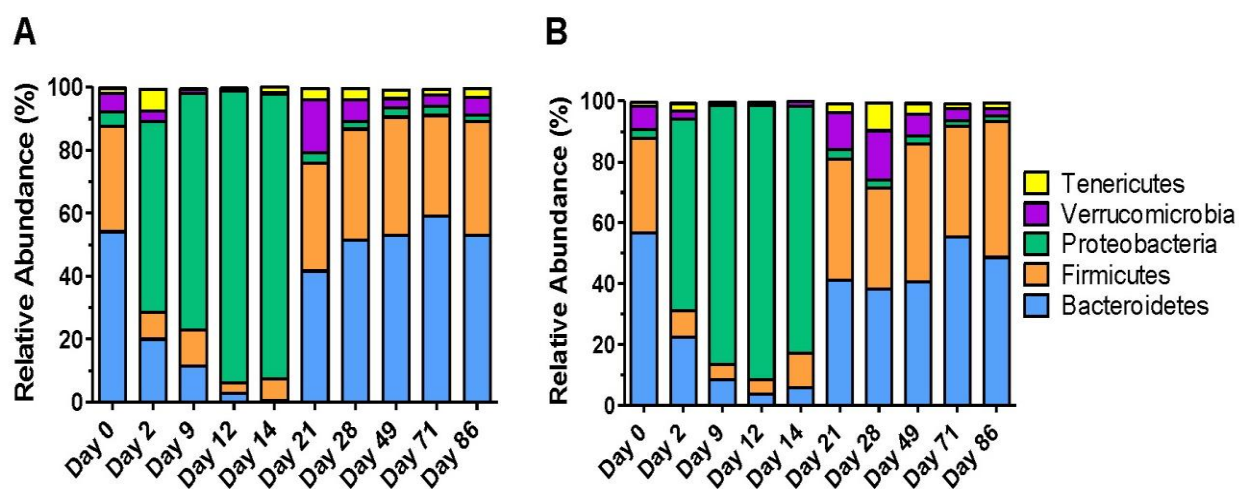


**Figure S3.** Relative abundance (%) of 16S bacterial community composition across all time points at phylum level in (A) WT, and (B) KO.

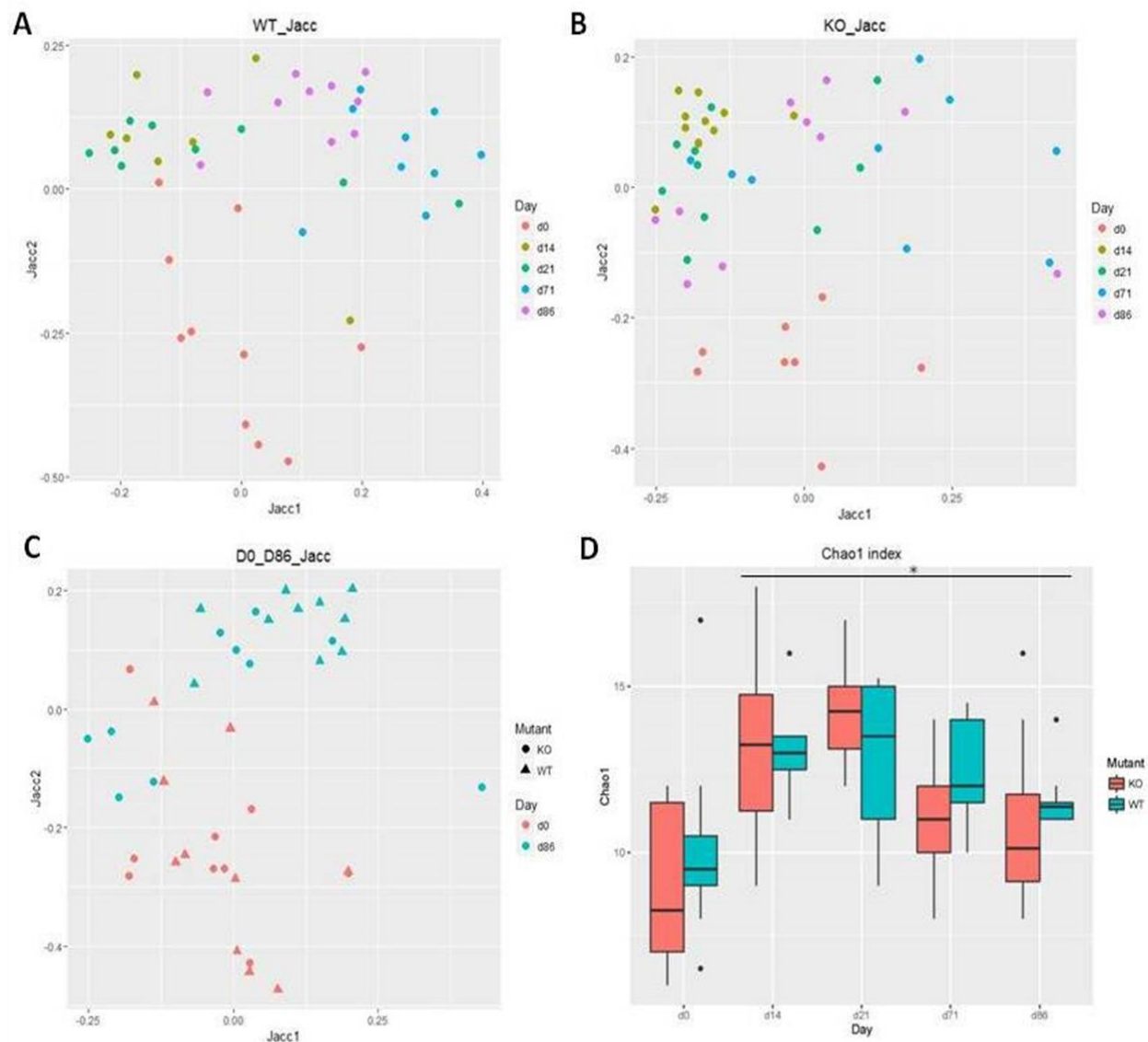


**Figure S4.** Principle coordinate analysis (PCoA) of fungi where Jacc1 explains 10.47% and Jacc2 explains 8.39% in **(A)** WT across time, **(B)** KO across time, and **(C)** WT (triangles) and KO (circles) at day 0 (pretreatment) (pink) and day 86 (blue). **(D)** Chao1 index demonstrating fungal richness in WT and KO across time. Time points (day 14, 21, and 71) in both genotypes are significant when compared to day 0 (Student's t-test,  $P < 0.05$ ).

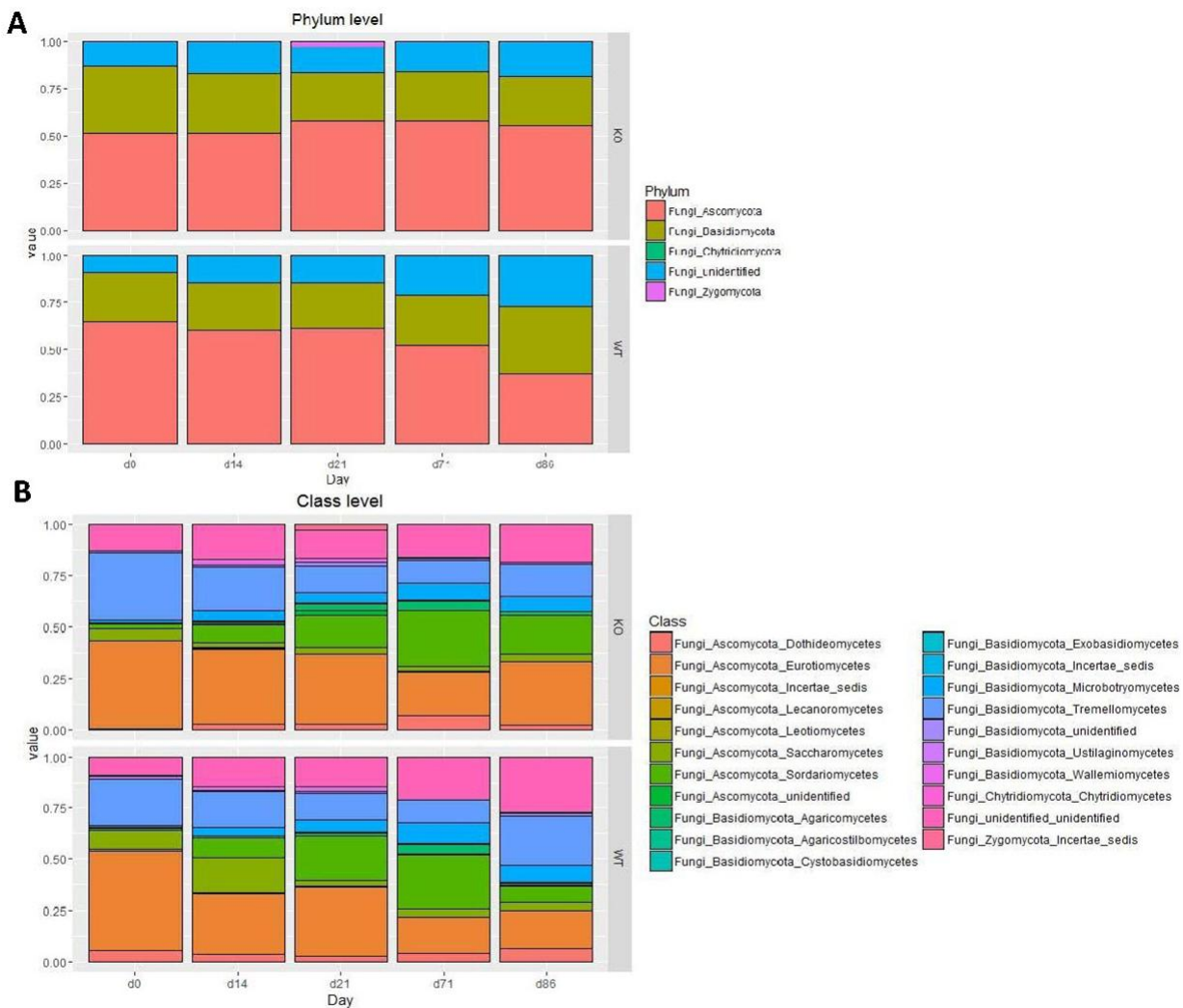


**Figure S5.** Fungal relative abundance (%) of community composition in KO and WT at (A) phylum level and (B) class level.

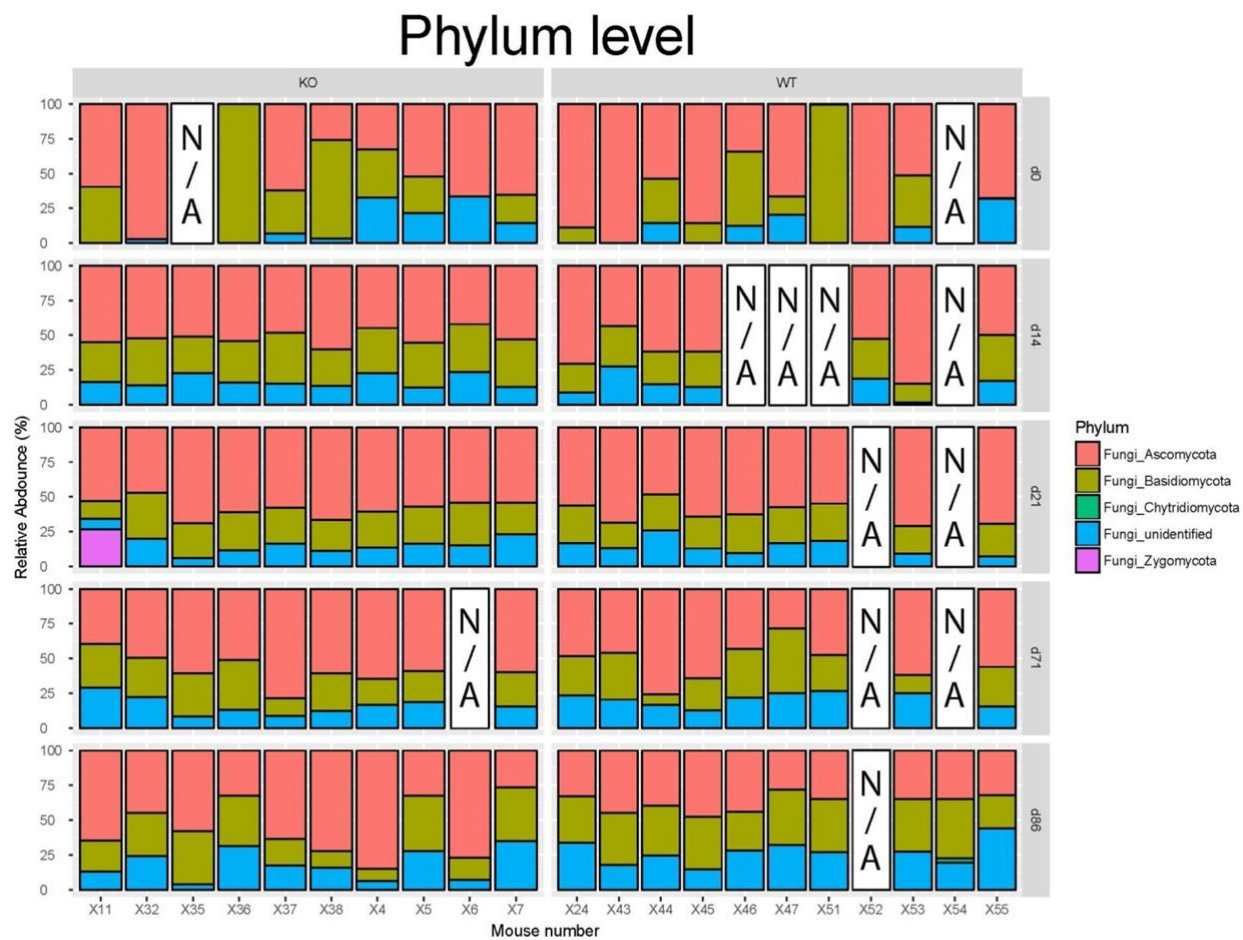


**Figure S6.** ITS1 fungal relative abundance (%) of phylum level community composition in all KO and WT individuals across time (days 9, 14, 21, 71, 86). N/A indicates sample unavailable.

**A**

Family/Genus	Target	Target Gene	Assay ID	Context Sequence
Enterobacteriaceae Phylum: Proteobacteria	ESBL	CTX-M group9	Pa04646127 s1	GCTTAATCAGCCTGTCGAGATCAAG
		SHV	Pa04646134 s1	CGCTTCCCATGATGAGCACCTTTA
		TEM	Pa04646128 s1	GCGGCCAACTTACTTCTGACAACGA
		OXA-1	Pa04646133 s1	TCATACACCAAAGACGTGGATGCAA
	AmpC Resistance	BIL/LAT/CMY	Pa04646135 s1	TAAGACGTTTAAACGGCGTGTGGGC
		ACT/MIR	Pa04646124 s1	ACCGTTACGCCGCTGATGAAAGCGC
	Carbapenem Resistance	VIM	Pa04646155 s1	GATGGTGATGAGTTGCTTTTGATTG
KPC		Pa04646152 s1	CCTCGTCGCGGAACCATTTCGCTAAA	
Enterococcus Phylum: Firmicutes	Vancomycin Resistance	vanA2	Pa04646147 s1	AGCTACTCCCGCCTTTTGGGTTATT
		vanB	Pa04646150 s1	AACTTAACGCTGCGATAGAAGCGGC
		vanC2-C3-2	Pa04646122 s1	TTGAGATCGGTTGCGGTATTTGGG

**B**

Target Gene	Target	Associated Phylum	Individual Mouse	Day Resistance Gene Present
ACT/MIR	AmpC Resistance	Proteobacteria	#46 WT	Day 14
ACT/MIR	AmpC Resistance	Proteobacteria	#55 WT	Day 71
vanC2-C3-2	Vancomycin Resistance	Firmicutes	#24 WT	Day 21 & Day 71
vanA2	Vancomycin Resistance	Firmicutes	#32 KO	Day 0
vanC2-C3-2	Vancomycin Resistance	Firmicutes	#35 KO	Day 14
vanC2-C3-2	Vancomycin Resistance	Firmicutes	#11 KO	Day 21
BIL/LAT/CMY	AmpC Resistance	Proteobacteria	#7 KO	Day 21

**Table S1. (A)** Assays employed in this study as part of the TaqMan® based microfluidic real time PCR system. **(B)** Summary of resistance genes present in individual mice from days 0, 2, 14, 21, and 71. Presence of resistance genes was determined by qPCR assays as listed in App. 2 Table S1A.

	Bacteroidetes	Proteobacteria	Verrucomicrobia	Firmicutes	Tenericutes
TreatmentWT	6,26E-01	1,38E-01	0,576497	8,23E-01	5,10E-01
factor(day)2	1,29E-05	5,72E-11	0,302459	2,94E-08	3,31E-01
factor(day)9	1,40E-11	0,00E+00	0,001512	1,11E-11	8,29E-03
factor(day)12	0,00E+00	0,00E+00	0,000808	3,87E-11	9,03E-03
factor(day)14	1,74E-14	0,00E+00	0,016084	2,96E-03	4,29E-03
factor(day)21	1,30E-01	8,27E-01	0,190371	3,10E-01	3,00E-01
factor(day)28	5,46E-02	5,50E-01	0,025025	8,18E-01	2,35E-02
factor(day)49	5,33E-03	5,38E-01	0,932214	2,24E-02	1,40E-02
factor(day)70	9,37E-01	1,80E-01	0,290782	5,25E-01	7,10E-01
factor(day)86	3,58E-01	1,04E-01	0,023226	1,71E-01	2,35E-01

**Table S2.** Exchangeable correlation matrix (GEE) of phylum level gut bacteria, where factors are time points across the longitudinal study and treatment is WT day 0 (pretreatment). Highlighted boxes indicate significance ( $P \leq 0.05$ ).

	Barnesiella	Parabacteroides	uncl. Porphyromonadaceae	Prevotella	Alistipes	Bacteroides	uncl. Bacteroidales	Parasutterella	Escherichia Shigella	Anaeroplasm	Akkermansia	Lactobacillus	Clostridium XIVa	uncl. Lachnospiraceae	uncl. Ruminococcaceae	uncl. Clostridiales
Treatment WT	0,045312	0,4866	2,34E-01	2,08E-01	2,41E-01	2,16E-01	0,40942	0,69085	0,70228	0,74512	4,95E-01	7,01E-01	2,27E-01	2,23E-01	7,72E-01	3,62E-01
factor(day)2	0	0,182	1,20E-08	8,29E-06	2,69E-01	1,89E-01	0,00702	0,55719	0	0,125309	3,87E-02	6,14E-01	1,83E-05	1,94E-13	1,95E-08	6,03E-01
factor(day)9	0	0,0396	2,22E-16	6,63E-10	7,44E-15	1,67E-06	0,21807	0,72818	0	0,000455	1,31E-07	3,44E-04	1,12E-02	1,94E-10	1,78E-05	1,11E-03
factor(day)12	0	0,1362	0,00E+00	5,55E-16	0,00E+00	5,60E-09	0,09343	0,00278	0	0,000339	1,54E-07	8,98E-06	6,55E-04	1,84E-13	8,18E-11	2,44E-06
factor(day)14	0	0,6734	0,00E+00	0,00E+00	0,00E+00	1,43E-02	0,00563	0,46939	0	0,633845	2,43E-05	1,22E-01	2,26E-06	4,35E-14	4,24E-12	5,31E-07
factor(day)21	0,000144	0,0241	5,32E-07	4,81E-02	3,98E-01	2,56E-01	0,13552	0,31411	0,00301	0,142477	2,44E-02	6,33E-01	1,40E-02	6,48E-01	4,23E-02	4,28E-01
factor(day)28	0,031842	0,0887	2,72E-02	3,98E-04	4,26E-01	5,28E-01	0,02707	0,2149	0,05153	0,018377	1,01E-01	7,80E-02	9,71E-03	9,53E-01	3,11E-01	6,40E-01
factor(day)49	0,535091	0,3141	5,96E-01	3,07E-10	9,81E-01	1,07E-01	0,1357	0,86042	0,03436	0,03386	3,19E-01	3,92E-02	3,62E-03	2,77E-01	2,70E-01	2,02E-02
factor(day)70	0,085452	0,1169	3,41E-01	4,62E-07	8,92E-04	8,38E-03	0,09318	0,96517	0,26435	0,765982	5,02E-02	2,39E-01	1,91E-02	8,26E-01	4,44E-01	1,89E-01
factor(day)86	0,415301	0,1269	7,12E-01	7,83E-11	3,53E-01	1,57E-03	0,14705	0,22099	0,68781	0,07713	1,54E-01	1,40E-01	2,14E-03	1,73E-01	1,85E-01	8,62E-02

**Table S3.** Exchangeable correlation matrix (GEE) of genus level gut bacteria, where factors are time points across the longitudinal study and treatment is WT Day 0 (pretreatment). Highlighted boxes indicate significance ( $P \leq 0.05$ ).

Groups	R	P-value %	Possible Permutations	Actual Permutations	Number $\geq$ Observed
<b>0, 14</b>	<b>0,809</b>	<b>0,002</b>	<b>462</b>	<b>462</b>	<b>1</b>
<b>0, 21</b>	<b>0,431</b>	<b>0,002</b>	<b>462</b>	<b>462</b>	<b>1</b>
<b>0, 71</b>	<b>0,791</b>	<b>0,002</b>	<b>462</b>	<b>462</b>	<b>1</b>
<b>0, 86</b>	<b>0,557</b>	<b>0,002</b>	<b>462</b>	<b>462</b>	<b>1</b>
14, 21	0,178	9,3	462	462	43
<b>14, 71</b>	<b>0,643</b>	<b>0,002</b>	<b>462</b>	<b>462</b>	<b>1</b>
14, 86	0,539	0,009	462	462	4
21, 71	0,041	27,7	462	462	128
21, 86	-0,002	47	462	462	217
71, 86	-0,069	66,9	462	462	309

**Table S4.** ANOSIM global test for differences between time groups of the viral communities ( $R = 0.406$ ;  $P = 0.001$ ).

Species	Group 0	Group 14	Av.Diss	Diss/SD	Contrib%	Cum.%
	Av.Abund	Av.Abund				
Phage cdtI DNA	0,00	2,28	3,13	1,77	5,01	5,01
Parabacteroides	2,69	0,90	2,46	1,66	3,95	8,96
Bacteroides	1,95	0,11	2,42	2,35	3,88	12,84
Edwardsiella	0,01	1,81	2,41	3,54	3,86	16,71
Croceibacter	1,86	0,06	2,35	3,04	3,77	20,48
Escherichia	0,13	1,80	2,33	1,91	3,73	24,21
Cellulophaga	1,73	0,30	1,93	1,39	3,09	27,31
Salmonella	0,31	1,67	1,84	2,70	2,95	30,25
Lactobacillus	1,93	1,23	1,71	1,27	2,74	32,99
Enterococcus	1,35	1,25	1,67	1,19	2,68	35,68
Cercopithecine herpesvirus 2	0,09	1,26	1,59	1,53	2,55	38,22
Vibrio	0,43	1,51	1,52	1,90	2,44	40,66
Stx2	0,09	1,15	1,44	1,69	2,30	42,97
Enterobacteria	0,59	1,32	1,07	1,54	1,72	44,69
Burkholderia	0,50	0,74	1,01	1,32	1,63	46,31
Weissella	0,74	0,01	0,95	1,77	1,52	47,84
Streptococcus	0,53	1,24	0,95	2,18	1,52	49,35
Brevibacillus	0,48	0,95	0,93	1,56	1,49	50,85
Mycobacterium	0,79	0,29	0,92	2,61	1,48	52,33
Clostridium	1,30	1,98	0,92	1,21	1,48	53,81
Ectocarpus siliculosus virus 1	0,30	0,96	0,89	1,80	1,42	55,23
Staphylococcus	0,57	0,45	0,76	1,26	1,22	56,45
Prochlorococcus	0,56	0,06	0,70	0,98	1,12	57,58
Synechococcus	0,29	0,80	0,66	1,11	1,06	58,64
Iodobacteriophage	0,00	0,47	0,65	1,15	1,05	59,68
Riemerella	0,63	0,26	0,65	1,93	1,05	60,73
Paenibacillus	0,57	0,19	0,64	1,25	1,03	61,76
Planktothrix	0,36	0,79	0,63	1,46	1,01	62,77
Ralstonia	0,16	0,44	0,61	0,61	0,98	63,75
Acholeplasma	0,00	0,46	0,61	0,98	0,98	64,73
Emiliana huxleyi virus 86	0,09	0,54	0,59	1,67	0,95	65,68
Paramecium bursaria Chlorella virus	0,52	0,07	0,59	2,21	0,94	66,62
Lactococcus	0,54	0,76	0,56	1,67	0,90	67,52
Rhodococcus	0,46	0,36	0,55	1,57	0,88	68,39
Tetrasphaera	0,42	0,00	0,54	1,65	0,87	69,26
Microviridae	0,34	0,36	0,54	1,07	0,86	70,12

**Table S5.** Pairwise test for time groups 0 and 14 of the viral community, where SIMPER analysis of average dissimilarity is 62.37.

Species	Group 0	Group 21	Av.Diss	Diss/SD	Contrib%	Cum.%
	Av.Abund	Av.Abund				
Parabacteroides	2,69	0,12	4,47	1,90	7,06	7,06
Enterococcus	1,35	2,58	3,27	1,18	5,18	12,24
Bacteroides	1,95	0,02	3,20	2,08	5,06	17,29
Croceibacter	1,86	0,18	2,84	2,11	4,48	21,78
Cellulophaga	1,73	0,13	2,76	1,43	4,36	26,14
Lactobacillus	1,93	2,53	2,64	1,15	4,18	30,31
Bacillus	1,87	1,48	1,98	1,36	3,13	33,44
Clostridium	1,30	1,47	1,98	1,59	3,13	36,57
Lactococcus	0,54	1,21	1,66	1,15	2,62	39,19
Streptococcus	0,53	1,06	1,34	1,45	2,11	41,30
Staphylococcus	0,57	0,71	1,21	1,24	1,91	43,21
Brevibacillus	0,48	0,78	1,17	1,18	1,84	45,05
Weissella	0,74	0,05	1,16	1,52	1,83	46,88
Riemerella	0,63	0,30	1,13	2,05	1,78	48,66
Geobacillus	0,52	0,69	1,12	0,93	1,78	50,44
Rhodococcus	0,46	0,31	0,89	1,00	1,41	51,85
Prochlorococcus	0,56	0,15	0,87	0,91	1,38	53,22
Paenibacillus	0,57	0,21	0,86	1,13	1,36	54,58
Mycobacterium	0,79	0,65	0,77	1,29	1,22	55,80
Klebsiella	0,24	0,42	0,76	0,75	1,21	57,00
Salmonella	0,31	0,44	0,76	1,17	1,19	58,20
Enterobacteria	0,59	0,34	0,74	1,28	1,17	59,37
Pseudomonas	0,43	0,54	0,71	1,52	1,12	60,49
Tetrasphaera	0,42	0,00	0,68	1,53	1,08	61,57
Cafeteria roenbergensis virus BV-PW1	0,47	0,28	0,64	1,82	1,02	62,59
Paramecium bursaria Chlorella virus	0,52	0,17	0,63	1,41	0,99	63,58
Planktothrix	0,36	0,39	0,61	1,20	0,97	64,55
Microviridae	0,34	0,09	0,60	0,65	0,95	65,50
Vibrio	0,43	0,40	0,58	1,47	0,91	66,41
Burkholderia	0,50	0,33	0,57	1,28	0,90	67,31
Pandoravirus	0,47	0,28	0,51	1,19	0,80	68,11
Ectocarpus siliculosus virus 1	0,30	0,36	0,45	1,38	0,70	68,82
Acanthamoeba polyphaga moumouvirus	0,32	0,12	0,43	1,55	0,68	69,50
Listeria	0,24	0,34	0,43	1,80	0,68	70,18

**Table S6.** Pairwise test for time groups 0 and 21 of the viral community, where SIMPER analysis of average dissimilarity is 63.27.

Species	Group 0	Group 71	Av.Diss	Diss/SD	Contrib%	Cum.%
	Av.Abund	Av.Abund				
Parabacteroides	2,69	1,28	3,83	1,79	6,48	6,48
Bacteroides	1,95	0,02	3,53	2,42	5,98	12,46
Enterococcus	1,35	2,65	3,40	1,38	5,75	18,21
Croceibacter	1,86	0,05	3,28	3,09	5,56	23,77
Cellulophaga	1,73	1,93	2,96	1,34	5,02	28,78
Lactobacillus	1,93	2,57	2,88	1,33	4,88	33,67
Bacillus	1,87	0,84	1,94	2,10	3,28	36,94
Weissella	0,74	0,00	1,33	1,83	2,26	39,20
Clostridium	1,30	0,88	1,24	1,76	2,11	41,31
Mycobacterium	0,79	0,28	0,97	1,94	1,65	42,95
Prochlorococcus	0,56	0,04	0,96	0,92	1,63	44,59
Enterobacteria	0,59	0,44	0,96	1,44	1,63	46,22
Paenibacillus	0,57	0,28	0,91	1,25	1,53	47,75
Rhodococcus	0,46	0,28	0,83	0,98	1,41	49,16
Geobacillus	0,52	0,33	0,82	1,66	1,40	50,56
Brevibacillus	0,48	0,31	0,79	1,11	1,33	51,89
Staphylococcus	0,57	0,16	0,76	0,88	1,29	53,17
Lactococcus	0,54	0,43	0,76	1,41	1,28	54,46
Tetrasphaera	0,42	0,00	0,75	1,67	1,28	55,73
Caulobacter	0,30	0,30	0,72	1,07	1,21	56,95
Pandoravirus	0,47	0,07	0,70	1,90	1,19	58,14
Microviridae	0,34	0,14	0,70	0,77	1,18	59,32
Cafeteria roenbergensis virus BV-PW1	0,47	0,08	0,67	2,39	1,13	60,45
Streptomyces	0,37	0,02	0,63	2,41	1,06	61,51
Burkholderia	0,50	0,16	0,62	1,43	1,05	62,56
Paramecium bursaria Chlorella virus	0,52	0,19	0,62	1,64	1,05	63,61
Riemerella	0,63	0,49	0,62	1,36	1,04	64,66
Vibrio	0,43	0,16	0,61	1,79	1,04	65,70
Pseudomonas	0,43	0,09	0,61	1,74	1,04	66,73
Streptococcus	0,53	0,23	0,59	1,73	0,99	67,73
Acanthocystis turfacea Chlorella virus 1	0,22	0,28	0,55	0,96	0,93	68,65
Listeria	0,24	0,34	0,53	1,06	0,90	69,56
Arthrobacter	0,19	0,22	0,53	0,80	0,90	70,46

**Table S7.** Pairwise test for time groups 0 and 71 of the viral community, where SIMPER analysis of average dissimilarity is 59.07.

Species	Group 0 Av. Abund	Group 86 Av. Abund	Av. Diss	Diss/SD	Contrib%	Cum. %
Parabacteroides	2,69	0,75	3,43	1,44	6,45	6,45
Bacteroides	1,95	0,10	2,91	2,06	5,48	11,93
Enterococcus	1,35	2,16	2,59	1,17	4,88	16,81
Croceibacter	1,86	0,38	2,53	1,89	4,76	21,57
Cellulophaga	1,73	2,39	2,51	1,30	4,71	26,28
Lactobacillus	1,93	2,31	2,28	1,20	4,29	30,56
Clostridium	1,30	1,49	1,17	1,48	2,20	32,77
Weissella	0,74	0,00	1,14	1,71	2,14	34,91
Riemerella	0,63	1,28	1,13	1,46	2,13	37,04
Bacillus	1,87	1,46	1,05	1,35	1,97	39,01
Lactococcus	0,54	0,95	0,99	1,29	1,87	40,88
Microviridae	0,34	0,41	0,84	0,89	1,57	42,45
Staphylococcus	0,57	0,52	0,82	1,12	1,53	43,99
Paenibacillus	0,57	0,30	0,81	1,17	1,51	45,50
Prochlorococcus	0,56	0,34	0,78	1,04	1,46	46,97
Rhodococcus	0,46	0,27	0,74	0,99	1,39	48,36
Brevibacillus	0,48	0,40	0,70	1,05	1,31	49,67
Geobacillus	0,52	0,34	0,68	1,90	1,27	50,94
Klebsiella	0,24	0,38	0,67	0,74	1,27	52,21
Ralstonia	0,16	0,42	0,65	1,04	1,23	53,44
Tetrasphaera	0,42	0,00	0,64	1,58	1,21	54,65
Streptococcus	0,53	0,67	0,63	1,46	1,18	55,83
Polaribacter	0,00	0,42	0,61	1,13	1,15	56,98
Enterobacteria	0,59	0,30	0,61	1,18	1,15	58,12
Paramecium bursaria Chlorella virus	0,52	0,52	0,60	1,55	1,12	59,24
Mycobacterium	0,79	0,56	0,57	1,38	1,07	60,32
Cafeteria roenbergensis virus BV-PW1	0,47	0,22	0,56	1,74	1,04	61,36
Pandoravirus	0,47	0,25	0,54	1,42	1,01	62,38
Salmonella	0,31	0,25	0,51	1,26	0,96	63,33
Streptomyces	0,37	0,06	0,48	1,74	0,90	64,23
Arthrobacter	0,19	0,28	0,47	0,83	0,89	65,12
Listeria	0,24	0,31	0,45	1,24	0,85	65,97
Bacteriophage	0,22	0,31	0,45	1,00	0,84	66,81
Burkholderia	0,50	0,25	0,45	1,19	0,84	67,64
Synechococcus	0,29	0,42	0,44	1,02	0,84	68,48
Vibrio	0,43	0,29	0,41	1,40	0,78	69,26
Pseudomonas	0,43	0,29	0,39	1,39	0,73	69,99
Cronobacter	0,22	0,12	0,37	1,67	0,69	70,68

**Table S8.** Pairwise test for time groups 0 and 86 of the viral community, where SIMPER analysis of average dissimilarity is 53.20.

## Appendix 3 – Fecal Transfer

	Patient 1	Patient 2	Patient 3	Patient 4	Patient 5
Age (y)	59	73	72	49	75
Sex	Female	Female	Male	Male	Female
Prior CDI episodes	3	1	2	2	>2
Anamnesis prior to CDI	Life-threatening recurrent diverticulitis, sigma resection	Gastric carcinoma, gastrectomy, diverticulitis	Immunosuppressed since kidney transplant in 1990, multimorbid	Immunosuppressed, HIV infection under antiviral therapy, multimorbid	Colon cancer with colon surgery
Reported antibiotic use before CDI	Ciprofloxacin, metronidazole	Diverse antibiotics	Diverse antibiotics	Cefuroxime, clindamycin	Diverse antibiotics
Additional relevant diagnoses	Pseudomembranous colitis	None	Loss of kidney function	HIV infection, epilepsy	Chronic heart failure, coronary heart disease
Antibiotic(s) used for CDI therapy	Metronidazole, Vancomycin	Metronidazole, Vancomycin	Vancomycin, Metronidazole, Rifaximin	Metronidazole, Vancomycin	Metronidazole, Vancomycin
Type of CDI (refractory or recurrent)	Recurrent	Atypical (currently not detectable)	Recurrent	Recurrent	Recurrent
Additional relevant medications or treatments	None	FMT (donor: husband, 28.03.2014), recurrent symptoms	Ciclosporin, perenterol ( <i>Saccharomyces boulardii</i> )	None	None
Donor	Son	Husband	Sister	Sister	Non-related donor
Date of IMEnT treatment	23 January 2014	20 June 2014	01 July 2014	11 December 2015	22 December 2015
Diarrhea resolution after IMEnT	Yes	Yes	Yes	Yes	Yes
Days to discharge from hospital	1	1	1	1	1
Days to symptom-free status	3	3	3	2	4
Symptom-free until to date	Yes	Yes	Yes	Yes	Yes

**Table S1.** Characteristics and treatment outcome of patients.

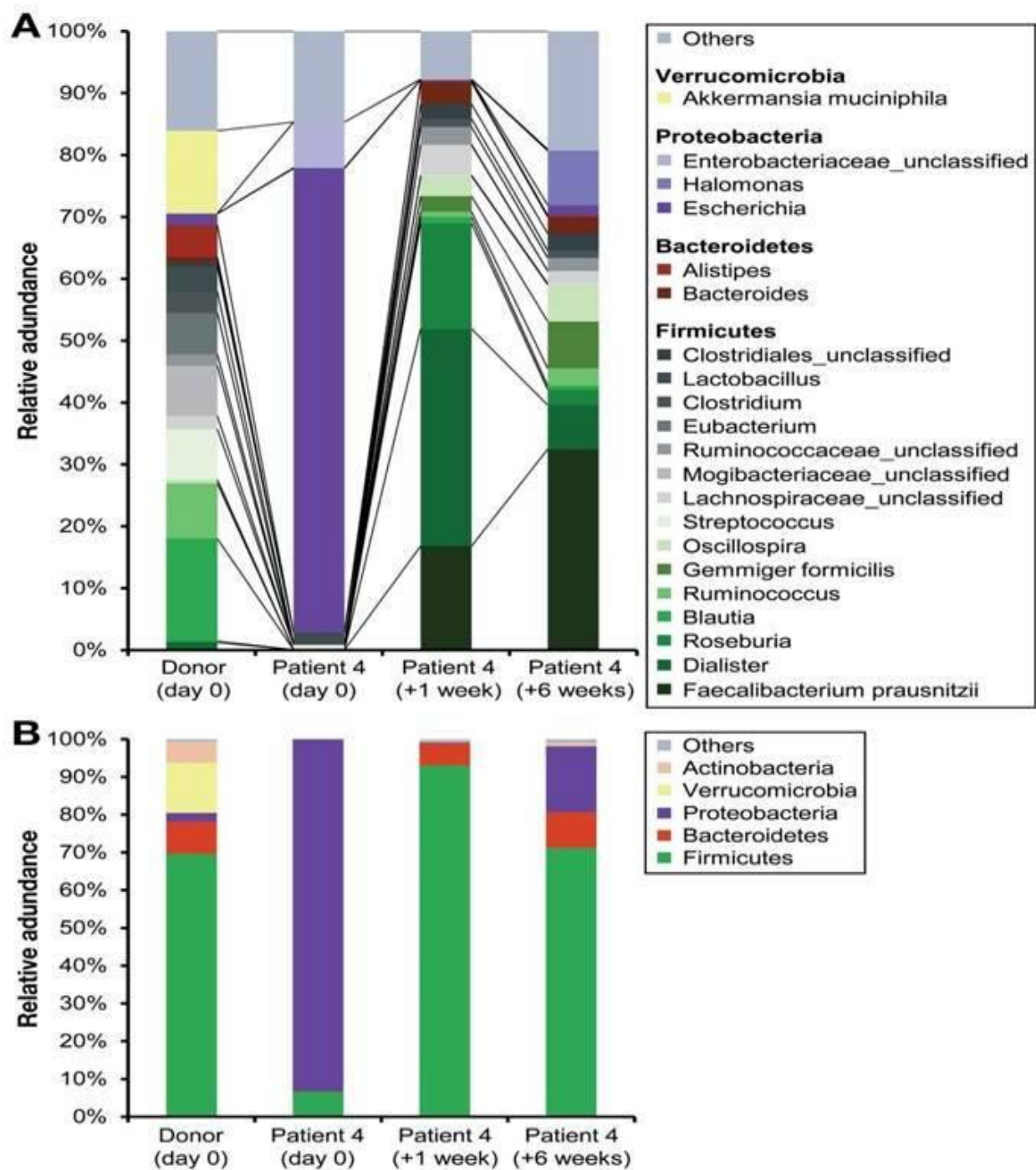


**Figure S1.** Relative abundance (%) of the bacterial community of patient 4 at the (A) genus level and (B) phylum level.

## Appendix 4 – Immunoglobulin A levels

	Mouse ID	B4GALNT2	Farm	Family	Group	Population	Gender	Haplotype	Haplogroup
1	JJM0202	Heterozygotes	JJM02	F2	G1	A11	male	h7	H8
2	JJM0203A	Heterozygotes	JJM02	F2	G1	A11	male	h21	H4
3	JJM0203B	Heterozygotes	JJM02	F2	G1	A11	male	h20	H4
4	JJM0204	C57BL6	JJM02	F2	G1	M08	male	h9	H8
5	JJM0205	Heterozygotes	JJM02	F2	G1	A11	male	h21	H4
6	JJM0206	Heterozygotes	JJM02	F2	G1	A11	female	h16	H4
7	JJM0207	C57BL6	JJM02	F2	G1	A11	male	h20	H4
8	JJM0208	C57BL6	JJM02	F2	G1	A11	male	h20	H4
9	JJM0209	Heterozygotes	JJM02	F2	G1	A11	female	h20	H4
10	JJM0210	Heterozygotes	JJM02	F2	G1	A11	male	h20	H4
11	JJM0901	C57BL6	JJM09	F7	G2	A05	male	h7	H8
12	JJM0902	C57BL6	JJM09	F7	G2	A05	female	h27	H2
13	JJM0903	C57BL6	JJM09	F7	G2	A08	male	h12	H11
14	JJM0904	C57BL6	JJM09	F7	G2	A05	female	h27	H2
15	JJM0906	C57BL6	JJM09	F7	G2	A05	female	h27	H2
16	JJM0908	C57BL6	JJM09	F7	G2	A05	male	h27	H2
17	JJM0909	C57BL6	JJM09	F7	G2	A05	female	h26	H2
18	JJM0910	C57BL6	JJM09	F7	G2	A05	female	h26	H2
19	JJM0911	C57BL6	JJM09	F7	G2	A05	male	h13	H11
20	JJM0912	C57BL6	JJM09	F7	G2	A05	female	h26	H2
21	MJJ0101	C57BL6	MJJ01	F11	G5	A04	male	h12	H11
22	MJJ0102	Heterozygotes	MJJ01	F11	G5	A04	male	h12	H11
23	MJJ0103	C57BL6	MJJ01	F11	G5	A04	male	h12	H11
24	MJJ0104	C57BL6	MJJ01	F11	G5	A04	male	h12	H11
25	MJJ0106	C57BL6	MJJ01	F11	G5	A04	male	h12	H11
26	MJJ0107	Heterozygotes	MJJ01	F11	G5	A04	male	h12	H11
27	MJJ0108	Heterozygotes	MJJ01	F11	G5	A04	male	h12	H11
28	MJJ0109	Heterozygotes	MJJ01	F11	G5	A04	male	h12	H11
29	MJJ0111	C57BL6	MJJ01	F11	G5	A04	male	h12	H11
30	MJJ0112	Heterozygotes	MJJ01	F11	G5	A04	female	h12	H11
31	MJJ0113	Heterozygotes	MJJ01	F11	G5	A04	male	h12	H11
32	MJJ0114	C57BL6	MJJ01	F11	G5	A04	male	h12	H11
33	MJJ0115	Heterozygotes	MJJ01	F11	G5	A04	male	h12	H11
34	MJJ0116	Heterozygotes	MJJ01	F11	G5	A04	male	h12	H11
35	MJJ0117	C57BL6	MJJ01	F11	G5	A04	male	h12	H11
36	MJJ0601	Heterozygotes	MJJ06	F13	G6	A13	male	h16	H4
37	MJJ0602	RIISJ	MJJ06	F13	G6	A13	male	h16	H4
38	MJJ0603	Heterozygotes	MJJ06	F13	G6	A13	male	h16	H4
39	MJJ0604	RIISJ	MJJ06	F13	G6	A13	male	h16	H4
40	MJJ0605	RIISJ	MJJ06	F13	G6	A13	male	h16	H4
41	MJJ0606	Heterozygotes	MJJ06	F13	G6	A13	female	h16	H4
42	MJJ0607	Heterozygotes	MJJ06	F13	G6	A13	male	h16	H4
43	MJJ0608	RIISJ	MJJ06	F13	G6	A13	male	h16	H4
44	MJJ0609	RIISJ	MJJ06	F13	G6	A13	male	h16	H4
45	MJJ0610	Heterozygotes	MJJ06	F13	G6	A13	male	h16	H4
46	MJJ0611	RIISJ	MJJ06	F13	G6	A13	male	h16	H4

**Table S1.** Characteristics of wild mice collected from the area of Espelette, France.

ID	Ileum	Cecum	ColonProx	ColonDist
JJM0202	0	2	0	0
JJM0203A	0	0.333333333	0.333333333	0.333333333
JJM0203B	0	0.666666667	0	0
JJM0204	1.333333333	1.333333333	1.666666667	0
JJM0205	1.666666667	0	1.333333333	0
JJM0206	0	0	0.333333333	NA
JJM0207	0	0.333333333	0	0
JJM0208	0.666666667	0	0.333333333	0.333333333
JJM0209	0	1.666666667	2	0
JJM0210	0	0.333333333	0	0
JJM0901	0.333333333	1.333333333	0.666666667	1
JJM0902	0	0.333333333	1	0
JJM0903	2	3	1	0.666666667
JJM0904	1	0.333333333	0.666666667	0.333333333
JJM0905	0	0.666666667	1.333333333	0
JJM0906	0	0.333333333	1.666666667	0
JJM0908	2	0.666666667	2	0
JJM0909	NA	0	0.333333333	0
JJM0910	0	1.333333333	0.333333333	1
JJM0911	0	1	0.333333333	0
JJM0912	3	0.666666667	0.333333333	1.666666667
MJJ0101	3.333333333	1.333333 333	2	1
MJJ0102	1.333333333	1	0.333333333	1
MJJ0103	1.666666667	0	0	1.333333333
MJJ0104	0	0	0.666666667	0.333333333
MJJ0105	NA	0	0.666666667	1
MJJ0106	0	1.333333333	1	0
MJJ0107	1	0.333333333	0.333333333	0.333333333
MJJ0108	0	0.666666667	0	0
MJJ0109	1.333333333	0.333333333	0.333333333	0
MJJ0111	0	0.333333333	0.333333333	1.333333333
MJJ0112	0	1.333333333	3	0.333333333
MJJ0113	0	1.333333333	1.666666667	0
MJJ0114	0	0.333333333	0.666666667	1
MJJ0115	1.333333333	0.333333333	0.333333333	0.333333333
MJJ0116	0.333333333	0.333333333	0	0.666666667
MJJ0117	0	1.333333333	1.666666667	1.666666667
MJJ0601	1	3.333333333	42.856	2
MJJ0602	0.333333333	1	0.333333333	2
MJJ0603	0	0	0.666666667	0
MJJ0604	NA	0	0.333333333	0.333333333
MJJ0605	0.333333333	0	0	0.333333333
MJJ0606	0.333333333	0	0	0
MJJ0607	0.666666667	0.333333333	0	0
MJJ0608	1.333333333	0	0.666666667	0
MJJ0609	0	0.666666667	0	0
MJJ0610	1	1	0	0
MJJ0611	0.333333333	0.333333333	0	0

**Table S2.** Intestinal scores of wild mice. NA indicates sample not available.

outlyers	ID	description	IgA level (ng/ml)
genotype	MJJ0603	heterozygote	368,8904
	MJJ0104	C57	227,7116
	JJM0906	C57	123,8358
	MJJ0607	heterozygote	54,5
farm	MJJ0603	heterozygote	368,8904
	MJJ0104	C57	227,7116
	JJM0906	C57	123,8358
gender	MJJ0603	male	277,4052
	MJJ0104	male	250,3236
	JJM0906	female	107,1934
	MJJ0607	male	43,49
	JJM0904	female	30,87475
haplogroup	MJJ0603	H4	368,8904
	MJJ0104	H11	227,7116
	JJM0906	H2	123,8358
	MJJ0607	H4	54,5
population	MJJ0603	A13	368,8904
	MJJ0104	A04	227,7116
	JJM0906	A05	123,8358
	MJJ0607	A13	54,5
	JJM0909	A05	18,07727
haplotype	MJJ0603	h16	368,8904
	MJJ0104	h12	227,7116
	JJM0906	h27	123,8358
	MJJ0611	h16	23,9

**Table S3.** Characteristics of wild mice with high fecal IgA levels. Colors indicate same individual mouse.

ID	Ileum	Cecum	ColonProx	ColonDist
MJJ0603	0	0	0.666666667	0
MJJ0104	0	0	0.666666667	0.333333333
JJM0906	0	0.333333333	1.666666667	0
MJJ0607	0.666666667	0.333333333	0	0
JJM0904	1	0.333333333	0.666666667	0.333333333
JJM0909	NA	0	0.333333333	0
MJJ0611	0.333333333	0.333333333	0	0

**Table S4.** Summary of intestinal scores from wild mice with high fecal IgA levels as determined by ELISA. NA indicates sample not available.

## Declaration

I, Jacqueline Moltzau Anderson, declare that the dissertation in form and content, and except for advices given by my supervisor, constitutes my own work. The manuscript, “NOD2 influences intestinal microbial resilience after antibiotic perturbation”, was submitted to Microbiome on July 5<sup>th</sup>, 2017, and is currently under revision. The manuscript, “Intestinal microenvironment transfer: a case series for therapy of *Clostridium difficile* infection”, was published in Gastroenterology in 2016. The manuscript, “The resilience of the intestinal microbiota influences health and disease”, was published in Nature Reviews Microbiology in 2017. The manuscript, “Antibiotics cause delayed resilience in the diverse murine virome”, is currently in preparation for future submission for publication. This thesis has not been submitted elsewhere. All work has been undertaken in compliance with the German Research Foundation’s (Deutsche Forschungsgemeinschaft, DFG) rules of good academic practice.

---

Jacqueline Moltzau Anderson  
Kiel, October 2017

# Curriculum Vitae

## Jacqueline Moltzau Anderson

Date of Birth: Dec. 4<sup>th</sup>, 1988 • Place of Birth: Oslo, Norway  
 Nationality: American • Home Town: Washington Crossing, USA  
 Permanent Address: Bremerstrasse 20, 24118 Kiel, Germany

Email: [j.anderson@ikmb.uni-kiel.de](mailto:j.anderson@ikmb.uni-kiel.de) | [j.anderson@evolbio.mpg.de](mailto:j.anderson@evolbio.mpg.de) • Telephone: +49 1512 3403702

### Education

**Institute of Clinical Molecular Biology (IKMB) & International Max-Planck Research School (IMPRS) for Evolutionary Biology**, PhD Student in Natural Sciences & Evolutionary Biology, Kiel & Plön, Germany, 2014-expected Dec. 2017

**University of Copenhagen**, Masters of Science in Biology specializing in Microbiology, CPH, DK, 2012-2014

**Grinnell College**, Bachelor of Arts double major in Biology and French Lit., Grinnell, IA, USA, 2007-2011

### Research Experience

#### **IKMB & IMPRS for Evolutionary Biology**

##### *PhD Student with Prof. Dr. med. Philip Rosenstiel*

- Used murine model deficient in the Crohn's Disease risk gene NOD2, to investigate influence of NOD2 on the longitudinal dynamics of host-microbial interactions.
- Examined the effects of perturbations on the stability and resilience of the gut bacteriome, mycobiome, and virome through community structure and function, using next-gen. sequencing technologies.
- Determined presence and prevalence of antibiotic resistance genes post antibiotic perturbation using TaqMan qPCR and metagenome sequencing.
- Characterized the human gut virome in sterile fecal transfer study of *C.difficile* infected patients.
- Screened Secretory Immunoglobulin A levels in different murine genotypes and determined inflammatory response.

**University of Copenhagen**, CPH, DK, Feb. 2012-March 2014

##### *Master Student Research with Postdoc. Thomas Baek Pedersen & Prof. Ylva Ardo*

- Examined the growth dynamics of DL-starter cultures during cheese production and early ripening.
- Used Pulsed-field gel electrophoresis to compare different Danish and Dutch DL-starters.
- Developed primers to differentiate between the two aroma forming bacterial groups of *Leuconostoc* and citrate positive *Lactococcus*, in addition to other lactic acid bacteria (LAB).
- Used next-gen. sequencing to determine community structure and composition from DNA and RNA samples collected from a dairy plant.
- Compared culture based methods with molecular methods.
- Evaluated aroma compounds in semi-hard cheese and the fat, salt, and water content.

**University of Copenhagen**, CPH, DK, Summer 2012

##### *Student Research Assistant with Associated Prof. Riikka Rinnan*

- Participated with the Center for Permafrost in an ongoing 24-year-old project in the Swedish Arctic to understand the impact of climate warming on a micro and macroscale.

- Analyzed plant-soil-microbe interactions, nutrient mineralization, and plant nutrient uptake.
- Measured volatile organic compounds (VOCs) and gas exchange at leaf and whole plant level.

**Coe College Field Station, MN, USA, Summer 2009 and 2010**

***Independent Research with Prof. Harlo Hadow***

- To study and determine dominance behavior among *Carpodacus purpureus* (Purple Finch).
- Applied evolutionary theories and developed hypothesis of first year female plumaged male adaptive trait from observed seasonal resource competition between the sexes.

**Certification and Awards**

- Awarded IMPRS stipend for 3 years funding from Dec. 2014-Dec. 2017.
- Workshop on Genomics; Cesky Krumlov. Certificate Jan. 2017.
- Introduction to Genomic Technologies by Johns Hopkins Uni. on Coursera. Certificate Aug. 2016.
- Genomic Data Science with Galaxy by Johns Hopkins Uni. on Coursea. Certificate Sept. 2016.
- Awarded travel grant from MPI for Evol Bio; Feb. 2016.
- Gentechnik-Einweisung: S2 organisms & facility (work with pathogens; e.g. *C. difficile*); March 2015.
- Animal Welfare Course: Einführungsseminar: Tierschutz & Versuchstiere in der Forschung, Jan. 2015.

**Relevant Experience**

- Guest speaker at Prof. Thomas C.G. Bosch lab; NOD2 Affects Microbial Resilience After Antibiotic Treatment In Mice; July 2016.
- Guest speaker at Prof. Dr. John Baines lab; Establishing IgA levels in mice: Does haplotype variation in wild mice populations influence IgA levels?; July 2015.
- Hosted Workshop; Scientific Publishing and Open Access; MPI for Evolutionary Biology; June 2015.
- Open Access Ambassador (for OA publishing); Max Planck Society; since Dec. 2014.

**Conference Presentations**

- The International Society for Evolution, Medicine & Public Health 3rd Meeting; Oral presentation confirmed; Groningen, Netherlands; Aug. 2017.
- European Society of Evolutionary Biology XVI Congress (ESEB); Poster presentation confirmed; Groningen, Netherlands; Aug. 2017.
- International Conference on Holobionts; Oral presentation delivered; Paris, France; April 2017.
- Joint Meeting of the German and Japanese Societies of Developmental Biologists; Oral presentation delivered; Kiel, Germany; March 2017.
- E:Med Systems Medicine meeting; Poster presentation delivered; Kiel, Germany; Oct. 2016.
- European Meeting of PhD Students in Evolutionary Biology (EMPSEB22); Oral presentation delivered; Gotland, Sweden; Sept. 2016.
- Max-Planck-Institute for Evol. Biology Meeting. Poster presentation delivered; Germany; Sept. 2016.
- International Society for Evolution, Medicine, and Public Health 2<sup>nd</sup> Annual Meeting; Poster presentation delivered; N. Carolina, USA; June 2016.
- International RTG Symposium; Poster presentation delivered; Kiel, Germany; June 2015.
- International 5<sup>th</sup> Annual Cluster Symposium: Inflammation at Interfaces; Poster presentation delivered; Kiel, Germany; Feb. 2015.
- Max-Planck-Institute for Evol. Biology Meeting. Oral presentation delivered; Germany; Sept. 2015.

**Publications**

**Moltzau-Anderson J**, Pan WH, Rehman A, Falk-Paulsen M, Lipinski S, Häsler R, Bharti R, Rosenstiel P. NOD2 influences intestinal microbial resilience after antibiotic perturbation. (Microbiome, submitted July 5<sup>th</sup>, 2017; under revision)

Ott J.S., Waetzig H.G., Rehman A., **Moltzau Anderson J.**, Bharti R., Cassidy L., Thley A., Fickenscher H., Seegert D., Rosenstiel P., Schreiber S. (2016). Intestinal microenvironment transfer: a case series for therapy of *Clostridium difficile* infection. Gastroenterology doi: <http://dx.doi.org/10.1053/j.gastro.2016.11.010>.

Sommer F., **Moltzau Anderson J**, Bharti R, Raes J., Rosenstiel P. (2017). The resilience of the intestinal microbiota influences health and disease. *Nature Reviews Microbiology*. doi:[10.1038/nrmicro.2017.58](https://doi.org/10.1038/nrmicro.2017.58)

**In Preparation**

**Moltzau Anderson J**, Lachnit T, Falk-Paulsen M, Lipinski S, Rosenstiel P. Antibiotics cause delayed resilience in the diverse murine virome. (Manuscript in preparation)

**Moltzau Anderson J.**, Pedersen B.T., Al-Soud A.W., Ardo Y. Diversity and dynamics of *Leuconostoc* in undefined mesophilic DL-starter cultures and manufacturing of Danish Danbo cheese (Manuscript in preparation).

